Copyright Warning & Restrictions

The copyright law of the United States (Title 17, United States Code) governs the making of photocopies or other reproductions of copyrighted material.

Under certain conditions specified in the law, libraries and archives are authorized to furnish a photocopy or other reproduction. One of these specified conditions is that the photocopy or reproduction is not to be "used for any purpose other than private study, scholarship, or research." If a, user makes a request for, or later uses, a photocopy or reproduction for purposes in excess of "fair use" that user may be liable for copyright infringement,

This institution reserves the right to refuse to accept a copying order if, in its judgment, fulfillment of the order would involve violation of copyright law.

Please Note: The author retains the copyright while the New Jersey Institute of Technology reserves the right to distribute this thesis or dissertation

Printing note: If you do not wish to print this page, then select "Pages from: first page # to: last page #" on the print dialog screen

ABSTRACT

A STUDY OF THE NEW YORK / NEW JERSEY COASTAL WATER: BIO-OPTICAL CHARACTERISTICS OF THE HARBOR ESTUARY AND THE EFFECTS OF HEAVY METALS ON BROWN TIDE ALGA OF THE BIGHT

by
Bin Wang

The New York / New Jersey (NY/NJ) coastal area is one of the most productive regions around the world and a major natural and scenic resource for New York and New Jersey. As a result of excessive nutrient loading in the water, algal blooms have been observed since 1950's. The NY/NJ coastal area includes the NY/NJ Bight and the NY/NJ Harbor Estuary, and in the former, brown tides (*Aureococcus anophagefferens*) were first observed in 1985 becoming a more serious water quality problem over the last 25 years. The influence of micronutrients, namely trace metals, on *A. anophagefferens* that are widespread in coastal waters is not as well understood. Growth rate and bioaccumulation from exposure to trace metals demonstrated that nickel promoted brown tide growth and that the occurrence of the blooms may significantly influence the fate of cadmium and zinc. On the other hand, in the NY/NJ Harbor Estuary diatom and dinoflagellate blooms dominate the area. Rapid assessment of alga blooms is critical in maintaining coastal waters and remote sensing is an effective tool for monitoring. To improve the accuracy of its application in the NY/NJ Harbor Estuary and to build a bio-optical database, in situ samples were collected from August 2008 to June 2009. Absorption spectra revealed contributions of 47 ± 18% color dissolved organic matter (CDOM), 18 ± 6% non-algal particles (NAP), and 35 ± 16% phytoplankton. The narrow variation in the NAP contribution demonstrates that it can be conveniently subtracted from the total absorption.

Furthermore, analysis showed that organics dominated the NAP spectra; in situ sources with minor terrigenous inputs dominated CDOM spectra; and, diatom and dinoflagellate governed phytoplankton contributions. The combination of pigment distribution analysis and package effect estimation indicates that cell size was a significant factor accounting for variability observed in the specific absorption coefficient. Overall, the obtained bio-optical characteristics, including the specific absorption coefficient and slopes of CDOM and NAP spectra, facilitate application of remote sensing models for water quality monitoring of the NY/NJ Harbor Estuary.

A STUDY OF THE NEW YORK / NEW JERSEY COASTAL WATER: BIO-OPTICAL CHARACTERISTICS OF THE HARBOR ESTUARY AND THE EFFECTS OF HEAVY METALS ON BROWN TIDE ALGA OF THE BIGHT

by
Bin Wang

A Dissertation
Submitted to the Faculty of
New Jersey Institute of Technology
in Partial Fulfillment of the Requirements for the Degree of
Doctor of Philosophy in Environmental Engineering

Department of Civil and Environmental Engineering

May 2011

APPROVAL PAGE

A STUDY OF THE NEW YORK / NEW JERSEY COASTAL WATER: BIO-OPTICAL CHARACTERISTICS OF THE HARBOR ESTUARY AND THE EFFECTS OF HEAVY METALS ON BROWN TIDE ALGA OF THE BIGHT

Bin Wang

Dr. Lisa Axe, Dissertation Co-Advisor — Date
Professor of Civil and Environmental Engineering, NJIT

Dr. Liping Wei, Dissertation Co-Advisor — Date
Assistant Professor of Chemistry and Environmental Science, NJIT

Dr. Zoi-Heleni Michalopoulou, Committee Member — Date
Professor of Mathematical Sciences, NJIT

Dr. Priscilla P. Nelson, Committee Member — Date
Professor of Civil and Environmental Engineering, NJIT

Dr. Thomas J. Olenik, Committee Member — Date
Associate Professor of Civil and Environmental Engineering, NJIT

BIOGRAPHICAL SKETCH

Author: Bin Wang

Degree: Doctor of Philosophy

Date: May 2011

Undergraduate and Graduate Education:

- Doctor of Philosophy in Environmental Engineering,
  New Jersey Institute of Technology, Newark, NJ, 2011
- Master of Engineering in Environmental Engineering,
  Beijing Technology and Business University, Beijing, P. R. China, 2003
- Bachelor of Engineering in Environmental Engineering,
  Beijing Technology and Business University, Beijing, P. R. China, 1999

Major: Environmental Engineering

Presentations and Publications:

Wang, B., Axe, L., Wei, L., Michalopoulou, Z.-H. The Effects of Cd, Cu, Ni, and Zn on brown tide alga *Aureococcus anophagefferens* growth and metal accumulation. (*Submitted*)

Wang, B., Axe, L., Wei, L., Michalopoulou, Z.-H., Ranheim, B., Tan, M., and Riman, R. Light variation of colored dissolved organic matter, phytoplankton, and non-algal particles in the New York/New Jersey Harbor Estuary. *(Manuscript)*

Wei, L., Kang, R., Wang, B., Axe, L., Huo, R. Factors affecting growth potential of *Aureococcus anophagefferens* - observation from laboratory cultures and preliminary field incubations. *(Manuscript)*

Wang, B., Axe, L., Wei, L., Michalopoulou, Z.-H., and Ranheim, B. Bio-optical characteristics of New York / New Jersey Coastal Water. *95th New Jersey Water Environment Association Annual Conference*, Atlantic City, New Jersey, May 9 - 14, 2010.

Wang, B., Axe, L., Wei, L., Bagheri, S., Michalopoulou, Z.-H., Ranheim, B. Variations in the light absorption coefficients of phytoplankton, non-algal particles, and color dissolved organic matter in the New York / New Jersey Harbor Estuary. *Fifth Symposium on Harmful Algae in the U.S.*, Ocean Shores, Washington, November 15 - 19, 2009.

Wang, B., Axe, L., Wei, L., Bagheri, S., Michalopoulou, Z.-H. Sensitivity of *Aureococcus anophagefferens* to heavy metals: the effect of metal adsorption on toxicity**.** *13th IACIS International Conference on Surface and Colloid Science and 83rd ACS Colloid and Surface Science Symposium*, Columbia University, New York City, New York, June 14 - 19, 2009. (Oral presentation)

Wang, B., Axe, L., Wei, L., Bagheri, S., Michalopoulou, Z.-H., Ranheim, B. Absorption coefficient of particles and colored dissolved organic matter at New York / New Jersey Harbor Estuary. *AGU 2008 Fall Meeting*, San Francisco, California, December 15 - 19, 2008.

Wang, B., Axe, L., Wei, L., Bagheri, S., Michalopoulou, Z.-H. Cadmium, copper, nickel, and zinc toxicity and bioavailability to *Aureococcus anophagefferens. Third Passaic River Symposium*, Montclair State University, Montclair, New Jersey, October 16, 2008.

Wang, B., Axe, L., Wei, L., Bagheri, S., Michalopoulou, Z.-H. Effect of cadmium, copper, nickel, and zinc on a minute golden brown alga *Aureococcus anophagefferens. Fourth Symposium on Harmful Algae in the U.S.*, Woods Hole, Massachusetts, October 28 - November 1, 2007.

Wang, B., Wang, Q., Dong, L., Xue, Y. Electrical methods to detect leaks on landfill geomembrane liners. *Research of Environmental Sciences*, 2004, 17(3): 50-54 (*in Chinese*).

Wang, B., Wang, Q., Dong, L., Liu, J. Study on electrical leakage detection for geomembrane liners used in landfill. *Research of Environmental Sciences,* 2003, 16(2): 54-57 (*in Chinese*).

Wang, B., Wang, Q., Dong, L. The comparison of leakage detection for landfill liners. *Research of Environmental Sciences,* 2002, 15(5): 47-48 (*in Chinese*).

This dissertation is dedicated to
my parents who set me on the path to education
and to my sister for her support.

谨以此博士论文献给在求学生涯上支持我的
父亲王连生，母亲叶秀英，以及姐姐王艳。

ACKNOWLEDGMENT

I would like to express my deepest appreciation to Dr. Lisa Axe, who not only served as my research supervisor, providing valuable and countless resources, insight, and intuition, but also constantly gave me support, encouragement, and reassurance. I also would like to express my sincere gratitude to Dr. Liping Wei, my co-advisor, for her guidance and encouragement, which made this work a great learning experience. Special thanks are given to Dr. Priscilla P. Nelson, Dr. Thomas J. Olenik, and Dr. Zoi-Heleni Michalopoulou for actively participating my committee and providing valuable input from their own areas of expertise.

My appreciation to the National Science Foundation Grant No. SBE-0547427 through the ADVANCED program at New Jersey Institute of Technology for providing financial support for this research.

I would like to thank Marine Science at New York City Department of Environmental and Passaic Valley Sewerage Commissioners for sampling conduction, and Heidi Maass from Bedford Institute of Oceanography, Canada for providing the program to analyze data. I would also wish to thank all professors, laboratory stuff, and the secretaries in the department of Civil and Environmental Engineering for constant guidance and help.

All my fellow graduate students are deserving of recognition for their support. I have cherished their friendship for five years, and this will go on and be an asset in my life forever.

TABLE OF CONTENTS

TABLE OF CONTENTS
(Continued)

Chapter **Page**

TABLE OF CONTENTS
(Continued)

Chapter **Page**

LIST OF TABLES

LIST OF TABLES
(Continued)

LIST OF FIGURES

LIST OF FIGURES
(Continued)

Figure **Page**

LIST OF FIGURES
(Continued)

Figure **Page**

CHAPTER 1

INTRODUCTION

Coasts are very important as they serve as physical buffers providing community protection from storm surges and flooding, nurseries for fish and shellfish, homes for much wildlife, and potential sources for oil and gas (Beatley et al., 2002). Although coastal waters represent less than 10 percent of the ocean's surface, they account for 50 percent of its biological productivity (Castro and Huber, 2007). Because 38% of the world's population lives within 100 km of the coast (Small and Cohen, 2004), coastal areas are used extensively. Consequently, these waters are potentially polluted by pathogens, oxygen-depleting substances, metals, nutrients, thermal inputs, polychlorinated biphenyls (PCBs), and other toxic organic chemicals (Sindermann, 2006). The outcome of coastal pollution includes bio-accumulation, a reduction in recreation and tourism, death of marine life, and production of algal blooms (Newman et al., 2002).

An algal bloom is a rapid increase in the algae population for an aquatic system. If algal blooms are unhealthy to human beings and other organisms, the blooms are referred to as harmful algal blooms (HABs); these have been observed in every coastal state of the U.S. (Boesch, 1997). HABs are formed through dispersal of HAB organisms, nutrient enrichment, and introduction and transport of cysts via ballast water transfers (Hallegraeff, 1993). Effects from their persistence include illness and possibly death through ingestion of toxins from contaminated seafood; mass mortalities of wild and farmed fish as well as mortalities of marine mammals, seabirds, and other predator

species; and, disturbances of marine food webs and ecosystems (Landsberg, 2002; Sellner et al., 2003).

The New York / New Jersey (NY/NJ) coastal area is part of the Western Atlantic coastline and includes two parts: (1) the NY/NJ Harbor Estuary, and (2) the NY/NJ Bight area from Montauk Point in Long Island, New York to Cape May, New Jersey (Figure 1.1). The Harbor Estuary is one of the most productive regions in the world (Marshall and Cohn, 1987) and has been declared as a major natural and scenic resource to both states. Significant development in the area has contributed to its pollution from a wide variety of harmful substances. The major pollutants in the coastal water are organic matter, nutrients, toxic metals, and pathogens, which impact the health of both ecosystems and humans. Sources of pollutants include municipal treatment plants, industrial discharges, combined sewer overflows, storm water, tributaries, landfill leachate, navigable vessels, and atmospheric deposition. To protect, preserve, and restore the environment of the NY/NJ coastal areas, state and federal programs have been established such as the NY/NJ Harbor Estuary Program (HEP), NY/NJ Clean Ocean and Shore Trust (COAST), and the NJ Coastal Management Program (CMP).

The water quality and physical environment determine if and when algal blooms will occur in the NY/NJ coastal area. One major HAB in the NY/NJ Bight is brown tides caused by *Aureococcus anophagefferens* (NJDEP, 1999, 2000), while dominant blooms in the NY/NJ Harbor Estuary are diatom and dinoflagellates (NJDEP, 2000, 2008a). A number of studies have been conducted on the causes of brown tide blooms (Bricelj and Lonsdale, 1997; Gobler et al., 2005); factors studied include nitrogen, phosphorus, temperature, and light. However, with the exception of iron, the effects of heavy metals

on *Aureococcus Anophagefferens* have not been addressed and are a focus of the research conducted in this work.

Figure 1.1 New York / New Jersey Coastal Area includes NY/NJ Bight (light green) and NY/NJ Harbor Estuary (dark green).

For the NY/NJ Harbor Estuary, one of the primary missions for water quality control is rapid monitoring of algal blooms (Bagheri et al., 2002; Hellweger et al., 2004). As an effective, economical, and real-time tool, remote sensing has been demonstrated as useful for algal monitoring in the area (Bagheri et al., 2002; Hellweger et al., 2004). In this research, in situ temporal and spatial sampling was conducted to build a requisite bio-optical database for the NY/NJ Harbor Estuary (Figure 1.2), namely Hudson/Raritan Bay, Jamaica Bay, and Inner Harbor. This work serves to aid in improving the accuracy of remote sensing algorithms. Specifically, characteristics of the absorption spectra with respect to particles and dissolved organic matter are investigated and the implications of the results are addressed. Moreover, application of these results resolving water quality characteristics is considered for remote sensing.

The following chapters include Chapter 2, Literature Review; Chapter 3, Hypotheses and Objectives; Chapter 4, Experimental Methods; Chapter 5, Effects of Cd, Cu, Ni, and Zn on Brown Tide Alga *Aureococcus Anophagefferens*; Chapter 6, Variations in the Bio-optical Characteristics of the New York / New Jersey Harbor Estuary; Chapter 7, The Specific Absorption Coefficient for the New York / New Jersey Harbor Estuary; Chapter 8, Pigment Retrieval from Phytoplankton Absorption Spectra; and, Chapter 9, Conclusions and Future Work.

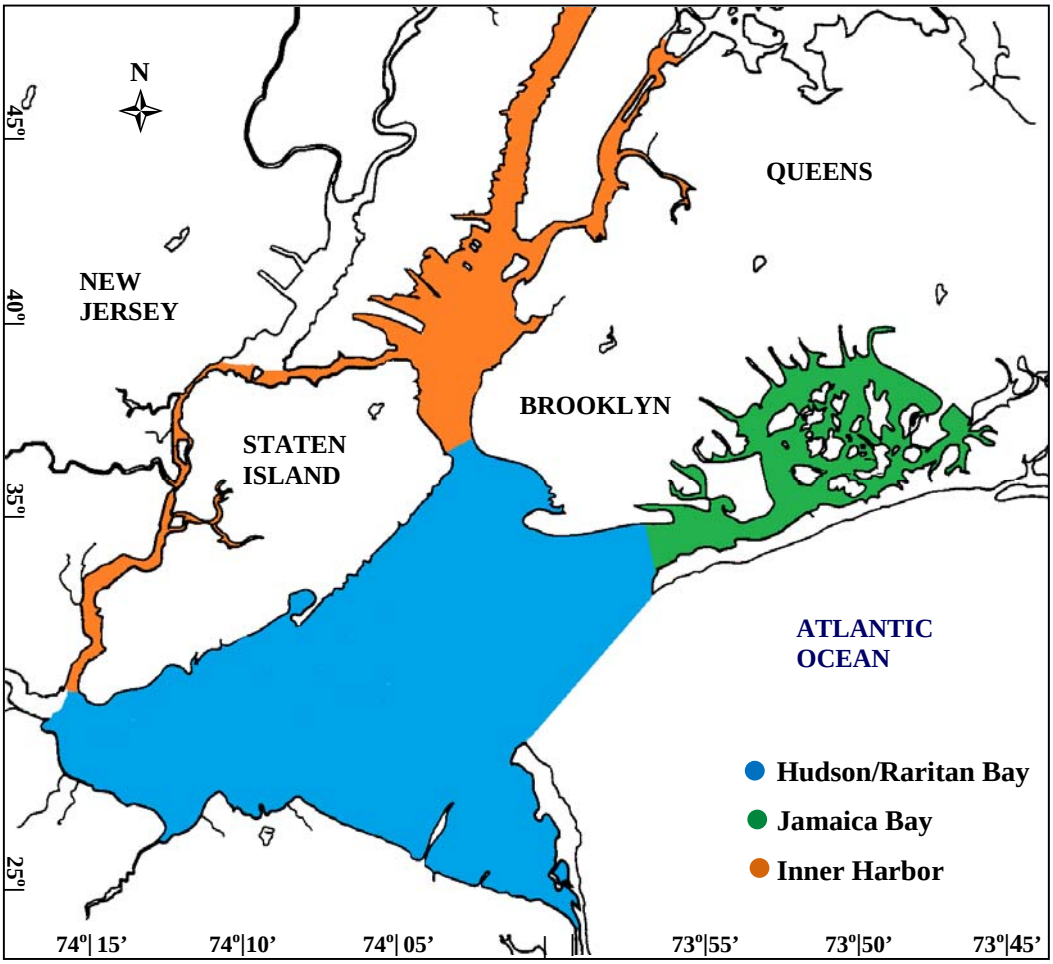

Figure 1.2 New York / New Jersey Harbor Estuary includes Hudson/Raritan Bay (blue), Jamaica Bay (green), and Inner Harbor (Brown).

CHAPTER 2

LITERATURE REVIEW

Harmful algal blooms (HABs) are influenced by many factors, such as water quality, temperature, nutrients, and sunlight. This review focuses on the features of HABs and phytoplankton in the NY/NJ coastal area: brown tide blooms in the NY/NJ Bight, and the bio-optical characteristics in the NY/NJ Harbor Estuary.

2.1 HABs in the New York / New Jersey Coastal Water

HABs have been recorded over the last 60 years for the NY/NJ coastal water (Table 2.1). As early as the 1960's, red tides were documented to be caused by several species of phytoflagellates, such as *Olishthodiscus leteus*, *Katodinium rotundatum*, and *Prorocentrum spp.* (Mahoney and McLaughlin, 1977). In recent years, major phytoflagellate red tides have been confined primarily to the NY/NJ Harbor Estuary, where diatoms (e.g. *Skeletonema costatum* and *Thalassiosira spp.*) are abundant during the cooler months and have dominated from mid to late summer (NJDEP, 2000). Brown tides were first confirmed in lower Barnegat Bay and adjacent Little Egg Harbor Bay of the NY/NJ Bight in 1995 (Nuzzi et al., 1996, No. 15), although they were suspected to have occurred between 1985 and 1986. In 1997, *A. anophagefferens* bloomed again in Barnegat Bay of the NY/NJ Bight and they were observed between 1999 and 2002 mainly as Category 2 (8.5×10^4 - 2.0×10^5 cells $m1^{-1}$) and Category 3 blooms (2.0×10^6 cells ml^{-1}) (Gastrich and Wazniak, 2002; Gastrich et al., 2004).

Table 2.1 HABs Observed in the New York / New Jersey Coastal Water, 1959 - 2010

Division/Classes	Species	Tides
Diatoms	*Asterionella*	
	Cerataulina pelagica	
	Chaetoceros sp.	
	Cylindrotheca closterium	
	Leptocylindrus sp.	
	Pseudonitzschia delicatissima	
	Pseudonitzschia seriata	
	Pseudonitzschia pungens multiseries	
	Pseudonitzschia (Nitzschia) spp	
	Rhizosolenia sp.	
	Skeletnema costatum	
	Thalassiosira spp	
Dinoflagellates	*Ceratium tripos*	Red
	Gyrodinium aureolum	Green
	Katodinium rotundatum	Red
	Pfiesteria piscicida	
	Prorocentrum lima	
	Prorocentrum micans	Red
	Prorocentrum redfieldi	Red
	Scripsiella trochoidea	
Pelagophyceae	*Aureococcus anophagefferens*	Brown
Raphidophy	*Olisthodiscus luteus*	Red
Chlorophytes	*Didymocystis sensu*	Green
	Nannochloris atomus	Green
Euglenids	*Eutreptia lanowii*	Red

Sources: NJDEP (1999, 2000, 2008 a, 2008 b, 2009, 2010)

As significant HABs in the NY/NJ coastal water, brown tides have been repeatedly observed in the NY/NJ Bight. Although brown tides have not been observed in the NY/NJ Harbor Estuary, other blooms have been documented. In Sections 2.2 and 2.3, studies conducted on brown tides are reviewed along with the bio-optical properties of the NY/NJ Harbor Estuary. The advantage to applying bio-optical properties is discussed as an approach for rapid characterization of the phytoplankton spectra.

2.2 Brown Tides at the New York / New Jersey Bight

Brown tides are caused by *A. anophagefferens* and *Aureoumbra lagunensis* (DeYoe et al., 1997), but only the former has been observed in the NY/NJ coastal water (Gobler et al., 2005). Bricelj et al. (1997) and Gobler et al. (2005) reviewed 20 years of studies on *A. anophagefferens* and its blooms. The early research and monitoring of brown tides (1985-1986) were conducted by the Suffolk County Department of Health Services, Office of Ecology, New York and New York Sea Grant (NYSG) funded by the National Oceanographic and Atmospheric Administration (NOAA) (Gobler et al., 2005). In 1995, the Brown Tide Research Initiative (BTRI) (Lomas and Gobler, 2004) was established by NOAA's Coastal Ocean Program (COP) and NYSG to understand the factors that lead to bloom initiation, persistence, and dispersion (Lomas and Gobler, 2004). Phase I (1996-1999) of the BTRI program funded eight projects to identify the factors and processes that stimulate and sustain brown tide blooms, while Phase II (1999-2002) funding took a slightly broader ecosystem-related view based on the outcome of prior research. Below is a review of research conducted over the last two decades on characteristics of *A.*

anophagefferens, causes and effects of brown tides, and factors influencing *A. anophagefferens* growth.

In 1985, blooms of the small phytoplankton, *A. anophagefferens*, were first observed in the eastern and southern bays of Long Island, NY, and Narragansett Bay, RI, and later confirmed as a member of phytoplankton communities in estuarine areas from Maine to Florida as well as those of South Africa (Gobler et al., 2005). Sieburth et al. (1988) originally assigned the brown tide organism to the algal class Chrysophyceae based on its ultrastructure and pigment composition. A few years later, based on further pigment analysis by Bidigare (1989) and Anderson et al. (1993), a new class, the Pelagophyceae, including *A. anophagefferens,* was resolved. The work confirmed that pigments in *A. anophagefferens* included chlorophyll *a*, chlorophyll *c*, fucoxanthin, diatinoxanthin, diatxantin, beta-carotene, and 19'-butanoyl-fucoxanthin. The classification of *A. anophagefferens* in Pelagohpyceae is also supported by analysis of physiological strains (18S rRNA) (DeYoe et al., 1997; Saunders et al., 1997; Bailey and Andersen, 1999) and sterol composition, (E)-24-propylidenecholesterol, 24-methylenecholesterol, and (Z)-24-propylidenecholse (Giner and Boyer, 1998).

Although *A. anophagefferens* has no direct impact on fish and human health, its blooms can negatively affect important estuarine nursery grounds by reducing eelgrass beds, commercially important shellfisheries, and plankton that are a base component of the food web (Cosper et al., 1987; Buskey and Stockwell, 1993; Gobler et al., 2005; Dooley, 2006). An intense brown tide can reduce sunlight penetration; subsequently inhibiting the growth of attached plants such as eelgrass (*Zostera marina*) that serve as a vital nursery for finfish and shellfish, and as a refuge for many other estuarine organisms

(Dennison et al., 1989). These impacts have resulted in fishery loss: annually $3.3 million loss for scallop (*Argopecten irradians*) harvest at Peconic and Gardiners Bays (Cosper et al., 1987); adult hard clams no longer feeding when brown tide cells reached approximately 3.5×10^4 cells/L (Greenfield, 2002); and, death of juvenile hard clams under bloom conditions (Greenfield et al., 2004).

A. anophagefferens, a microscopic alga (2-3 μm), can grow and bloom under a wide range of temperatures from 0 ºC to 25 ºC (Cosper et al., 1987; Gobler et al., 2002). At temperatures greater than 25ºC, the bloom often diminishes (Gobler et al., 2005). Although *A. anophagefferens* can survive in water with a low salinity, the species grows best in water with higher levels of salinity found in estuaries (> 25‰) (Cosper et al., 1987; LaRoche et al., 1997). *A.anophagefferens* is also adaptable in its use of light and can maintain intense brown tides ($>10^8$ cell L^{-1}) under severe attenuation (1% light depth 1-2 m) where other algae are unable to survive (Milligan and Cosper, 1997; MacIntyre et al., 2004). This ability to grow quickly under low light levels may give *A. anophagefferens* a distinct advantage over other phytoplankton.

Most algal blooms are attributed to elevated nutrient loading, including dissolved organic nitrogen and/or phosphorus. When dissolved inorganic nitrogen levels are high, other algae out-compete *A. anophagefferens* (Lomas et al., 2004). In contrast, brown tides often occur when the levels of dissolved inorganic nitrogen are low (Gobler and Sañudo-Wilhelmy, 2001; Gobler et al., 2002). Therefore, brown tides are not a result of eutrophication but rather dominate under conditions where inorganic nutrients are depleted and organic matter is available and plentiful (LaRoche et al., 1997; Gobler and Sañudo-Wilhelmy, 2001). Organic nutrients therefore promote *A. anophagefferens*

blooms. The use of organic N, in combination with the inorganic form, allows for maximal photosynthetic rates for *A. anophagefferens* under low light conditions (Pustizzi et al., 2004). *A. anophagefferen* can also consume C from organic compounds (Dzurica et al., 1989; Mulholland et al., 2002). Even though P stimulation of *A. anophagefferens* growth rates during a brown tide is not reported, additional P may have been required for *A. anophagefferens* to use the large amounts of dissolved inorganic nitrogen (DIN) and dissolved organic nitrogen (DON) (Gobler et al., 2002; 2005).

The nutrient concentrations in the NY/NJ Bight from Montauk, NY to Cape May, NJ range from 4.4 to 1,000 μg total N/L and 1.1 to 280 μg P/L (Zimmer and Groppenbacher, 1999). The primary factors controlling the concentration of nutrients tend to be the input from anthropogenic sources and the uptake of nutrients through primary productivity. Related factors include loss of nutrients from tissue to the water column through senescence, incorporation of both inorganic and organic nutrients into the sediments, resuspension from the sediments, and fixation of nitrogen from the atmosphere. Brown tides have been observed in the area (Bricelj and Lonsdale, 1997; Gobler et al., 2005) when DIN concentrations were low, 2.5 ± 1.9 μM, and DON were greater than 32 ± 6.5 μM (Gobler et al., 2002).

One key factor promoting brown tides is the reduction in mortality processes that would otherwise decrease *A. anophagefferens* populations. These processes are microzooplankton grazing and viral lysis (Gobler et al., 1997). During brown tide blooms, microzooplankton may preferentially avoid *A. anophagefferens* choosing instead to consume other species of phytoplankton (Lonsdale et al., 1996; Gobler et al., 2002). Moreover, multiple cultures of microzooplankton are unable to grow on a diet of *A.*

anophagefferens (Caron et al., 1989; Mehran, 1996). Reduced microzooplankton grazing of brown tides may be due to *A. anophagefferens* having extracellular polysaccharide secretions (EPS) (Sieburth et al., 1988) and dimethylsulphoniopropionate (DMSP) (Lonsdale et al., 1996). EPS contains a dopamine-like compound that is capable of inhibiting ciliary motion in bivalves (Gainey and Shumway, 1991). This sheath may have a similar effect on the cilia of microzooplankton contributing to the observed lowered grazing rates on the brown tide. Alternatively, DMSP may also inhibit protozoan grazing (Wolfe et al., 1997). Gobler et al. (2002) first concluded that reduced grazing pressure on *Aureococcus* was a factor that can contribute to the proliferation of brown tide blooms in the NY/NJ coastal waters. In addition to the above two key factors, reduced freshwater flow, high salinities, and long residence times in shallow estuaries promote the occurrence of brown tides (Gobler et al., 2005).

Trace metals, particularly Fe, Mn, Cu, Zn, Co, Ni, and even the nonessential metal Cd, also play key roles in marine phytoplankton carbon, nitrogen, and phosphorus acquisition (Morel and Price, 2003). In coastal waters several of these metals, such as Cd, Cu, Ni, and Zn, are common contaminants from industrial wastewater and sewage discharges, antifouling paints, fossil fuel combustion, and urban and agricultural runoff (Förstner et al., 1979). Dissolved metal concentrations are compared for coastal waters of the Northeast where brown tides have been observed (Table 2.2). A number of coastal algal blooms were found to have heavy metal links. Iron was involved in the occurrence of harmful algal blooms of the dinoflagellate *Gymnodinium breve* in southern Florida (Ingle and Martin, 1971), cobalt has been implicated in the incidence of blooms of prymnesiophyte *Chrysochromulina polylepis* at Kattegat in south-east Sweden (Graneli

and Risinger, 1994), and selenium has also been identified as a potentially important factor in *Gymnodinium nagasakiense* dinoflagellate blooms in Tanabe Bay, Japan (Koike et al., 1993). Some nonessential metals such as Cd may also promote algal growth by substituting for nutrient metals when essential metals are depleted. For example, Price and Morel (1990) found that Cd addition resulted in a Zn-deficient diatom *Thalassiosira weissflogii* which grew at 90% of its maximum growth rate.

Table 2.2 Dissolved Metal Concentrations (nM) in Coastal Water of U.S. Northeast

Coastal Areas	Cd	Cu	Ni	Zn
Peconics Estuary, NY	0.025 - 0.4	9 - 51	1 - 13	6 - 57
Long Island Sound, NY	0.06 - 0.36	9 - 36	10 - 55	5 - 53
Great South Bay, NY	0.042 - 1.60	5 - 39		
Narragansett Bay, RI	0.29 - 0.80	12 - 28	17.3 - 90.8	16 - 72
Overall total dissolved	0.025 - 1.6	5 - 51	1 - 90.8	5 - 72

Sources: Breuer et al. (1999), Clark et al. (2006), Kozelka and Bruland (1998), and Wells et al. (2000).

The occurrence of algal blooms, particularly in shallow coastal waters, may affect metal speciation and biogeochemical cycling (Cloern, 1996). Development of diatom and dinoflagellate blooms in a sub-estuary of the Chesapeake Bay rapidly reduced arsenate to arsenite and methylated species, and increased organically complexed copper from an initial 20 - 40% to 60 - 100% of the total dissolved copper (Sanders and Riedel, 1993). Diatom blooms in the southern portion of the San Francisco Bay reduced concentrations

of dissolved Zn, Cd, and Ni by as much as 75% of their pre-bloom concentrations, while dissolved Cu increased 20% (Luoma et al., 1998). Apparently the phytoplankton assemblage and the productivity greatly affect total dissolved and bioavailable metal concentrations.

The role of heavy metals on *A. anophagefferens* growth and metal sequestration has been studied only with Fe, where it was found that *A. anophagefferens* required low levels for growth (a 5 nM quota of iron was needed for a bloom of 10^6 cell/mL) (Nichols et al., 2001). The effects of other heavy metals on the brown tide bloom initiation and consequent heavy metal sequestration has not been studied to date. One hypothesis in this research is that *A. anophagefferens* growth is inhibited by addition of what is considered a toxic metal, such as Cd, and elevated micronutrient metals, such as Cu, Ni, and Zn.

Brown tides have been observed over the last 25 years along the NY/NJ coastline in Long Island, NY and Barnegat and Little Egg Bay, NJ, but not in the NY/NJ Harbor Estuary. This exception can be explained based on the water quality not being conducive for *A. anophagefferens* growth. To comprehensively study the water quality and phytoplankton assemblages in the NY/NJ Coastal Area, bio-optical properties of the water will be examined.

2.3 The Bio-optical Properties for Remote Sensing in the New York / New Jersey Harbor Estuary

The NY/NJ Harbor Estuary is a major part of the NY/NJ coastal area (Figures 1.1 and 1.2) and was named “Estuary of National Significance” by the U.S. Environmental Protection Agency in 1981. The area has being threatened by increased pollutants, especially nutrient enrichment. In recent years, the area has been dominated by a diverse

assemblage of diatoms in mild to full bloom proportions from mid to late summer. Prevailing diatoms include *Skeletonema costatum*, *Asterionella glacialis, Thalassiosira nordenskioeldii*, *Nitzschia spp.* and *Cylindrotheca closterium* (NJDEP, 2000, 2008b, 2010). Dinoflagellates detected were *Gyrodinium undulans, Olisthodiscus luteus,* and *Prorocentrum micans*. In addition, *Pseudonitzschia spp.* and *Dinophysis spp.* both potentially toxic species were found at concentrations below that of a bloom (NJDEP, 2008a).

Traditionally, algal groups are quantified with microscopy by identifying and counting cells, measuring their size, and converting the resulting volumes (V) to carbon (C) biomass on the basis of previously established equations (Strathmann, 1967; Montagnes and Franklin, 2001). However, depending on the equation chosen for this conversion, calculated C concentrations may vary for a specific taxonomic group (Havskum et al., 2004; Llewellyn et al., 2005). Moreover, intra-class variations up to ~30-fold in the C:V ratios of phytoplankton were observed (Llewellyn et al., 2005). Overall, microscopic examination of the water samples is slow, laborious, and intermittent.

A more recent method to estimate the distribution of phytoplankton groups is through measuring pigment composition of cells with high performance liquid chromatography (HPLC) analysis (Mantoura and Llewllyn, 1983; Rodriguez et al., 2002). This technique is faster and more appropriate for the identification of pico- and nano-phytoplankton than the microscope approach (Veldhuis and Kraay, 2004). To relate the measured pigment composition to the distribution of phytoplankton groups, statistical techniques are applied including multiple linear regression (Tester et al., 1995) or matrix

factorization used in CHEMTAX (Mackey et al., 1996). However, simple multiple linear regression analysis has several shortcomings compared to CHEMTAX, such as the occurrence of negative contributions to total Chl *a* (Henriksen et al., 2002). CHEMTAX, which uses predefined pigment:Chl *a* ratios, is a powerful and robust approach for the taxonomic classification of phytoplankton assemblages (Mackey et al., 1996; Schlüter et al., 2000; Rodriguez et al., 2002). Nevertheless, only *in vitro* samples are acceptable for HPLC pigment measurement (Jeffrey et al., 1997), which means pigments must be extracted from samples in solvents, such as acetone and methanol (Jeffery et al., 1997). Furthermore, HPLC system should be calibrated with standardized pigments that are subject to decay over short periods of time (< 3 months) (Jeffery et al., 1997).

A better alternative to estimate algal communities is through remote sensing. The ocean color (reflectance) is first acquired by the sensor mounted on a satellite, an aircraft, or some other remote platform. The obtained remote sensing data are processed through inverse models to obtain water quality properties (Figure 2.1). For Case 1 Waters, open ocean water, universal algorithms have been developed and can be expressed as a function of the chlorophyll *a* concentration (IOCCG, 2000). Beside phytoplankton and their by-products which dominate in Case 1 Waters, total suspended solid (TSS) and color dissolved organic matter (CDOM) make up important contributions as well in Case 2 Waters (coastal and inland waters) (Prieur and Sathyendranath, 1981; Babin et al., 2003). The universal algorithms are therefore not appropriate for Case 2 Waters (IOCCG, 2000).

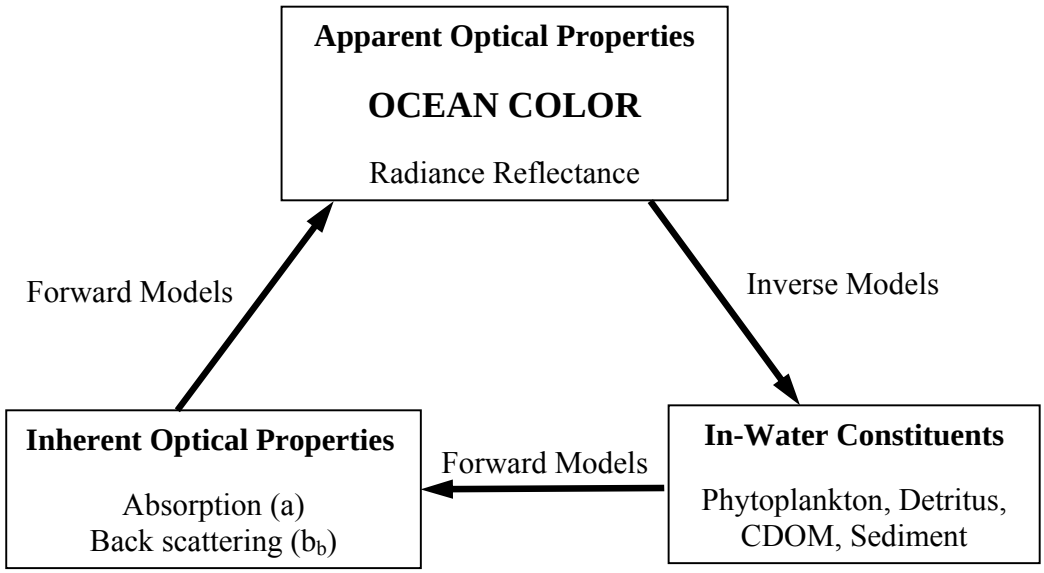

Figure 2.1 Schematic diagram for the interrelationships between apparent optical properties such as color, in-water constituents, and inherent optical properties.

Source: IOCCG (2000)

For Case 2 Waters, an effective alternative to the universal algorithm is to retrieve inherent optical properties (IOPs) from reflectance (IOCCG, 2006) and hence water quality characteristics, including particulate and dissolved contributions (Twardowski et al., 2005). Understanding regional IOP parameterization is critical in building and improving remote sensing systems for Case 2 Waters, as algorithms and/or sensors need to be specific to different water bodies and IOP characters (IOCCG, 2006). For example, MODIS (the Moderate Resolution Imaging Spectroradiometer) is appropriate for monitoring water quality in Tampa Bay, FL (Hu et al., 2004), but not for the New York Harbor (Hellweger et al., 2004). Semi-analytical algorithms have been successful for

modeling the Florida shelf in Key West, Florida (Lee et al., 2002), but not for Tampa Bay due to its high turbidity (Hu et al., 2004).

As a primary IOP, the absorption coefficient, $a(\lambda)$, has been studied worldwide for Case 2 Waters, for example, in Europe coastal waters: English Channel, Adriatic Sea, Baltic Sea, Mediterranean Sea, and North Sea (Babin et al., 2003); in North America: Florida Bay (Gould and Arnone, 1997) and the Northern Gulf of Mexico (D'Sa et al., 2006); in East Asia: Funka Bay in Japan (Sasaki et al., 2005); in South America: Patagonian Shelf-break Front (Ferreira et al., 2009); and, in Australia: Jervis Bay (Phillips and Kirk, 1984).

The total absorption coefficient, $a(\lambda)$, is expressed as

$$a(\lambda) = a_w(\lambda) + a_{ph}(\lambda) + a_{NAP}(\lambda) + a_{CDOM}(\lambda) \tag{2.1}$$

where *w*, *ph*, *NAP*, and *CDOM* represent pure water, phytoplankton, non-algal particles, and color dissolved organic matter, respectively (Prieur and Sathyendranath, 1981; Roesler et al., 1989; Carder et al., 1991). These components are characterized by different spectral absorption features and are present in variable proportions for various water columns (Oubelkheir et al., 2007). The $a_w(\lambda)$ is well studied (Pope and Fry, 1997). The $a_{CDOM}(\lambda)$ spectrum typically fits the exponential function (Jerlov, 1968; Bricaud and Sathyendranath, 1981; Kirk, 1994; Hellweger et al., 2004):

$$a_{CDOM}(\lambda) = a_{CDOM}(\lambda_r) e^{S_{CDOM}(\lambda_r - \lambda)} \tag{2.2}$$

where λ_r (nm) is a reference wavelength, $a_{CDOM}(\lambda_r)$ is the absorption coefficient at λ_r, and S_{CDOM} (nm^{-1}) is the spectral slope of the $a_{CDOM}(\lambda)$ spectrum, which varies between 0.01 and 0.026 nm^{-1} (Kirk, 1994; Hellweger et al., 2004).

The coefficients $a_p(\lambda)$ and $a_{NAP}(\lambda)$ are measured directly, while $a_{ph}(\lambda)$ is obtained by subtracting $a_{NAP}(\lambda)$ from $a_p(\lambda)$. The obtained $a_{ph}(\lambda)$ can then be decomposed into Gaussian curves that reflect (maker) pigments of the phytoplankton present (Hoepffner and Sathyendranath, 1991; Stuart et al., 1998). Based on the specific absorption coefficient (absorbance per unit pigment mass), pigment compositions from Gaussian curves are therefore quantitatively evaluated (Hoepffner and Sathyendranath, 1992; Stuart et al., 1998).

Similar with $a_{CDOM}(\lambda)$, $a_{NAP}(\lambda)$ can be expressed as an exponential function

$$a_{NAP}(\lambda) = a_{NAP}(\lambda_r) e^{S_{NAP}(\lambda_r - \lambda)} \tag{2.3}$$

where λ_r (nm) is a reference wavelength, $a_{NAP}(\lambda_r)$ is the absorption coefficient of non algal particulates at λ_r, and S_{NAP} (nm^{-1}) is the spectral slope of the $a_{NAP}(\lambda)$ spectrum. $a_{CDOM}(\lambda)$ and $a_{NAP}(\lambda)$ impact the accuracy of $a_{ph}(\lambda)$, especially for coastal water (Babin et al., 2003); therefore, properly expressing $a_{CDOM}(\lambda)$ and $a_{NAP}(\lambda)$ is critical.

In situ absorption measurements are essential to improve the accuracy of regional remote sensing and hence water quality studies (Stuart et al., 1998; IOCCG 2006). The variation of $a_{ph}(\lambda)$ is used to estimate the diversity of phytoplankton communities and even detect harmful algal blooms, such as dianoflagellate blooms caused by *Gymnodinium breve* (Millie et al., 1997) and *Alexandrium tamarense* (Leong and

Taguchi, 2006). The spectra of $a_{CDOM}(\lambda)$ and $a_{NAP}(\lambda)$ reflect the their possible sources (Carder et al., 1989; Babin et al., 2003) and are associated with biochemical cycles. The spectra of $a_w(\lambda)$ is constant for a body of water and has been well studied (Smith and Baker, 1981).

Remote sensing has proved useful in water quality studies in the NY/NJ Harbor Estuary, for example, water leaving radiance spectra and chlorophyll concentrations were retrieved from NASA/AVIRIS (airborne visible infrared imaging spectrometer) data (Bagheri et al., 2005), and chlorophyll *a* concentrations and Secchi Depth were estimated from Landsat Thematic Mapper (TM) data (Hellweger et al., 2004). However, characterization of temporal and spatial variation of in situ absorption has not been conducted, and is needed to improve the accuracy of the remote sensing algorithms.

2.4 Summary

This literature review has demonstrated that HABs of significance in the NY/NJ coastal waters include brown tides for the NY/NJ Bight and blooms of diatom and dinoflagellate for the NY/NJ Harbor Estuary. Brown tides negatively impact ecosystems by reducing the plankton which is a base component of the food web. The brown tide alga *Aureococcus anophagefferens* is unique in that it can utilize both organic and inorganic nitrogen, while most other species feed only on organic nitrogen. However, in addition to macronutrients, trace metals are critical to algae growth; yet with the exception of Fe, no other trace metals have been investigated for their impact on algal growth. One aspect of this research is to investigate the relationships between metals and brown tide alga *Aureococcu anophagefferens*.

To mitigate the occurrence of HABs in the NY/NJ Harbor Estuary, monitoring systems for algal blooms are of primary importance for water quality control. Remote sensing has proven to be useful for monitoring blooms. However, because of the complex Case 2 Water in the NY/NJ Harbor Estuary, universal algorithms used for Case 1 Waters are not appropriate. As an alternative, retrieving inherent optical properties from reflectance is applied for Case 2 Waters. To link the water quality and remote sensing data, field work is needed to improve remote sensing algorithms. This type of research provides a temporal and spatial understanding of absorption coefficients for CDOM, phytoplankton, and non-algal particles, as well as their relative contribution to total absorption for the NY/NJ Harbor Estuary. In the next chapter, research objectives and hypotheses are presented.

CHAPTER 3

HYPOTHESES AND OBJECTIVES

This research is focused on investigating the effect of heavy metals on the brown tide alga *Aureococcus anophagefferens* observed in the NY/NJ Bight, and, developing a bio-optical database and approach to rapidly characterize algal composition in the NY/NJ Harbor Estuary. A number of metals serve as micronutrients to algae; however, the affect as a function of concentration and bioavailability on *A. anophagefferens* is not understood (except for iron). The research focuses on addressing sensitivity, toxicity, and bioavailability as well as the effects of resulting blooms on the biochemical cycle of metals. A viable method will allow assessment of water quality characteristics and potential impacts from development of harmful algal blooms. With the onset of HABs, mitigative measures can be implemented prior to the onset of ecosystem consequences. In this research, the following hypotheses are tested:

1. Dissolved Cu, Zn, and Ni at environmentally relevant concentrations can promote *A. anophagefferens* growth. Cd additions will inhibit the growth due to its toxicity and its presence may impede the ability to uptake micronutrients.

2. Heavy metal contamination in coastal waters may be an important factor in the development of brown tide blooms.

3. Brown tide occurrences may significantly impact the fate metal species in coastal waters.

4. A database of *in situ* bio-optical characteristics (absorption vs. water quality) can be developed for obtaining water quality characteristics from absorption spectra in the NY/NJ Harbor Estuary (includes Jamaica Bay, Inner Harbor, and Hudson/Raritan Bay).

5. The bio-optical characteristics vary greatly in the NY/NJ Harbor. Although phytoplankton is the most significant contribution to absorption, CDOM and non-algal particles play important roles also.

The objectives include studies to

1. Evaluate *A. anophagefferens* growth rate, growth inhibition, and toxicity from exposure to dissolved metals.

2. Assess *A. anophagefferens* cellular and intracellular metal distribution to estimate metal sequestration.

3. Estimate the metal biochemical cycling by *A. anophagefferens* blooms.

4. Measure spatial and temporal absorption coefficients for CDOM, phytoplankton, and non-algal particles in the NY/NJ Harbor Estuary.

5. Investigate the variation of absorption spectra and possible pollution sources of CDOM and non-algal particles.

6. Quantitatively analyze algal pigments based on spectra decomposition.

In the next chapter, methods are presented to test the hypotheses and address the objectives.

CHAPTER 4

EXPERIMENTAL METHODS

The current research covers the coastal water of the NY/NJ Bight and the NY/NJ Harbor Estuary. For the brown tide studies in the NY/NJ Bight, the relationship between heavy metals and *A. anophagefferens* is investigated in two experiments: long-term and short-term. The media, measured properties, and analyses are described in this section. For the bio-optical characterization of the NY/NJ Harbor Estuary, the approach reviews sampling and is followed by methods to evaluate bio-optical characteristics, relative measurements, and data analysis.

4.1 Effects of Heavy Metals on *Aureococcus Anophagefferens*

The relationship between heavy metals and *A. anophagefferens* is studied through both long-term and short-term batch experiments conducted in the laboratory following Quality Assurance/Quality Control as described in the 21st Edition of Standard Methods for the Examination of Water and Wastewater (Eaton et al., 2005). The procedures followed for the long-term and short-term experiments are based on standard methods (Fisher et al., 1984; Errécalde and Campbell, 2000) applied in evaluating the effect of metal contaminants on phytoplankton and in this case, *A. anophagefferens*. Long-term studies are conducted to evaluate growth rate, growth inhibition, and toxicity as a function of free ion concentration through three transfer cycles (Nichols et al., 2001). Short-term experiments are used to assess cellular and intracellular metal distribution and metal tolerance mechanism(s) to elevated concentrations of metals over 72 hours of

incubation during the exponential phase (Errécalde and Campbell, 2000; Wang and Wang, 2008; Debelius et al., 2009).

Axenic *Aureococcus anophagefferens* (CCMP 1984) was purchased from the Bigelow Laboratory for Ocean Sciences, Maine, and maintained in artificial seawater media Aquil-Si (Aquil without silicate addition, Appendix A) (1988/1989) in a Thermo Scientific 818 Precision diurnal growth chamber with 12 h:12 h light: dark cycle, 120 μmol/(photons·m^2·s) illumination at 19 ± 0.2 ^oC. Media and cultures were handled in a HEPA (high efficiency particulate air) filtered laminar flow hood. The culture media Aquil-Si were prepared following Price et al. (1988/1989). Briefly, Chelex-100-treated and microwave sterilized synthetic ocean water (SOW, Appendix B) was supplemented with 0.2 μm-filter-sterilized nitrate, phosphate, and vitamin mixture with trace metal addition (containing EDTA (ethylenediaminetetraacetic acid), Fe, Mn, Co, Cu, Zn, and Cd). In control media (Aquil-Si), Cu and Zn ion concentrations were pCu 13.8 and pZn 10.7 (pMe = -log [Me^{2+}]), and Cd and Ni were not added. Throughout this study the metal speciation was calculated with the thermodynamic equilibrium model MINEQL (Westall et al., 1976) with an updated database from Schecher (2001). Polycarbonate bottles (Nalgene®) of 125 ml (long-term and short-term) and 250 ml (short-term) used for culture incubation were cleaned using the procedure outlined by Price et al. (1988/1989): soaked in detergent for 24 h with a distilled water rinse, followed by 1 N HCl soak for 24 h, Milli-Q water rinse, dried in a laminar hood, and stored in sealed plastic containers before use.

The media for the long-term metal studies were prepared by adding equimolar Cd-EDTA, Cu-EDTA, Ni-EDTA, or Zn-EDTA solutions to Aquil-Si containing either 10 or 100 μM EDTA to adjust Cd, Cu, Ni, and Zn concentrations (Table 4.1). The range of $[Me^{2+}]$ used in the study (Table 4.1) was determined by (1) The $[Me^{2+}]$ is not less than that observed in natural coastal water, and (2) Total EDTA for buffering free metal ion concentrations must be less than 500 μM as greater concentrations may be toxic to the culture (Price et al., 1988/1989). To prepare media for short-term radioisotope labeling experiments, radioisotopes ^{109}Cd (6.10 – 61 kBq L^{-1} in 0.5 M HCl), ^{63}Ni (3.53 – 354 kBq L^{-1} in 0.5 M HCl), and ^{65}Zn (3.62 – 36.2 kBq L^{-1} in 0.5 M HCl) (all were from Eckert & Ziegler Isotope Products) were added to heavy-metal-free and EDTA-free Aquil-Si. Ni concentrations in media were further elevated by adding nonradioactive Ni_2SO_4 (Alfa Aesar, > 99.97%). A Cu radioisotope was not obtained for this study. After adding the metals and adjusting the pH to 8.1 ± 0.1, the culture media were equilibrated overnight. The resulting total metal concentrations ranged from 6.51×10^{-10} to 6.50×10^{-9} M for Cd, 1.64×10^{-10} to 1.55×10^{-7} M for Ni, and 6.43×10^{-9} to 6.43×10^{-8} M for Zn, with free metal ion concentrations of $10^{-10.76}$, $10^{-10.26}$, and $10^{-9.76}$ M for Cd^{2+}; 10^{-10}, 10^{-9}, 10^{-8}, and 10^{-7} M for Ni^{2+}; and, $10^{-8.57}$ and $10^{-7.57}$ M for Zn^{2+} (Table 4.1).

4.1.1 Long-term Experiments

The experimental procedure was similar to that in Ahner et al. (1995) and Wei et al. (2003). *A. anophagefferens* was inoculated in the control media (Aquil-Si) and the metal amended media (Aquil-Si with the ranges of Cd^{2+}, Cu^{2+}, Ni^{2+}, or Zn^{2+} concentrations in Section 4.1). After acclimation for two weeks over two sequential transfers and sub-culturing, the mid-exponential growth rate, μ (d^{-1}), was obtained from the third sub-

Table 4.1 Metal Concentrations of Cd, Cu, Ni, and Zn in Experiments and Coastal Waters Where Brown Tides Were Observed. [Me_T] is total metal concentration, [Me′] is total inorganic metal concentration ([Cd′] = [Cd^{2+}] + [CdOHCl(aq)] + [$CdCl^+$] + [$CdCl_3^-$] + [$CdCl_2$(aq)]; [Cu′] = [Cu^{2+}] + [$CuOH^+$] + [$Cu(OH)_2$(aq)] + [$CuCl^+$] + [$CuCO_3$(aq)] + [$Cu(CO_3)_2^{-2}$] + [$CuSO_4$(aq)]; [Ni′] = [Ni^{2+}] + [$NiHCO_3^+$] + [$NiCl^+$] + [$NiCO_3$(aq)] + [$NiSO_4$(aq)]; [Zn′] = [Zn^{2+}] + [ZnOHCl(aq)] + [$ZnCl_3^-$] + [$ZnCl^+$] + [$ZnCl_2$(aq)] + [$ZnCO_3$(aq)] + [$ZnSO_4$(aq)].), and pMe = - log [Me^{2+}].

Metal	Control	Metal concentration in long-term study					Total EDTA	Metal concentration in short-term study (nM)	Metal concentration in coastal waters (nM)
Cd									
[Cd_T]	Not added	30 nM	0.3 μM	3 μM	30 μM			0.65 - 6.5	0.025 - 1.6 [a]
[Cd']	N/A	0.18 nM	1.8nM	17.6 nM	176 nM		100 μM + [Cd_T]	0.65 - 6.5	0.05 - 0.22 [b]
pCd	N/A	11.33	10.33	9.33	8.33			pCd 10.76 - 9.76	11.7 - 11.2 [b]
Cu									
[Cu_T]	20 nM	0.12 μM	1.2 μM	12 μM	120 μM				5 - 51 [a]
[Cu']	0.15pM	8.8 pM	88.1 pM	0.88 nM	8.8 nM		100 μM + [Cu_T]		0.003 - 0.025 [b]
pCu	13.8	12.03	11.03	10.03	9.03				13.7 - 11.7 [b]
Ni									
[Ni_T]	Not added	3 μM	30 μM	30 μM	300 μM		10 μM + [Ni_T] (pNi ≤ 9.23)	0.16 - 155	1 - 90.8 [a]
[Ni']	N/A	9.5 pM	95 pM	0.95 nM	9.5 nM		100 μM + [Ni_T] (pNi ≥ 10.23)	0.16 - 155	0.5 - 64 [c]
pNi	N/A	11.23	10.23	9.23	8.23			pNi 10 - 7	9.5 - 7.4 [d]
Zn									
[Zn_T]	80 nM	6 nM	60 nM	0.6 μM	6 μM	60 μM		6.4 , 64	5 - 72 [a]
[Zn']	47.2 pM	3.5 pM	35.4 pM	0.35 nM	3.54 nM	35.4 nM	100 μM + [Zn_T]	6.4 , 64	0.6 - 26.6 [b]
pZn	10.7	11.8	10.8	9.8	8.8	7.8		pZn 8.57, 7.57	9.5 - 7.9 [b]

[a] Breuer et al. (1999), Clark et al. (2006), Kozelka and Bruland (1998), and Wells et al. (2000). [b] Kozelka and Bruland (1998). [c] [Ni′] = 50 - 70 % of [Ni_T] according to Slaveykova et al. (2009). [d] [Ni^{2+}] is estimated by MINEQL (Westall et al., 1976) based on 0.5 - 64 nM Ni′ in synthetic ocean water (Price et al., 1988/1989).

culturing based on daily measurements of *in vivo* fluorescence (Turner Designs Trilogy fluorometer): $\ln X_t = \mu \cdot t + \ln X_0$, where X_t and X_0 are *in vivo* fluorescence of culture at time t (d) and 0 d, respectively. The control and amended cultures were conducted in triplicate and were set up in parallel. One way analysis of variance (ANOVA) with Tukey's multiple comparison (family error rate 5%) was used to test statistically significant effects of long-term Cd, Cu, Ni, and Zn exposure on *A. anophagefferens* growth rate.

4.1.2 Short-term Experiments

Cultures of *A. anophagefferens* from the exponential phase were collected by gentle filtration (< 120 mm Hg vacuum), briefly rinsed with SOW, and then transferred to radioisotope spiked media to yield an initial cell density of approximately 10^7 cell/mL (large initial biomass was necessary for quantifiable metal uptake or adsorption). The short-term experiments were conducted over 48 h for Cd and 72 h for Ni and Zn. Cultures were set up in triplicate.

The experimental procedure to determine metal uptake was similar to those of Errécalde and Campbell (2000). At time intervals of 6 h, 12 h, 24 h, 48 h, and 72 h, two identical aliquots were withdrawn. Each aliquot was gently filtered through two layers of 0.8 μm and 25 mm polycarbonate membranes (namely, the upper and lower membranes). Only one set of these filters was further rinsed with 5 - 10 mL of 100 μM EDTA (dissolved in SOW). The upper and lower membranes from each filtration were placed into separate scintillation vials containing 6 ml of Ready Value cocktail (Beckman), and the radioactivity was determined with a liquid scintillation counter (LS 6500, Beckman). The total radioactivity in culture suspensions was also determined to ensure no significant

loss of radioactivity during the short-term incubation. Liquid scintillation counting times were such that counting errors were generally < 2%. At each sampled time, cell density was estimated using a coulter counter (Multisizer^{TM} 3, Beckman). External quench curves (empirical relationship between H number and count efficiency) were developed for each radioisotope, which were used to convert cpm (counts per min) to dpm (disintegration per min).

Metal concentrations associated with the total cellular and intracellular (Me_{cell} and Me_{int}, respectively) at each sampling time were calculated:

$$Me_{cell} = \frac{R_1 - R_2}{R_3 V} \times \frac{C}{N} \tag{4.1}$$

$$Me_{\text{int}} = \frac{R_1^{'} - R_2^{'}}{R_3 V} \times \frac{C}{N} \tag{4.2}$$

where R_1 and R_2 are radioactivity on upper and lower filters, respectively, without EDTA rinse (dpm), $R_1^{'}$ and $R_2^{'}$ are those with EDTA rinse (dpm), R_3 is the radioactivity of the 1 mL culture suspension (dpm), V is the volume of culture filtered (mL), C is the total metal concentration (M), and N is the cell density (cell/L). Me_{cell} and Me_{int} are in units of mole of metal/cell. Adsorbed metal (Me_a) concentrations were calculated by subtracting Me_{int} from Me_{cell}. The steady state concentrations were determined based on an ANOVA test of logarithmic Me_{int} or Me_a as a function of time with Tukey's multiple comparison at a family error rate of 5%.

4.2 Bio-optical Characteristics of the New York / New Jersey Harbor Estuary

The database of bio-optical characteristics for the NY/NJ Harbor Estuary in this research is focused on the absorption coefficient, spatial-temporal observations and variability, and contributions from phytoplankton, non-algal particles, and CDOM determined by spectrophotometry measurements. The spectra of phytoplankton are then decomposed into Gaussian bands representing pigment concentrations, which are used to build correlations with standards from HPLC analysis.

4.2.1 Sampling

Sampling was conducted during six cruises (two days of each cruise) from August 2008 to June 2009 in the NY/NJ Harbor Estuary, which includes the Inner Harbor, Jamaica Bay, and Hudson/Raritan Bay (Figure 4.1). In total, 29 stations were visited and 123 samples were collected in cooperation with the New York City Department of Environmental Protection (NYCDEP) and the Passaic Valley Sewerage Commission (PVSC). At a 1 m depth below the water surface, 2 L of seawater were collected with Niskin bottles (26 stations) or polyethylene containers (3 stations), and stored at the same temperature as the sea surface in amber high density polyethylene (HDPE) bottles cleaned using a detergent-water and Milli-Q water rinse. At the same time, hydrographic data were collected with a SBE model 11 Plus CTD deck unit (SeaBird Inc). After sampling, water samples were processed within hours at the laboratory. Water quality and associated conditions collected during sampling are listed in Appendix C (provide by NYCDEP and PVSC), which include latitude, longitude, water depth of sampling, salinity, temperature, dissolved O_2, conductivity, pH, dissolved organic carbon (DOC), total Kjeldahl nitrogen (TKN_N), NH_3_N, (NO_3 + NO_2)_N, total P, ortho-P, TSS, Chl *a*,

SiO_2, fecal coliform, sigma-t (density of a sea-water sample as a function of temperature and salinity), wind, and current. NYCDEP has been conducting measurements since 1985 and the data are partially available online (http://www.nyc.gov/html/dep/html/news/hwqs.shtml).

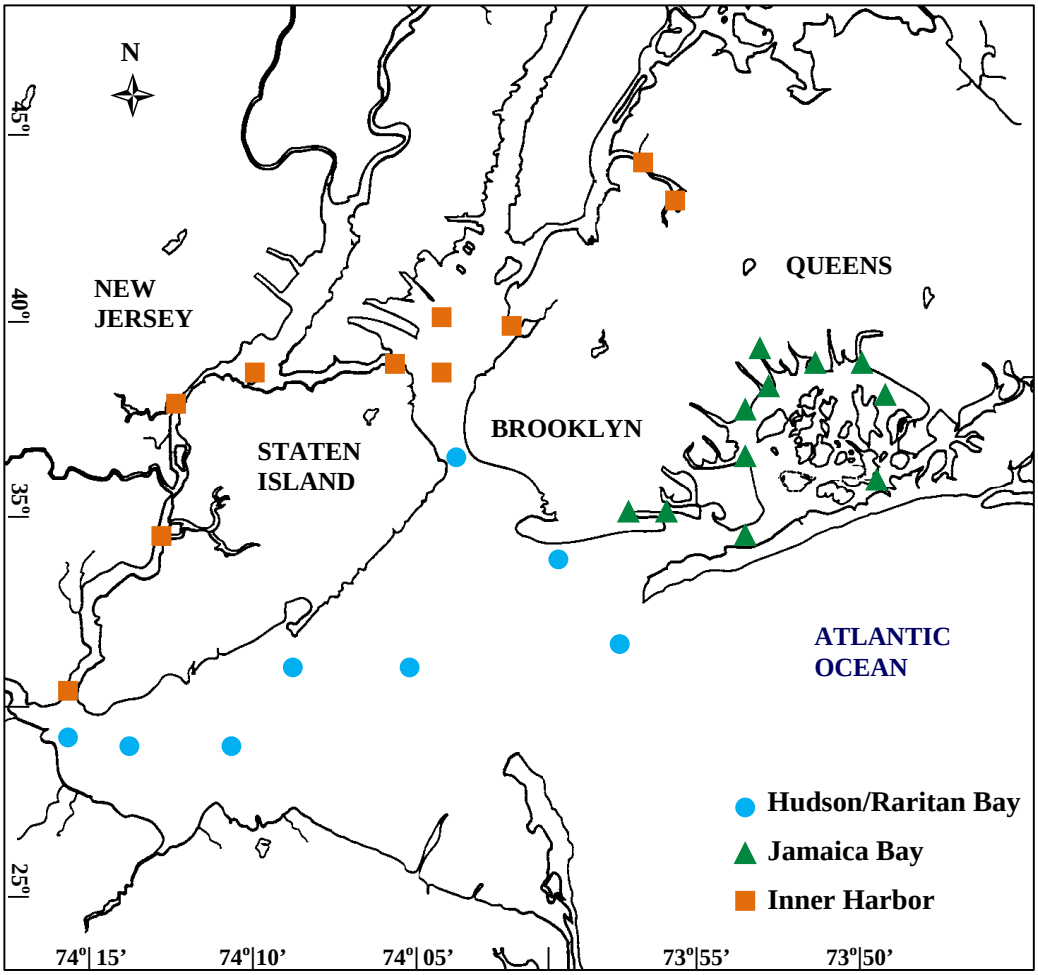

Figure 4.1 Sampling locations at New York / New Jersey Harbor Estuary including Hudson/Raritan Bay, Jamaica Bay, and Inner Harbor.

4.2.2 CDOM Absorption Coefficient

Samples for CDOM measurements were prepared according to Mitchell et al. (2000). Briefly, polycarbonate membranes (0.2 μm pore size, Nuclepore, Whatman®) were soaked in 10% HCl (ACS) for 15 min and rinsed with Milli-Q water three times. Qorpak bottles were soaked in dilute detergent, rinsed with distilled water, then soaked in 10% HCl followed by a final rinse with ample Milli-Q water. The acid cleaned Qorpak bottles were then heated at 450 ^{o}C for 4 - 6 h to remove residual organics. Caps of the Qorpak bottles were soaked in 10% HCl, rinsed with Milli-Q water five times, and finally dried at 70 ^{o}C for 4 - 6 h. Seawater samples were then filtered through pretreated polycarbonate membranes into 100 ml clear Qorpak bottles under low vacuum (~120 mm Hg). The absorbance of the filtered seawater was measured in a 10 cm length quartz cuvette (rinsed with 10% HCl, Milli-Q water, and sample) between 350 and 750 nm with 1 nm increments using a spectrophotometer (Agilent 8453). Milli-Q water was used as reference. The measured optical absorbance, OD_{CDOM} (λ), was converted to the absorption coefficient, a_{CDOM} (λ) (Figure 4.2), by

$$a_{CDOM}(\lambda) = \frac{2.303(OD_{CDOM}(\lambda) - OD_{CDOM}(\lambda_{null}))}{l} \tag{4.3}$$

where l is the light path length through the liquid sample, 0.1 m, and λ_{null} is the null point where CDOM absorption is negligible, averaged from 685 to 690 nm (Babin et al., 2003). Because of the chemical complexity of CDOM, the concentration is expressed using the absorption coefficient at some reference wavelength, typically either 355 nm, 375 nm, or 440 nm (Kirk, 1994). Here, absorption at 440 nm was used to analyze the CDOM spectra.

The slope of CDOM spectra, S_{CDOM}, was then obtained from a linear log-transformed regression between 350 and 500 nm based on Eq. (2.2)

$$a_{CDOM}(\lambda) = a_{CDOM}(\lambda_r) e^{S_{CDOM}(\lambda_r - \lambda)} \quad (2.2)$$

where, $a_{CDOM}(\lambda_r)$ is the absorption coefficient of CDOM (m^{-1}) at reference wavelength, λ_r, 440 nm.

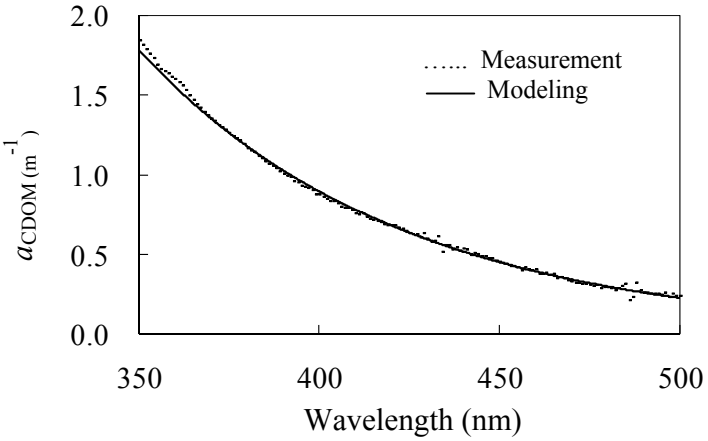

Figure 4.2 Example of CDOM absorption coefficient measurement

4.2.3 Particle Dry Weight

The total suspended solids (TSS) concentration was used to determine the particle dry weight according to Standard Methods 2540D (Eaton et al., 2005). GF/F filters (25 mm, Whatman) were rinsed with 20 ml distilled water three times, dried at 103 - 105 ^{o}C for 1 h, and weighed after cooling in desiccators. Subsequently, seawater (≤ 200 mL) was gently (~120 mm Hg vacuum) filtered through a prepared GF/F filter, which was then rinsed briefly with 10 ml distilled water three times. The filter with collected particles was dried

at least 1 h at 103 to 105 ^{o}C and weighed. TSS concentration (mg/L) was calculated from the difference between the two weights and volume of seawater filtered.

4.2.4 NAP and Phytoplankton Absorption Coefficients

Seawater (100 mL - 600 mL) was gently (~120 mm Hg vacuum) filtered through a GF/F filter (25 mm, Whatman) pre-wet with 0.2 μm filtered seawater. Filters with particles were then wrapped in aluminum foil, labeled, and stored in liquid nitrogen up to 2 months before analysis. The particulate absorption coefficient was measured following the transmission and reflection (T-R) method developed by Tassan and Ferrari (2002). The measurement was conducted between 400 and 750 nm with 1-nm increments using a dual beam spectrophotometer (Perkin Elmer, Lambda 9) equipped with a 60-mm integrating sphere. The spectrophotometer was calibrated using Holmium Oxide filters. Absorbance of the particles on the filter (OD_s) is determined as

$$OD_s(\lambda) = \log\left(\frac{1}{1 - a_s(\lambda)}\right) \tag{4.4}$$

where, $a_s(\lambda)$ is the absorption coefficient due to normally incident parallel light beam on a single pathway, and is expressed as

$$a_s(\lambda) = \frac{1 - \rho_T + R_f(\rho_T - \rho_R)}{1 + R_f \rho_T \tau(\lambda)} \tag{4.5}$$

where, ρ_T is the ratio of transmittance of the sample filter to that of the reference filter (GF/F filter hydrated with Milli-Q water) in transmission mode, ρ_R is the ratio of reflectance of the sample filter to that of the reference filter measured in reflectance mode, R_f is the reflectance of the reference filter in reflectance mode, and $\tau(\lambda)$ is the factor that accounts for radiation backscattered by the filter on the particle deposit and is diffuse radiation. $\tau(\lambda)$ is calculated by

$$\tau(\lambda) = 1.15 - 0.17 OD_{tr}(\lambda)^* \tag{4.6}$$

where, $OD_{tr}(\lambda)^* = OD_{tr}(\lambda) - 0.5 OD_{tr}(750)$, and $OD_{tr}(\lambda)$ is the optical density measured in transmission mode. Because of path length amplification, OD_s is converted to OD_{sus}, optical density of the particle suspension, by the equation (Tassan and Ferrari, 2002)

$$OD_{sus} = (0.423 \pm 0.0125)\, OD_s + (0.479 \pm 0.06)\, OD_s^2 \tag{4.7}$$

The absorption coefficient, a_p (Figure 4.3), for total particulate is obtained with

$$a_p(\lambda) = \frac{2.303 OD_{SUS}(\lambda)}{X} \tag{4.8}$$

where, X is the ratio of the filtered seawater volume to the filter clearance area.

The absorption coefficient of NAP, $a_{NAP}(\lambda)$ (Figure 4.3), was determined after at least 30 minutes depigmentation in a sodium hypochlorite solution with 0.12% active chloride (Ferrari and Tassan, 1999). The measurement and data processing were the same

as that for total particulate describe above. Similar with CDOM spectra, NAP spectra were analyzed using 440 nm as the reference wavelength. The slope of non-algal particles, S_{NAP}, is obtained from Eq. (2.3)

$$a_{NAP}(\lambda) = a_{NAP}(\lambda_r)e^{S_{NAP}(\lambda_r - \lambda)} \tag{2.3}$$

where, $a_{NAP}(\lambda_r)$ is the absorption coefficient of non-algal particles at reference wavelength, λ_r, 440 nm. The phytoplankton absorption coefficient is obtained by subtracting a_{NAP} from a_P in the following equation and as depicted in Figure 4.3:

$$a_{ph}(\lambda) = a_p(\lambda) - a_{NAP}(\lambda). \tag{4.9}$$

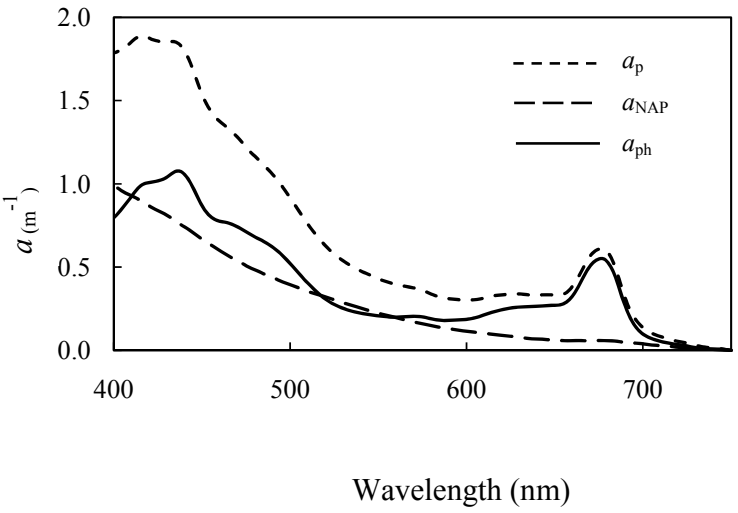

Figure 4.3 Example of particle absorption coefficient measurement.

4.2.5 HPLC Pigment Analysis

Pigment concentrations were measured using high performance liquid chromatography (HPLC) according to the procedure of Wright et al. (1991) (Table 4.2). Seawater filtration and particulate sample storage procedures were the same as those in particle absorption measurements described in Section 4.2.4. To extract pigment, filters were retrieved from liquid nitrogen, extracted using an ultrasonic bath with 3 ml acetone for 30 minutes, and the resulting mixture stored at -20^{o}C for 24 h. The extraction mixtures were then centrifuged for 3 min at 700 × g, and the supernatant was filtered through 0.45 μm PTFE syringe filters (Acrodisc). After adding 0.1 mL of Milli-Q water to 1 mL filtered supernatant, a 100 μL sample was injected into the HPLC system (Thermo Finnigan Suvery) equipped with a reversed phase column, Spherisorb ODS-2, 25 cm × 4.6 mm (Waters). Data were collected by a photodiode array detector (Thermo Finnigan Suvery) set at 436 and 450 nm and analyzed using Xcalibur^{TM} software. Based on the pigment composition of the dominant algal groups in the area (Table 4.3), pigment standards for calibration were purchased from Sigma-Aldrich (chlorophyll *a*, chlorophyll *b*, and ß-carotene) and DHI (Chlorophyll c_2, diadinoxanthin, fucoxanthin, and peridinin). Chl *a* represents the sum of chlorophyll *a* and chlorophyll *a* isomer and epimer.

4.2.6 Spectra Decomposition

A curve fitting program (Hoepffner and Sathyendranath, 1991; Stuart et al., 1998) was used to decompose phytoplankton spectra into as much as 13 Gaussian bands. The input specifications for spectra decomposition include: (1) measured phytoplankton spectra; and, (2) the band center and bandwidths at the half height. The program was then setup to run a maximum of 25 iterations per spectrum or terminate earlier only if the convergence

criterion had been met. The output includes (1) retrieved phytoplankton spectra; and, (2) modified band center and bandwidths at half heights. Additional details of the analysis are provided in Chapter 8.

Table 4.2 HPLC Eluent Gradient Program

Time (min)	Solvents			Conditions
	%A	%B	%C	
0.0	100	0	0	Linear
2.0	0	100	0	Linear
2.6	0	90	10	Linear
13.6	0	65	35	Linear
18.0	0	31	69	Hold
23.0	0	31	69	Linear
25.0	0	100	0	Linear
26.0	100	0	0	Hold
34.0	100	0	0	Inject

A: methanol : 0.5 M ammonium acetate (80:20 v:v, pH 7.2)
B: Acetonitrile: water (90:10 v:v)
C: 100% ethyl acetate

Source: Weight et al. (1991).

Table 4.3 Pigment Composition of Dominant Algal Classes (divisions) in the New York / New Jersey Harbor Estuary

Pigments	Classes (Division)	
	Diatom	Dinoflagellate
Chlorophyll *a*	●	●
Chlorophyll c_1	●	
Chlorophyll c_2	●	●
ß-carotene	▲	▲
Diadinoxanthin	●	●
Diatoxanthin	▲	▲
Dianoxanthin		◆
Fucoxanthin	●	
P-457+P-468		▲
Peridinin		●
Peridininol		▲
Pyrhoxanthin		▲

●: major pigment (>10%);
◆ : minor pigment (1-10%);
▲: trace pigment (<1%) of the total chlorophylls or carotene.

Sources: Marshall and Cohn (1987) and Gould et al. (1997).

CHAPTER 5

EFFECTS OF CD, CU, NI, AND ZN ON BROWN TIDE ALGA *AUREOCOCCUS ANOPHAGEFFERENS*

In this chapter, results are presented on effects of *Aureococcus anophagefferens* exposure to heavy metals which cause brown tide blooms in the NY/NJ Bight. Based on the *A. anophagefferens* growth from long-term exposure and metal uptake in short-term exposure, the implications on *A. anophagefferens* are addressed.

5.1 *Aureococcus Anophagefferens* Growth Response to Long-term Cd, Cu, Ni, and Zn Exposure

A. anophagefferens grew at 0.50 ± 0.01 d^{-1} in control media (Aquil-Si) containing pCu (-log[Cu^{2+}]) 13.8, pZn 10.7, and no Cd and Ni. Long-term exposure to Cd, Cu, Ni, or Zn resulted in a number of effects including growth enhancement, inhibition, and no significant impact when studied in parallel with control cultures (Figure 5.1). Specifically, Cu addition at pCu 11.03 stimulated *A. anophagefferens* growth by 11% compared to the control. More interestingly, Ni addition dramatically promoted *A. anophagefferens* growth, which increased by 37% at a pNi of 11.23 and by 68 - 77% for pNi from 10.23 to 8.23. *A. anophagefferens* tolerated moderately elevated concentrations of Cd and Zn up to pCd 10.33 and pZn 9.8 with growth rates comparable to that of the control cultures. With further increases in Cd, Cu, and Zn, growth inhibition was observed relative to the control cultures (Figure 5.1): 21% and 67% at pCd 9.33 and 8.33, respectively; 11% and 100% at pCu 10.03 and 9.03, respectively; and, 16% at pZn 8.8 - 7.8. All differences observed were statistically significant using Tukey's multiple comparison with one way analysis of variance (ANOVA) ($p < 0.05$).

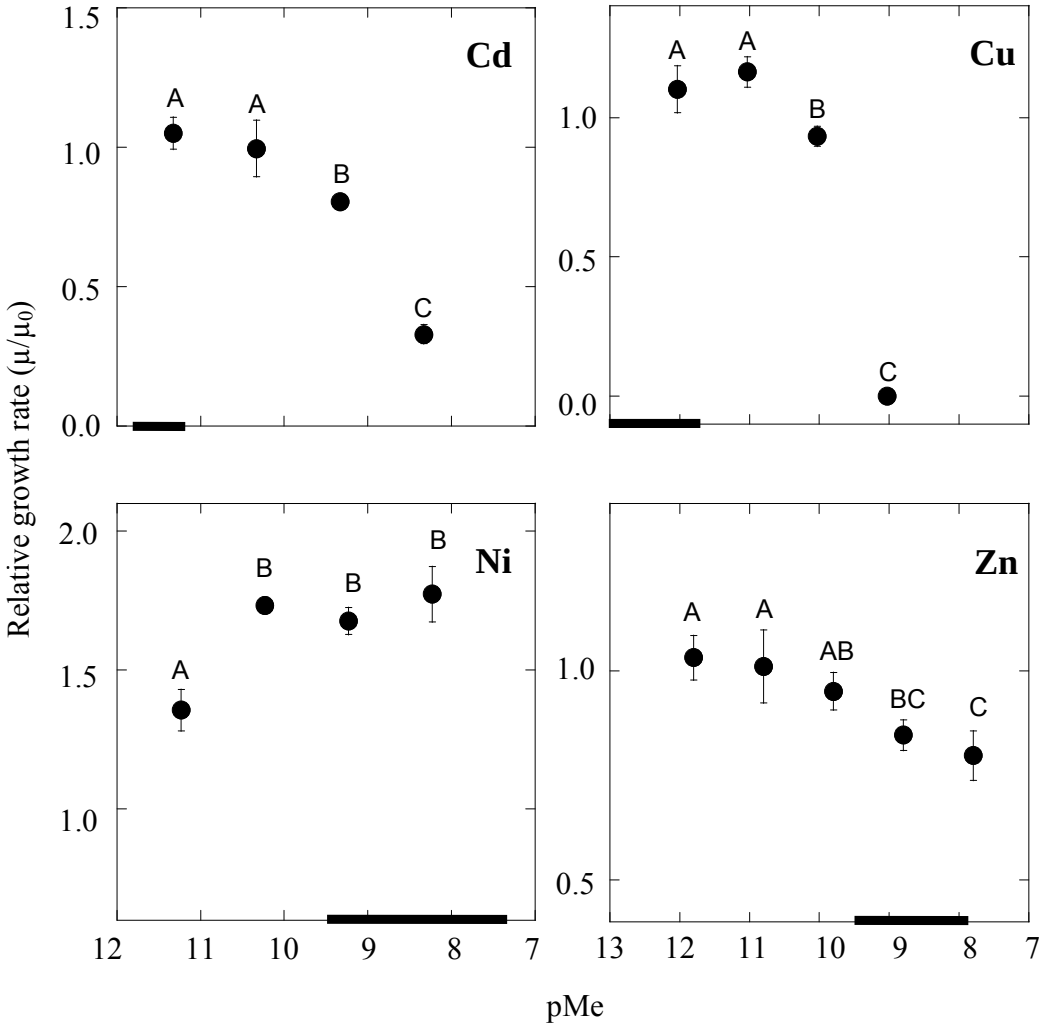

Figure 5.1 Relative growth rate (μ/μ_0) of *Aureococcus anophagefferens* as a function of free ion concentration (pMe = - log[Me]) in Aquil-Si during 3rd sub-culturing. μ is the growth rate while μ_0 is the growth rate of control. In the control, pCu = 13.8, pZn = 10.7, and there is no addition of Cd and Ni. Bold lines on X-axis reflect the range of pMe in natural seawater (listed in Table 4.1). Letters (A, B, and C) above the symbol signify a significant difference ($p < 0.05$) by ANOVA analysis. Error bars represent the standard deviations from triplicate cultures.

5.2 Heavy Metal Bioaccumulation in *Aureococcus Anophagefferens*

During short-term metal exposure, *A. anophagefferens* continued to grow exponentially with rates comparable to the control cultures (data not shown). The metal concentration associated with the total cell (Me_{cell}) includes intracellular (Me_{int}) and adsorbed (Me_a) ones. Cd_{int} increased with time and reached steady state at 24 - 48 h (Figure 5.2 a), while Cd_a plateaued at 12 - 24 h for pCd 10.76 and 10.26, and 24 - 48 h for pCd 9.76 (Figure 5.2 b). Steady state Ni_{int} was reached at 48 - 72 h for pNi 10, and 6 - 72 h for pNi 9 - 7 (Figure 5.2 c). However, steady state Ni_a was reached at 24 - 72 h for pNi 10 and 9, and at 48 - 72 h for pNi 8 and 7 (Figure 5.2 d). The steady state Ni_{int} may be reached more rapidly if the external Ni^{2+} concentration is greater, suggesting that uptake may be kinetically controlled: Ni^{2+} internalization is a relatively rapid process as compared to binding to the Ni^{2+} ion channel (Hudson, 1998). Steady state concentrations of Zn_{int} were observed during the entire 6 - 72 h as 0.033 and 0.094 amol/cell for additions of pZn 8.57 and 7.57, respectively (Figure 5.2 e) (amol = 10^{-18} moles). On the other hand, at the lower end of the initial Zn^{2+} concentration (pZn 8.57), Zn_a increased with time and reached a plateau at 24 - 48 h then decreased slightly at 72 h. At the greater end of the initial Zn^{2+} concentrations (pZn 7.57), Zn_a increased monotonically with time and did not reach a steady state within 72 h.

Once the concentration was invariant with time, the associated data were fit with the Langmuir adsorption isotherm. Total dissolved Cd, Ni, and Zn concentrations in the culture media remained relatively constant (> 98 % of initial concentration) throughout the short-term incubation; therefore in metal bioaccumulation models the initial metal concentrations added to solution are used.

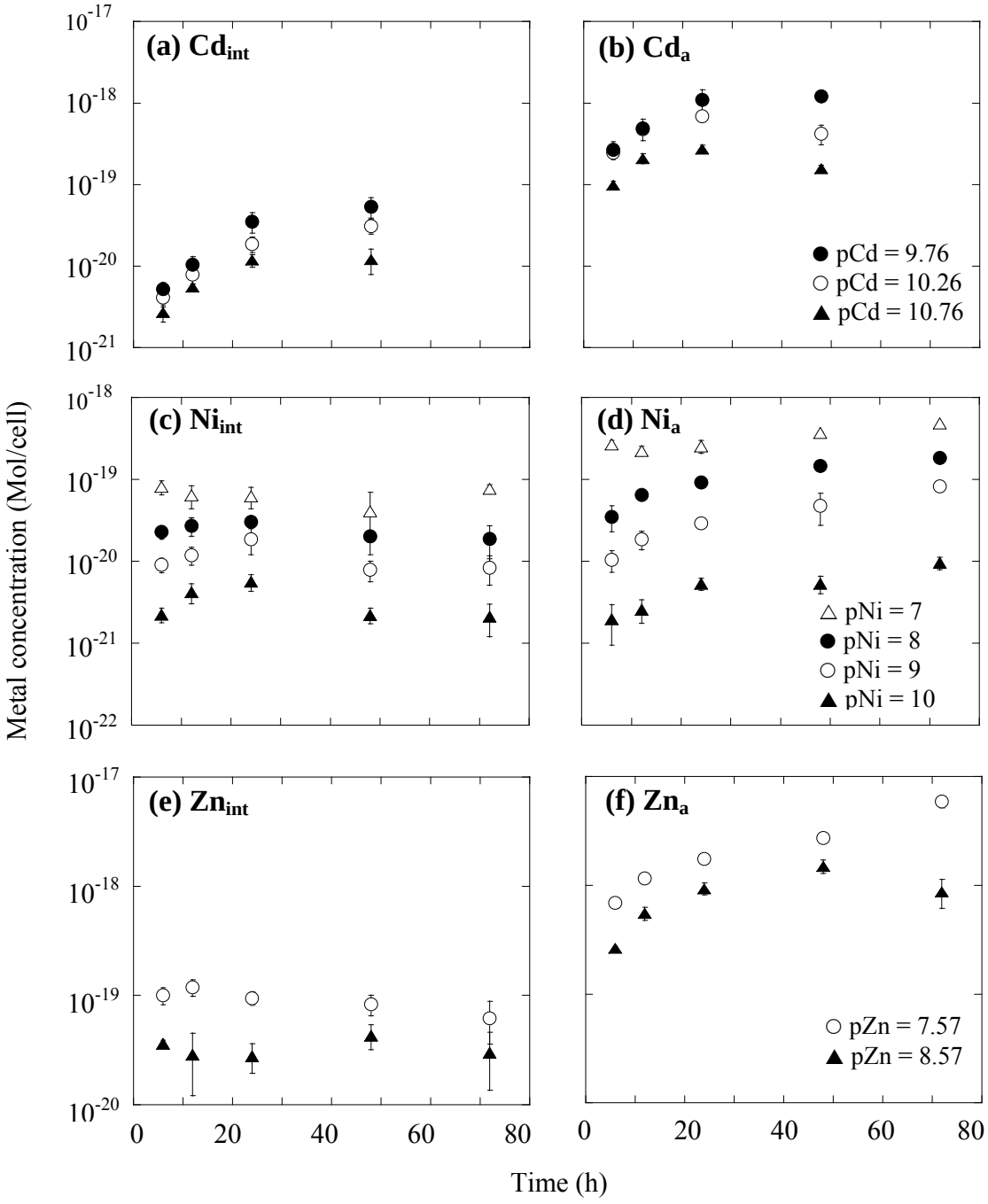

Figure 5.2 Intracellular (Me_{int}) and adsorbed (Me_a) metals (mol/cell) as a function of time during short-term exposure. The media were Aquil-Si without EDTA and without trace metal mixture. Error bars represent the standard deviations from triplicate cultures.

Intracellular (non-EDTA extractable) metal concentration, [Me_{int}] (mol/cell), is calculated and modeled as:

$$[Me_{\text{int}}] = [Me_{\text{int, max}}] \frac{K_{\text{int}}[Me^{2+}]}{1 + K_{\text{int}}[Me^{2+}]} \tag{5.1}$$

where [$Me_{int, max}$] is the maximum intracellular metal concentration (mol/cell), [Me^{2+}] is the equilibrium free metal ion concentration (M), and K_{int} (L/mol) is the average binding constant to the transport sites on the algal membrane.

Similarly, adsorbed (EDTA extractable) metal, [Me_a] (mol/cell), is expressed as

$$[Me_a] = [Me_{a,\max}] \frac{K_a[Me^{2+}]}{1 + K_a[Me^{2+}]} \tag{5.2}$$

where [$Me_{a, max}$] is the maximal adsorbed metal concentration (mol/cell), and K_a (L/mol) is the average binding constant for adsorption.

The overall *A. anophagefferens* cell associated metal quantity, [Me_{cell}] (mol/cell), is sum of [Me_a] and [Me_{int}] and therefore calculated as

$$[Me_{cell}] = [Me^{2+}]\left(\frac{K_{\text{int}}[Me_{\text{int,max}}]}{1 + K_{\text{int}}[Me^{2+}]} + \frac{K_a[Me_{a,\max}]}{1 + K_a[Me^{2+}]}\right) \tag{5.3}$$

[$Cd_{int, max}$] and [$Cd_{a, max}$] were 0.20 and 2.06 amol/cell, respectively, and the binding constants, K_{int} and K_a, were 1.79×10^9 and 7.18×10^9 L/mol, respectively (Table 5.1, Figure 5.3) for Cd. The maxima for Ni were found to be 0.079 and 0.514 amol/cell for

[$Ni_{int,\ max}$] and [$Ni_{a,\ max}$], respectively, with binding constants, K_{int} and K_a, of 4.76×10^7 and 4.88×10^7 L/mol, respectively (Table 5.1, Figure 5.3). The observed [$Zn_{int,\ max}$] and [$Zn_{a,\ max}$] during the 72 h exposure were 1.2 and 2.7 amol/cell for pZn 8.57 and 7.57, respectively (Figure 5.2 f). Because of limited data, Zn bioaccumulation is not modeled using the Langmuir isotherm. The cell associated metal concentrations, [Me_{cell}], is therefore expressed as:

$$[Cd_{cell}] = [Cd^{2+}]\left(\frac{3.58\times10^{-8}}{1+1.79\times10^{9}[Cd^{2+}]} + \frac{1.48\times10^{-6}}{1+7.18\times10^{9}[Cd^{2+}]}\right) \quad (5.4)$$

$$[Ni_{cell}] = [Ni^{2+}]\left(\frac{3.69\times10^{-10}}{1+4.76\times10^{7}[Ni^{2+}]} + \frac{1.48\times10^{-9}}{1+4.88\times10^{7}[Ni^{2+}]}\right) \quad (5.5)$$

Table 5.1 Langmuir Isotherm for Metal Bioaccumulation in *Aureococcus Anophagefferens*

	$Me_{in,\ max}$ (amol/cell)	$Me_{a,\ max}$ (amol/cell)	K_{int} (L/mol)	K_a (L/mol)
Cd	0.20	2.06	1.79×10^9	7.18×10^9
Ni	0.079	0.514	4.76×10^7	4.88×10^7

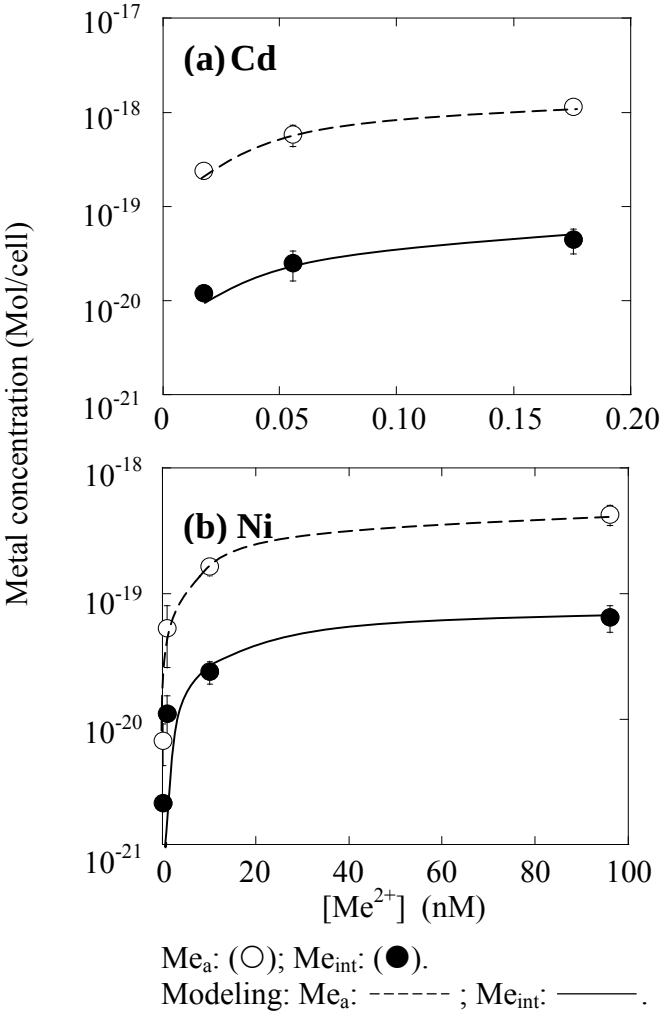

Figure 5.3 Langmuir isotherms (adsorbed Me_a and intracellular Me_{int} (mol/cell)) in *Aureococcus anophagefferens* as a function of free metal ion concentration, $[Me^{2+}]$ (nM). Aquil-Si media was applied without EDTA and without trace metal mixture. Error bars represent one standard deviation from triplicate cultures.

The ratios of [Me_{int}] to [Me_a] are compared for Cd, Ni, and Zn. The ratio of [Zn_{int}] to [Zn_a] was on the order of 3% at initial pZn 8.57 - 7.57 based on direct measurements. For Cd and Ni the [Me_{int}]/[Me_a] can be estimated from the Langmuir isotherm model results. For example, the ratio of [Me_{int}]/[Me_a] at any given [Me^{2+}] can be calculated by [Me_{int}]/[Me_a] = [$Me_{int,\ max}$]/[$Me_{a,\ max}$] and was approximately 5% for pCd << 9.25 and 15% for pNi << 7.68.

5.3 Implication of Metal Effects on *Aureococcus Anophagefferens*

One hypothesis in this research was that heavy metal contamination in coastal waters may be an important factor in the development of brown tide blooms. Therefore, the degree to which heavy metals may be sequestered by brown tide blooms was studied. Cd, Cu, Ni, and Zn concentrations in U.S. Northeast coastal waters (i.e. Peconics Estuary (Breuer et al., 1999), Great South Bay, NY (Clark et al., 2006), and Narrananestt Bay, RI (Kozelka and Bruland, 1998; Wells et al., 2000) with brown tide bloom occurrence were reported at pCd 11.7 - 11.2, pCu 13.7 - 11.7, pNi 9.5 - 7.4, and pZn 9.5 - 7.9 (Table 4.1). *A. anophagefferenss* tolerated Cd and Cu up to pCd 10.33 and pCu 11.03 without growth inhibition. Yet at pZn 8.8 - 7.8 growth inhibition of 16% was found. Brown tide algae growth would likely not be affected by Cd and Cu and only slightly inhibited by Zn concentrations observed in coastal waters. However, Ni addition promoted *A. anophagefferens* growth rate up to 77% with pNi as great as 8.23 in laboratory culture experiments, suggesting that brown tide alga may benefit substantially from elevated Ni levels in these coastal waters.

If other algae species are sensitive to Cd, Cu, Ni, and Zn concentrations found in waters with brown tide blooms, metal contamination may promote a niche for *A. anophagefferens* to grow. To compare metal sensitivity of *A. anophagefferens* with other marine microalgae species, the medium effective concentration EC_{50} (Me^{2+}) from long-term exposure, which reduces 50% of control growth rate, was calculated using the logistic model:

$$Y = \frac{c}{1 + e^{b(X-a)}} \tag{5.6}$$

where Y is inhibition (% of control value), c is the control (= 100%), a is log EC_{50} (M), b is the slope, and X is logarithmic free metal ion concentration (M).

A. anophagefferens EC_{50} (Cd^{2+}) was $10^{-8.73}$ M, indicating sensitivity to cadmium compared to many other marine algal species: 96-h EC_{50} (Cd^{2+}) for two common marine phytoplankton *Thalassiosira weissflogii* (diatom) and *Prorocentrum minimum* (dinoflagellate) grown in Aquil were $10^{-6.9}$ - $10^{-5.8}$ M and $10^{-6.0}$ - $10^{-5.2}$ M, respectively (Miao and Wang, 2006). Payne and Price (1999) studied eleven marine species representing five classes and reported the long-term (at least thirty generations) EC_{50} (Cd^{2+}) varied from $10^{-6.23}$ M for *Emiliania huxleyi* to $10^{-8.79}$ M for Synechococcus *sp* in Aquil. Thus *A. anophagefferens* sensitivity to cadmium is comparable to cyanobacteria *Synechococcus sp*, while it is much more sensitive than the diatom, dinoflagellate, or cocolithophore *E. huxleyi*. As a non-essential element, cadmium sensitivity may be related to the algae cell's capability to detoxify Cd by inducing phytochelatin synthesis or Cd efflux (Ahner and Morel, 1995; Lee et al., 1996; Wei et al., 2003).

EC_{50} (Cu^{2+}) for *A. anophagefferens* was $10^{-9.86}$ M, suggesting *A. anophagefferens* is rather insensitive to copper compared with many other species. Brand et al. (1986) conducted an extensive study of 38 marine phytoplankton species in nitrilotriacetic acid (NTA) buffer system, cyanobacteria were most sensitive with an EC_{50} (Cu^{2+}) of $10^{-10.88}$ M after 4 - 5 weeks exposure, and the diatoms were least sensitive with an EC_{50} (Cu^{2+}) of $10^{-10.04}$ M. Relatively *A. anophagefferens* is therefore much more tolerant of copper than cyanobacteria, and its insensitivity to copper is comparable to (or even slightly more insensitive than) that of the diatoms. As a micronutrient, Cu plays an important role in respiratory and the photosynthetic systems where it is a component of plastocyanin which can substitute for the iron-containing cytochrome C6 (Raven et al., 1999). However, at elevated concentrations copper affects photosynthetic electron transport on the reducing side of photosystem I and the oxidizing side of photosystem II (Miao et al., 2005).

The extrapolated EC_{50} (Zn^{2+}) was $10^{-5.96}$ M for *A. anophagefferens*. This value is comparable to many algae in previous studies, such as $10^{-5.28}$ M for a phytoplankton population studied from the Seine River, France (Seidl et al., 1998). Zn acts as a cofactor in numerous enzymes: carbonic anhydrase (CA), deoxyribonucleic acid (DNA), and alkaline phosphatase (AP) (Sunda, 2006). Nevertheless elevated Zn^{2+} concentrations impact the enzymatic activity of, for example, protochlorophyllide reductase involved in the reduction of protochlorophyll to chlorophyll (Miao et al., 2005).

A. anophagefferens growth inhibition with Ni addition was not observed in this study. In contrast, addition of $10^{-11.23}$ to $10^{-8.23}$ M Ni^{2+} stimulated *A. anophagefferens* growth. Although there is considerable literature on the toxicity of nickel to algae (Förstner et al., 1979; Sunda, 2006), Ni has been identified as an essential cofactor in

both urease and Ni-superoxide dismutase (Ni-SOD) (Dupont et al., 2010). Baker et al. (2009) demonstrated that ureas is an important nickel-containing enzyme in *A. anophagefferens*, and Gobler et al. (2011) recently confirmed three nickel-containing ureas in this organism. Furthermore, there are more nickel-containing enzymes in *A. anophagefferens* as compared to other similar phytoplankton (Gobler et al., 2011), which may provide a niche for *A. anophagefferens* blooms in nickel contaminated coastal water. Because nitrate (NO_3^-) as opposed to urea was used as the nitrogen source in this study, the promotion of *A. anophagefferens* growth with elevated Ni^{2+} may due to Ni-SOD as well. The activation of Ni-SOD may provide the cell additional protection from oxidative stress inherent in oxygenic photosynthesis and aerobic respiration. Dupont et al. (2008, 2010) found that Ni-SOD tends to lead to an obligatory need of Ni to maintain maximum growth rates, as was observed in most marine species of *Synechococcus* and *Prochlorococcus*.

A. anophagefferens is comparable to cyanobacteria in its sensitivity to cadmium, and is much more susceptible than diatoms, but given the relatively low concentrations of cadmium in coastal waters it would not actually exert growth inhibition. Furthermore, *A. anophagefferens* is comparable to the diatoms in its resistance to copper toxicity (and is much more tolerant than that of the cyanobacteria), which allows it to survive in coastal waters (Table 4.1). This brown tide alga is likely to benefit from nickel contamination found in coastal waters. However, its sensitivity to zinc is comparable to many other algal species; dissolved zinc in coastal water may slightly inhibit its growth. These factors may have contributed to *A. anophagefferens* survival, growth, and bloom initiation in coastal waters.

Algal blooms in shallow coastal bays may substantially affect metal bioavailability and biogeochemical cycling. The short-term experimental results along with the modeling can be used to estimate sequestration of Cd and Ni in brown tide bloom waters. A presumptive Category 3 brown tide bloom of 10^6 cell/mL would sequester 0.031 - 0.104 nmol/L of Cd and 0.127 - 0.397 nmol/L of Ni from total dissolved metal concentrations of 0.3 - 0.8 nmol/L for Cd and 17.3 - 90.8 nmol/L for Ni as was seen in Narragansett Bay, RI. This effect would represent 10.23 - 12.95% of the total dissolved Cd and 0.44 - 0.74% of the total dissolved Ni in Narragansett Bay, RI (Table 5.2). Compared to other coastal algal blooms such as a diatom bloom in San Francisco Bay where nearly 75% of dissolved Cd, Ni, and Zn were removed (and up to 25% of Cu) (Luoma et al., 1998), brown tide blooms only slightly affect total dissolved Ni (< 0.8% removed), but could possibly cause a greater decrease in Cd (< 13% removed). Zn removal was approximately 2.61 - 7.43 % of total dissolved. If 20% of Zn was removed by brown tide bloom, the resulting concentrations may place some algae species at a disadvantage, for example, green algae, as it has a relatively high Zn quota (thus probably a greater Zn requirement as well) compared to other algal groups (Ho et al., 2003).

In summary, this research demonstrated that *A. anophagefferens* is sensitive to Cd and insensitive to Cu, which, when present in coastal water, is unlikely to adversely affect *A. anophagefferens* growth rate given the typical concentrations in coastal water. Interestingly, however, *A. anophagefferens* growth may be substantially promoted by dissolved Ni. Zn contamination in coastal water may result in a slight growth inhibition for *A. anophagefferens*. The cellular and intracellular Cd, Ni, and Zn bioaccumulation

potential in brown tide blooms is not likely to cause dramatic changes in Ni concentrations, but may cause decreases in the total dissolved Zn and Cd, which in turn may affect the growth of other algal species.

Table 5.2 Estimated Metal Removal (%) by a Hypothetical Brown Tide Bloom of 10^6 cell mL^{-1} in Narraganasett Bay, Rhode Island

	Dissolved (nM)	**Sequester in Me_a (%)** [d]	**Sequester in Me_{int} (%)** [d]	**Total removal (%)**
Cd_T	0.3 – 0.8 [a]	9.74 - 12.35	0.49 - 0.61	10.23 - 12.95
Cd′	0.05 – 0.22 [a]	44.89 - 58.44	2.20 - 2.92	47.10 - 61.36
Ni_T	17.3 - 90.8 [b]	0.38 - 0.64	0.06 - 0.10	0.44 - 0.74
Ni′	8.65 - 64 [c]	0.55 - 1.28	0.08 - 0.19	0.63 - 1.47

′ Refers to the free ion and inorganic complexes with the free ion. [a] Kozelka and Bruland (1998). [b] Wells et al. (2000). [c] [Ni′] = 50 - 70% of [Ni_T] according to Slaveykova et al. (2009). [d] Me_a and Me_{int} are calculated based on Langmuir isotherm shown in Table 5.1, and the free metal ion concentrations are obtained based on Table 4.1.

CHAPTER 6

VARIATIONS IN THE BIO-OPTICAL CHARACTERISTICS OF THE NEW YORK / NEW JERSEY HARBOR ESTUARY

Water quality characteristics of coastal water significantly impact the diversity and viability of algae. One bloom is brown tide found in the NY/NJ Bight, and in this research the impact of metal concentrations present in coastal waters was considered. An aspect of this research was to assess the potential ability to characterize harmful algae blooms rapidly. In this chapter and the remaining ones, bio-optical characteristics of the remaining portion of the NY/NJ coastal area, namely the NY/NJ Harbor Estuary, are considered with respect to remote sensing application.

6.1 Absorption Constituents in Relation to Water Quality in the New York / New Jersey Harbor Estuary

The 29 sampling stations in the NY/NJ Harbor Estuary included 27 NYCDEP (New York City Department of Environmental Protection) conventional stations and two tributary stations. Data obtained covered three orders of magnitude for Chl *a* concentrations, two orders of magnitude for TSS concentrations, and one order of magnitude for absorption coefficients of CDOM at 440 nm, $a_{CDOM}(440)$ (Table 6.1). The correlation among these three variables was very low, $r^2 < 0.03$, which is typical for Case 2 Waters (Groom et al., 2009).

The Chl *a* concentrations ranged from 0.21 to 70.24 mg m^{-3} with a mean of 8.58 ± 13.34 mg m^{-3} (Table 6.1). The peak concentrations of Chl *a* were observed in spring (March - May, 22.68 ± 17.65 mg m^{-3}); this was followed by summer (August), autumn (September), and winter (November) (Figure 6.1 a). In spring and early summer, Chl *a* is

Table 6.1 Summary of Concentrations of Chl *a* (mg m^{-3}), TSS (g m^{-3}), and a_{CDOM} (440) (m^{-1}) in the NY/NJ Harbor Estuary during August 2008 - June 2009

	Number of Samples	Range	Mean	SD
Chl *a* (mg m^{-3})	95	0.21 - 70.24	8.58	13.34
TSS (g m^{-3})	98	1 - 32.8	12.84	6.58
a_{CDOM} 440 (m^{-1})	103	0.23 - 0.88	0.52	0.16

SD: represents standard deviation.

likely dominated by diatoms (e.g. *Skeletonema costatum*, *Asterionella glacialis*, *Thalassiosira nordenskioeldii, Nitzschia spp., and Cylindrotheca closterium*) and dinoflagellates (e.g. *Gyrodinium undulans, Olisthodiscus luteus*, and *Prorocentrum micans*) (Marshall and Cohn, 1987; NJDEP, 2000, 2008). The Chl *a* in summer (August, 6.10 ± 3.25 mg m^{-3}) in this study was much lower than that in August 1999 (Bagheri et al., 2002) (25.28 ± 14.47 mg m^{-3}) for the same area. The difference may be due to meteorological factors and different sampling locations. Average Chl *a* concentrations were no more than 3 mg m^{-3} during autumn and winter. Spatially, Jamaica Bay consistently showed greater concentrations than the Inner Harbor and Hudson/Raritan Bay. Specifically, the peak Chl *a* concentration in Jamaica Bay was 70.24 mg m^{-3} in spring, while in the Inner Harbor and Hudson/Raritan Bay they were 50.07 and 35.20 mg m^{-3}, respectively, during the same sampling period. Jamaica Bay's geographical properties may be responsible for the greater Chl *a* concentrations in this area. Jamaica Bay is an urban estuarine embayment with a national park consisting of tidal wetlands,

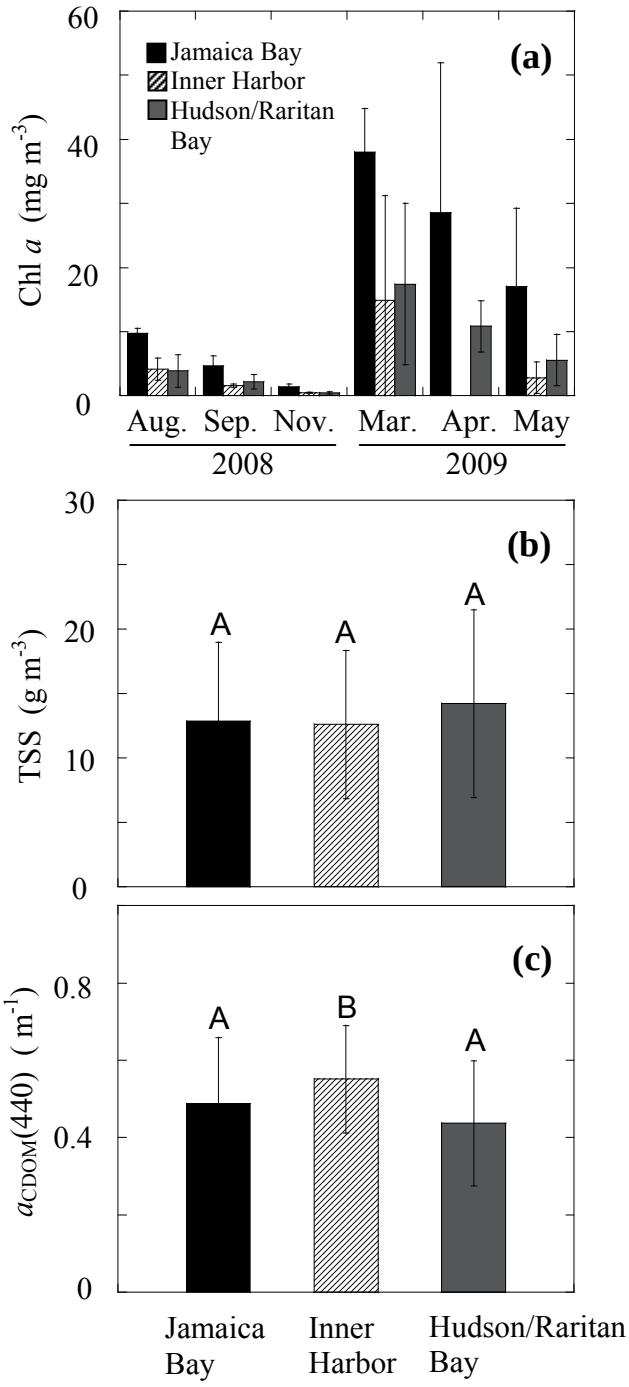

Figure 6.1 Distribution of (a) Chl *a* (mg m^{-3}), (b) TSS (g m^{-3}), and (c) a_{CDOM} (m^{-1}). Letters (A and B) in (b) and (c) show significant difference by ANOVA analysis.

upland areas, and open waters; while Inner Harbor is surrounded by residential and commercial developments, and the Hudson/Raritan Bay is mostly open water. Furthermore, the sampling stations in Jamaica Bay were for the most part in the vicinity of its tributaries and dead-end canals (Figure 4.1), which are prone to reduced water quality due to surface water runoff and poor flushing.

The total suspended solids (TSS) concentrations ranged from 1 to 32.8 g m^{-3}, with an average of 12.84 ± 6.58 g m^{-3} comparable to earlier work in the area with total suspended matter (TSM, similar to TSS) of 15.00 ± 6.98 g m^{-3} (Bagheri et al., 2002). Temporal and spatial variability was not significant in the studied area (Figure 6.1 b).

CDOM is expressed as the absorption coefficient of CDOM at 440 nm, $a_{CDOM}(440)$, ranging from 0.23 to 0.88 m^{-1} with an average of 0.52 ± 0.16 m^{-1} (Table 6.1). Compared to the observation (0.25 ± 0.14 m^{-1}) by Bagheri et al. (2002) ten years ago, $a_{CDOM}(440)$ has doubled. During this study, no significant temporal change of $a_{CDOM}(440)$ was observed. Spatially, however, the Inner Harbor exhibited greater $a_{CDOM}(440)$ (0.55 ± 0.14 m^{-1}) than either the Hudson/Raritan Bay (0.44 ± 0.16 m^{-1}, $p < 0.001$) or Jamaica Bay (0.48 ± 0.17 m^{-1}, $p = 0.005$) (Figure 6.1 c). High $a_{CDOM}(440)$ coincided with low water quality conditions reported for these areas, and low $a_{CDOM}(440)$ reflected higher water quality conditions. For example, some areas in the Inner Harbor (specifically the Kills system) are only suitable for fish, shellfish, and wildlife survival, and do not meet the requirement for primary and secondary contact in recreation and fish propagation, while the Hudson/Raritan Bay is the only area, among the three areas in this study, that meets the requirement of primary and secondary contact recreation and fishing (NYCDEP, 2009). The residential and commercial developments along the Inner Harbor, and the

industrial development on the New Jersey side of the Kills likely contributes to the high $a_{CDOM}(440)$ observed. On the other hand, the openness to the Atlantic Ocean supports the low $a_{CDOM}(440)$ found in the Hudson/Raritan Bay.

In summary, compared to the data of ten years ago (Bagheri et al., 2002), suspended particle concentrations did not show a significant change, CDOM doubled, and Chl *a* concentrations varied significantly.

6.2 The Absorption Budget

Total absorption (without pure water contribution, $a - a_w$) at wavelength of 440 nm was analyzed by creating an absorption budget with a ternary plot (Figure 6.2): partitioning the total absorption into associated contributions from CDOM, a_{CDOM}; phytoplankton, a_{ph}; and, NAP, a_{NAP}. IOCCG (2000) reported and discussed how results may fall throughout a budget diagram at 440 nm for coastal waters. However, the water samples in the NY/NJ Harbor Estuary were found to reside in the vicinity of the left axis, with a low and narrow variability in the NAP contribution, and variable CDOM and phytoplankton (*ph*) contributions.

The NAP contribution at 440 nm, $a_{NAP}/(a - a_w)$, in the NY/NJ Harbor Estuary was 0.18 ± 0.06, which is comparable to that found for European coastal waters, 0.22 ± 0.13, (Babin et al., 2003). Interestingly, the variance was less than 60% of that found for European coastal waters. Because there was no significant temporal and spatial variation in $a_{\mathrm{NAP}}/(a - a_{\mathrm{w}})$ at 440 nm (Figure 6.2, Table 6.2), $a_{NAP}(\lambda)$ can be conveniently subtracted from $a(\lambda)$ in remote sensing applications for the entire body of water in the

NY/NJ Harbor Estuary. To the best of our knowledge, this study is the first to address temporal and spatial variability of a_{NAP} in the NY/NJ Harbor Estuary.

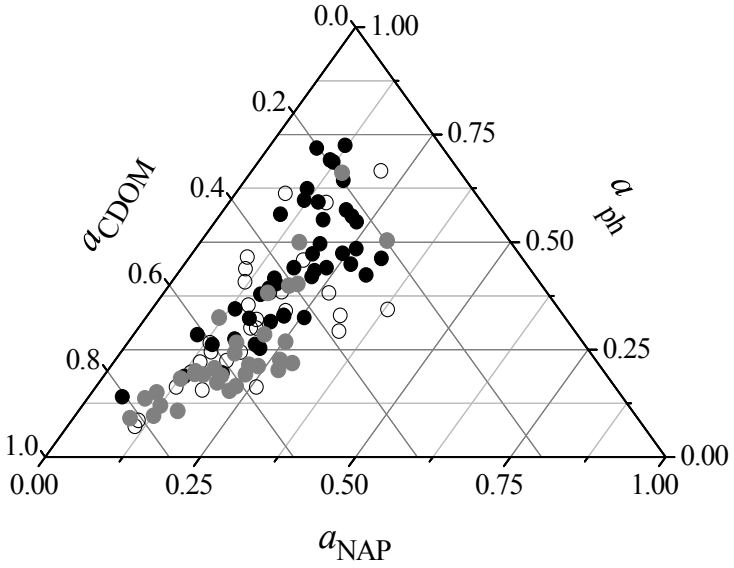

Figure 6.2 Absorption budget: ternary plots of relative contribution of CDOM (a_{CDOM}), phytoplankton (a_{ph}), and non-algal particle (a_{NAP}) to absorption (a - a_w) at 440 nm for (●) Jamaica Bay; (●) Inner Harbor; and (○) Hudson/Raritan Bay during 2008-2009.

The absorption budget indicates significant variability of CDOM and phytoplankton contributions to total absorption at 440 nm in the NY/NJ Harbor Estuary (Figure 6.2). Categorizing the Estuary into sub-areas would benefit remote sensing applications; thus, absorption contributions from CDOM and phytoplankton were statistically analyzed (Table 6.2).

Table 6.2 Relative Absorption Contributions of CDOM ($a_{CDOM}/(a\text{-}a_w)$), Non-algal Particle ($a_{NAP}/(a\text{-}a_w)$), Phytoplankton ($a_{ph}/(a\text{-}a_w)$)

Variable	Area	Sample Number	Range	Mean	SD	Statistically different from areas
$a_{CDOM}/(a\text{-}a_w)$	Jamaica Bay	39	0.15-0.81	0.38	0.16	Inner Harbor, Hudson/Raritan Bay
	Inner Harbor	30	0.19-0.82	0.57	0.16	Jamaica Bay
	Hudson/Raritan Bay	28	0.13-0.82	0.50	0.17	Jamaica Bay
	Total	97	0.13-0.82	0.47	0.18	
$a_{NAP}/(a\text{-}a_w)$	Jamaica Bay	39	0.05-0.31	0.18	0.06	
	Inner Harbor	30	0.09-0.30	0.19	0.06	
	Hudson/Raritan Bay	28	0.08-0.38	0.18	0.07	
	Total	97	0.05-0.38	0.18	0.06	
$a_{ph}/(a\text{-}a_w)$	Jamaica Bay	39	0.14-0.73	0.44	0.15	Inner Harbor Hudson/Raritan Bay
	Inner Harbor	30	0.09-0.66	0.24	0.13	Jamaica Bay Hudson/Raritan Bay
	Hudson/Raritan Bay	28	0.07-0.66	0.32	0.15	Jamaica Bay Inner Harbor
	Total	97	0.07-0.73	0.35	0.16	

Based on CDOM contribution, $a_{CDOM}/(a - a_w)$, the studied area can be divided into two sub-areas: a low CDOM contribution area of Jamaica Bay (0.38 ± 0.18) and high CDOM contribution areas including Inner Harbor (0.57 ± 0.16) and the Hudson/Raritan Bay (0.50 ± 0.17) (Table 6.2). The resulting CDOM contribution was consistent with that based on remote sensing for the Hudson/Raritan Bay (Chang and Gould, 2006), but varied greatly in the different waters studied. Researchers have reported contributions up to 90% or more of CDOM in the total absorption spectra at 440 nm in coastal waters (Ferrari and Dowell, 1998) and river plumes (Odriozola et al., 2007).

Phytoplankton absorption contributions, $a_{ph}/(a - a_w)$, differed significantly among Jamaica Bay, Inner Harbor, and Hudson/Raritan Bay ($p < 0.05$ for any two of the three sub-areas) (Table 6.2). The contribution was greatest in Jamaica Bay (0.44 ± 0.15), intermediate in Hudson/Raritan Bay (0.32 ± 0.15), and lowest in Inner Harbor (0.24 ± 0.13). This trend is consistent with Chl *a* measurements using HPLC (Figure 6.1), further demonstrating the accuracy of absorption measurements.

Overall, for the NY/NJ Harbor Estuary the absorption contribution from NAP was relatively constant at 0.18 ± 0.06, and was lower than that from phytoplankton and CDOM. Phytoplankton absorption contributed more than CDOM in Jamaica Bay, while in the Inner Harbor and Hudson/Raritan Bay, CDOM contributions were greater than phytoplankton.

6.3 Particulate Absorption Spectra

Both phytoplankton and non-algal particles contributed to particulate absorption (Eq. 4.9). Phytoplankton absorption results from algal pigments. Non-algal particle absorption is mainly from suspended mineral particles (IOCCG, 2000) along with non-bleachable organic remains of cell debris. In the following subsection, the NAP spectra are analyzed in an effort to relate the spectra features to the sources of pollution – organic or inorganic.

6.3.1 NAP Absorption Spectra

The absorption coefficient of non-algal particles at 440 nm, a_{NAP} (440), ranged from 0.06 to 0.98 m^{-1} with an average of 0.25 ± 0.16 m^{-1}. A relationship was not observed between a_{NAP} (440) and TSS (including total suspended cells and suspended mineral particles) concentration, suggesting variable contributions of organic particles to TSS and a_{NAP} (440) in the water samples. However, Babin et al. (2003) found for European coastal water a relationship (R^2=0.56) between a_{NAP} (443) and suspended particulate matter (SPM) and Binding et al. (2008) reported a stronger relationship (R^2=0.76) for Lake Erie; SPM is similar to TSS measured in this study.

NAP absorption spectra showed some variability (Figure 6.3). The exponential slope of NAP spectra, S_{NAP}, ranged from 0.0102 to 0.0193 nm^{-1}, with a mean value of 0.0138 ± 0.0015 nm^{-1}. This value was slightly greater than 0.011 nm^{-1} (Roesler et al., 1989) and 0.0123 ± 0.0013 nm^{-1} (Babin et al., 2003) reported for European coastal waters, and 0.0121 nm^{-1} (Perkins et al., 2009) for Finger Lakes, NY. Given this S_{NAP}, $a_{NAP}(\lambda)$ can be expressed as

$$a_{NAP}(\lambda) = a_{NAP}(440)e^{0.0138\ (440-\lambda)} \tag{6.1}$$

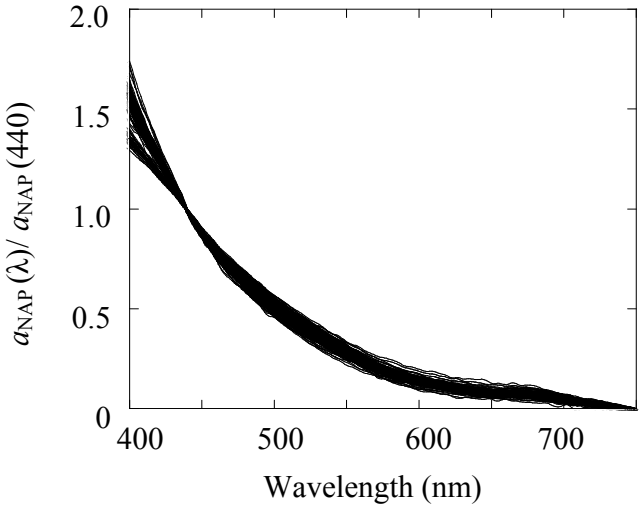

Figure 6.3 Absorption spectra of non-algal particles (a_{NAP}) normalized to a_{NAP} at 440 nm as a function of wavelength (nm).

The mean S_{NAP} value of 0.0138 ± 0.0015 nm^{-1} suggests the dominance of organic particles in the NY/NJ Harbor Estuary. Other studies show that the variability of S_{NAP} was due to inconsistent contributions of minerals and organic particles (Binding et al., 2008). Low S_{NAP} suggests the dominance of mineral particles, such as 0.011 nm^{-1} for Irish Sea (Bowers et al., 1996), while greater S_{NAP} values indicate high particulate organic matter concentrations, for example, 0.0128 nm^{-1} at Baltic Sea (Babin et al., 2003). In this research, spring and summer samples showed slightly greater S_{NAP} (0.0141 ± 0.0015 nm^{-1}) than the autumn and winter samples (0.0134 ± 0.0014 nm^{-1}) ($p = 0.015$), coinciding with greater phytoplankton density in the spring and summer. Besides phytoplankton, other organic particles, dredged sediments, waste, precipitated aerial particles, and particles transported by rivers converging to the NY/NJ Harbor Estuary,

could be important as well. Komada et al. (2002) found that during the resuspension of dredged sediment in the NY/NJ Harbor Estuary, particulate organic matter, mostly protein-like and humic-like matter, was released. The particulates may also originate from municipal wastewater treatment plants, industrial discharges, stormwater, and landfills. Gao et al. (2002) confirmed increasing concentrations of particles (< 2.5 μm) in the NY/NJ Harbor Estuary caused by in situ precipitation and vicinal precipitation transported via waterways to the NY/NJ Harbor Estuary.

6.3.2 Phytoplankton Absorption Spectra

Phytoplankton absorption spectra, $a_{ph}(\lambda)$, showed both seasonal and spatial variability, consistent with Chl *a* concentrations: $a_{ph}(\lambda)$ was greater in the spring and summer than in autumn and winter, and it was greater in Jamaica Bay than the Inner Harbor and Hudson/Raritan Bay (Figure 6.4). The ratio of a_{ph} at the blue wavelength (~ 440 nm) to that at red (~ 675 nm) was 1.6 -1.7 during spring and summer, and was comparable among the three areas; however, the ratios increased two to three times during autumn and winter, suggesting a greater proportion of accessory pigments to Chl *a* in autumn and winter.

Broadening of the autumn and winter phytoplankton spectra between 400 and 440 nm, especially in the Inner Harbor and Hudson/Raritan Bay (Figure 6.4 b and c), suggests great phaeopigment concentrations, which strongly absorbs light at short wavelengths (Roesler et al., 1989; Babin et al., 2003). Algal communities generally show greater phaeopigment concentrations in oligotrophic waters than in eutrophic waters (Babin et al., 2003; Bricaud et al., 2004). On the other hand, Binding et al. (2008) argued that the high phytoplankton absorption at short wavelengths could be due to the bleaching of particle-

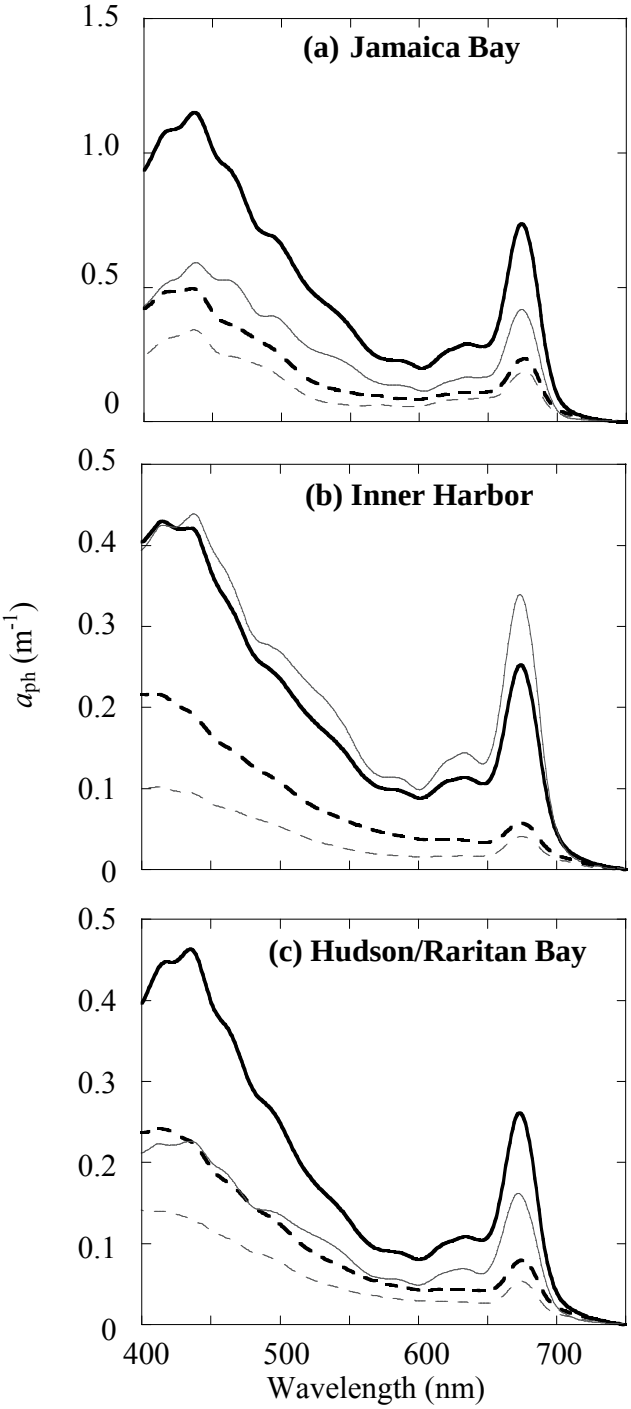

Figure 6.4 Average phytoplankton absorption (m^{-1}) of spring/summer (bold solid lines) and autumn/winter (bold dashed lines) samples with standard derivation (gray solid lines for spring/summer and gray dashed lines for autumn/winter) from 400 to 750 nm wavelength in (a) Jamaica Bay, (b) Inner harbor; and (c) Hudson/Raritan Bay.

bound organic matter by sodium hypochlorite. They observed that the $a_{ph}(\lambda)$ between 400 and 440 nm increased with increasing a_{CDOM} (440). Nevertheless, this correlation (between a_{CDOM} (440) and $a_{ph}(\lambda)$ over 400 to 440 nm) was not observed in this research, suggesting that bleaching is an unlikely cause of the broadening in the phytoplankton spectra from 400 to 440 nm.

A power relationship between a_{ph} (440) and Chl *a* concentrations, $a_{ph}(440) = 0.180(chl\ a)^{0.576}$, is observed for the NY/NJ Harbor Estuary (Figure 6.5). This curve lies above that of $a_{ph}(440) = 0.0654(chl\ a)^{0.728}$, developed by Bricaud et al. (2004) for the world's ocean water (Case 1 Waters) (Figure 6.5). The upward shift may be explained by how Chl *a* is defined: Bricaud et al. (2004) used TChl *a* including chlorophyll *a*, divinyl-Chl *a*, and even phaeopigment (just for oligotrophic water). In this research, Chl *a* includes chlorophyll *a*, chlorophyll *a* isomer, and epimer.

Specific phytoplankton absorption, $a^*_{ph}(\lambda)$ (obtained by normalizing $a_{ph}(\lambda)$ to Chl *a*, i.e. phytoplankton absorption per unit Chl *a*, m^2 mg^{-1} Chl *a*) showed variability in the NY/NJ Harbor Estuary (Figure 6.6). The $a^*_{ph}(\lambda)$ ranged from 0.028 to 0.34 m^2 mg^{-1} Chl *a* with a mean value of 0.125 ± 0.077 m^2 mg^{-1} Chl *a*. As is the case with many studies (Bricaud et al., 1995; Babin et al., 2003; Bricaud et al., 2004), $a^*_{ph}(\lambda)$ decreased as Chl *a* increased (Figure 6.5), which is caused by a "package effect" and/or pigment composition (Bricaud et al., 1995; Babin et al., 2003). Accessory pigments, especially carotenoids, contribute significantly to the absorption in the blue range at low Chl *a* concentrations (Babin et al., 2003). Because the dominant algal communities in this water body are diatoms and dinoflagellates (NJDEP, 2008b), the major carotenoids are

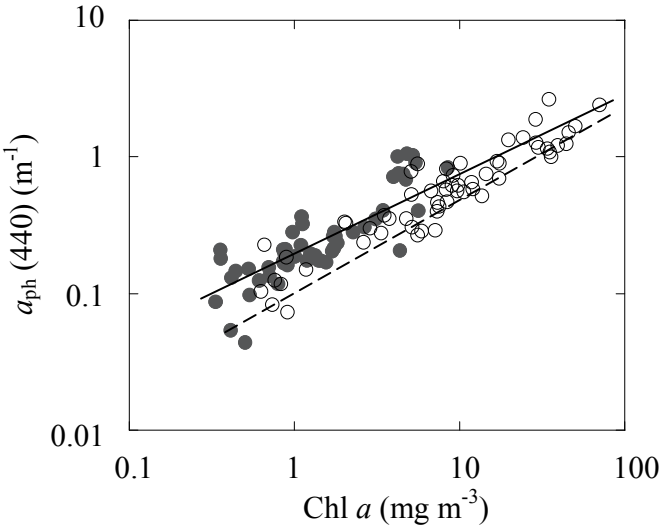

Figure 6.5 Scatter plots of phytoplankton absorption coefficients at 440 nm, $a_{ph}(440)$ (m^{-1}), as a function of Chl *a* concentration (mg m^{-3}) in autumn/winter (●) and spring/summer (○) samples. Solid line: New York/New Jersey Harbor Estuary (Case 2 water), $a_{ph}(440) = 0.196[\text{Chl } a]^{0.576}$, $r^2 = 0.82$; dashed line: Europe ocean water (Case 1 water) from Bricaud et al. (2004), $a_{ph}(440) = 0.0654(chl\ a)^{0.728}$.

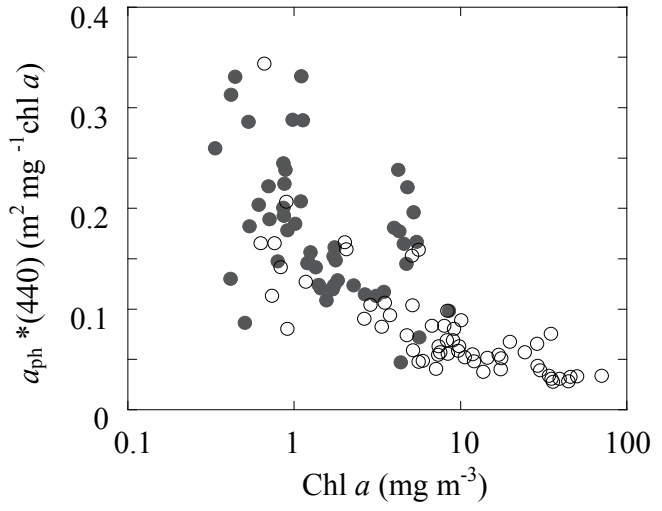

Figure 6.6 Scatter plots of (a) a_{ph}*(440) (m^2 mg^{-1} Chl *a*) as a function of Chl *a* concentration (mg m^{-3}) for autumn/winter (●) and spring/summer (○) samples.

chlorophyll c_1, chlorophyll c_2, diadinoxanthin, fucoxanthin, and peridinin (Jeffrey et al., 1997). Because of the large cell size of diatoms and dinoflagellates, where absorption of surface pigments dominates, the package effect is possibly a significant factor in the variation of $a^*_{ph}(\lambda)$ (Babin et al., 2003). Further interpretation of the pigment composition and packaging effect will be discussed in the Chapter 7.

6.4 CDOM Absorption Spectra

The range of CDOM absorption at 440, $a_{CDOM}(440)$, has been discussed in Section 6.1 (also see Table 6.1, Figure 6.1). The negative linear relationship between $a_{CDOM}(440)$ and salinity (Figure 6.7 a) suggests the dilution of estuary CDOM by marine water. Almost all CDOM absorption spectra (103 out of 104) fit Eq. (2.2); the resulting slope, S_{CDOM}, is 0.0160 ± 0.0023 nm^{-1}, similar to other studies for Case 2 waters. For example, Warnock et al. (1999) found 0.016 - 0.017 nm^{-1} for the Southern Bight of the North Sea and the English Channel, and, Babin et al. (2003) measured 0.0176 ± 0.0020 nm^{-1} for European coastal waters. Temporal and spatial variations of S_{CDOM} were not observed in this research. Further no significant correlation was found between S_{CDOM} and $a_{CDOM}(440)$, which is consistent with other oceanic and coastal water studies (Carder et al., 1999; Babin et al., 2003; Binding et al., 2008). Equation (2.2) is therefore rewritten below for the entire the NY/NJ Harbor Estuary:

$$a_{CDOM}(\lambda) = a_{CDOM}(440)e^{0.016(440-\lambda)} \tag{6.2}$$

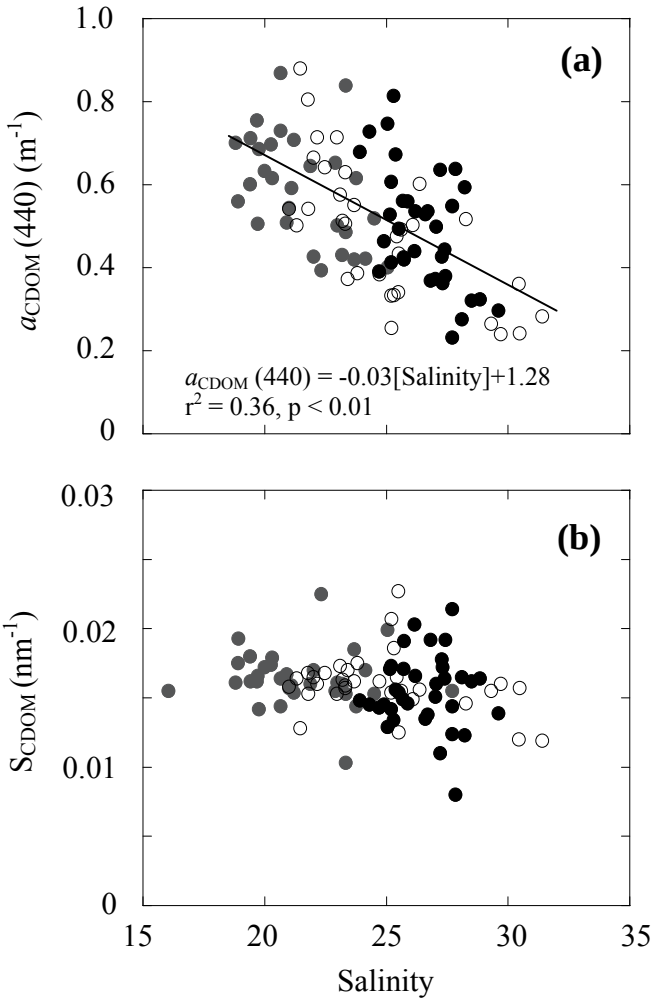

Figure 6.7 (a) Absorption coefficient of CDOM at 440 nm (a_{CDOM}, m^{-1}), and (b) Slope of CDOM spectra (S_{CDOM}, nm^{-1}) as a function of salinity for (●) Jamaica Bay; (●) Inner Harbor; and (○) Hudson/Raritan Bay.

Similar to S_{NAP}, S_{CDOM} can be used to determine whether CDOM was of terrigenous or in situ (e.g. phytoplankton, zooplankton, and sediments) sources (Carder et al., 1989; Stedmon and Markager, 2001; Binding et al., 2008). Terrigenous S_{CDOM} is generally constant (Astoreca et al., 2009), where it has been reported as 0.018 nm^{-1} for the Greenland Sea (Stedmon and Markager, 2001) and 0.0169 - 0.0191 nm^{-1} for the Southern North Sea (Astoreca et al., 2009). In contrast, S_{CDOM} from in situ sources varies

widely, for example, 0.009 - 0.027 nm^{-1} for coastal waters in Europe and South America (Stedmon and Markager, 2001; Astoreca et al., 2009). Though S_{CDOM} for the NY/NJ Harbor Estuary varied from 0.0080 to 0.0227 nm^{-1}, the mean value of S_{CDOM} was 0.0160 nm^{-1} with a standard deviation of 0.0020 nm^{-1} (12.5%). In situ CDOM sources may influence the majority of water bodies in this study, but individual sites may have significant terrigenous CDOM input. Although a correlation between Chl *a* concentration and $a_{CDOM}(440)$ was not observed, phytoplankton may still be the major source of CDOM in the NY/NJ Harbor Estuary. Some researchers (Bricaud and Sathyendranath, 1981; Nelson et al., 1998) have argued the presence of a time lag in Chl *a* contributing to CDOM, which may be a factor for this region during spring and early summer 2009. Specifically, in relating a_{CDOM} (samples during March, April, and May) as a function of Chl *a* concentration, the correlation coefficient increased from 0.09 (March) to 0.40 (April) and then decreased slightly to 0.37 (May). In addition to phytoplankton, suspended organic particles may possibly contribute to CDOM after dissolution. Overall, CDOM in the NY/NJ Harbor Estuary is dominated by in situ sources, combinations of phytoplankton, zooplankton, and sediments, along with terrigenous sources.

6.5 Summary

The in situ measurements of absorption and the characterization of CDOM, phytoplankton, and non-algal particle contributions for the NY/NJ Harbor Estuary over four seasons provide useful information on the water quality conditions as well as support for future remote sensing applications in the area. The results showed that $a_{NAP}/(a\text{-}a_w)$ varied within a relatively narrow range. The S_{NAP} (0.0138 ± 0.0015 nm^{-1}) was slightly

greater than most reported values for coastal waters, indicating significant organic particulate input. On the other hand, the wide range (0.0080 - 0.0227 nm^{-1}) and narrow variation (0.0160 ± 0.0020 nm^{-1}) of S_{CDOM} suggest that in situ sources dominate for CDOM while a few sites have greater terrigenous sources than others. A time lag of dissolved pigment, Chl *a*, contributing to CDOM suggests that phytoplankton is a source for CDOM. A relationship was not found between TSS and non-algal particles indicating that the source is likely comprised of complex organic particulates. Overall, absorption contributions (phytoplankton, CDOM, and NAP) aid addressing impacts to water quality conditions.

CHAPTER 7

THE SPECIFIC ABSORPTION COEFFICIENT FOR THE NEW YORK / NEW JERSEY HARBOR ESTUARY

The composition and variation of the absorption coefficient with contributions from CDOM, NAP, and phytoplankton were evaluated for the NY/NJ Harbor Estuary and discussed in Chapter 6. This chapter is focused on the specific absorption coefficient, absorption coefficient of phytoplankton per unit of ch *a*, $a^*_{ph}(\lambda)$, m^2 mg^{-1} Chl *a*, which was initially assumed as constant for any water (Bricaud et al., 1995). However, many researchers (e.g., Mitchell and Kieper, 1988; Bricaud et al., 1995; Babin et al., 2003) have found variability in $a^*_{ph}(\lambda)$ and concluded that the two contributing factors were pigment composition (Bidigare et al., 1990; Hoepffner and Sathyendranath, 1992; Bricaud et al., 2004) and the "package effect" (Kirk, 1975; Bricaud et al., 2004). The later one involves cell size and intracellular pigment composition (Morel and Bricaud, 1981). The larger cells "package" pigments and therefore absorb less light compared to smaller cells containing the same concentration of pigment. On the other hand, the variation of intracellular pigment distribution also results in variability of the specific absorption coefficient. The phytoplankton communities are made of algal cells typically representing a number of species, each of which has their own distinct pigment composition. In this chapter, the pigment composition and the resulting specific absorption coefficient are presented and followed by how the pigment composition and package effect impact the variability of the coefficient.

7.1 Pigment Composition

In the NY/NJ Harbor Estuary, the algal species detected over the last decade include two dominant ones diatom and dinoflagellate (Table 7.1), and to a lesser extent raphidophyceae (NJDEP, 2000, 2005, 2008a). Harmful algal blooms observed have involved *Skeletonema costatum* and *Thalassiosira spp.* in the Hudson/Raritan Bay (NJDEP, 2008). As reviewed in the methods, HPLC analysis is used to characterize the pigment concentrations and the analysis confirmed the presence of Chl *a*, Chl *b*, Chl c_2, diadinoxanthin, fucoxanthin, peridinin, and ß-carotene (Figure 7.1) in the water samples from the NY/NJ Harbor Estuary. Among accessory pigments, fucoxanthin (50.9% ± 25.4% of total accessory pigments, Table 7.2) is a bio-marker pigment for the diatom (Jeffery et al., 1997), which is dominant in the studied area consistent with historical observations (Marshall et al., 1987; NJDEP 2000, 2005, 2008a).

Table 7.1 Species of Diatom and Dinoflagellate Observed in the New York / New Jersey Harbor Estuary

Division/Class	Genus /Species [a]	Maker Pigments [b]
Diatom	*Skeletonema costatum, Asterionella glacialis, Thalassiosira minima, Nitzschia spp., Cylindrotheca closterium, Rhizosoplenia delicatula*, and *Leptocylindrus danicus*.	Chl c_1, Chl c_2, diadinoxanthin , fucoxanthin.
Dinoflagellate	*Gyrodinium undulans, Prorocentrum sp.*, *Katodinium sp., Ceratium fusus*, *Ceratium lineatum, Ceratium longipes,* and *Ceratium tripos*.	Chl c_2, peridinin, diadinoxanthin.

Source: [a] NJDEP (2000, 2005)
[b] Maker pigment > 10 % of total pigments (Jeffery et al., 2007)

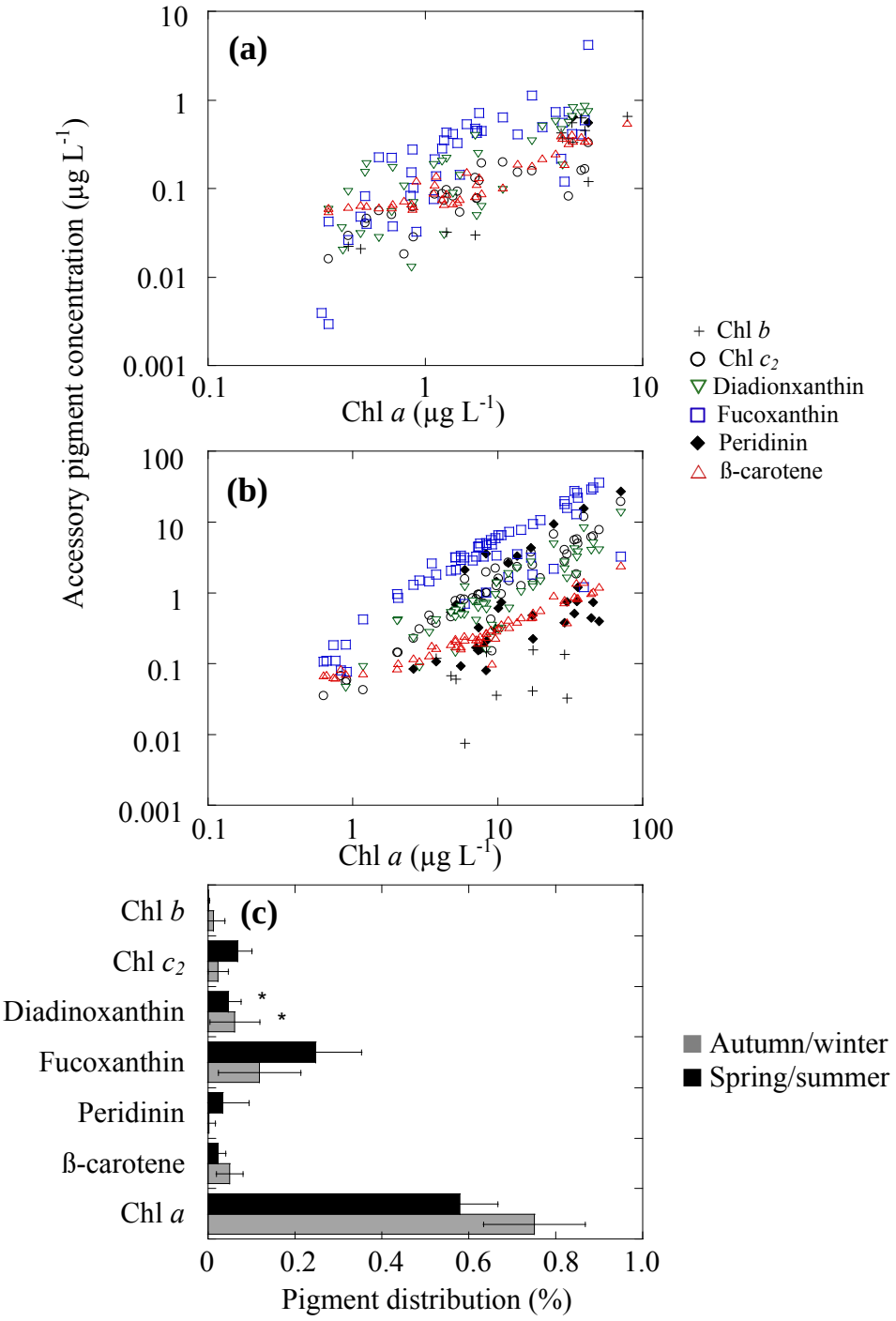

Figure 7.1 Pigment composition: accessory pigment concentration as a function of Chl *a* for samples of (a) autumn/winter samples, and (b) spring/summer samples; (c) pigment distribution where star (*) means no significant difference.

Table 7.2 Percent Contribution (%) of Accessory Pigments

Accessory pigment	Spring and Summer	Autumn and Winter	Total*
Chl *b*	0.2 ± 0.7	5.0 ± 11.0	2.4 ± 7.8
Chl c_2	16. 1 ± 10.8	7.7 ± 7.7	12.3 ± 9.1
Diadinothanxin (Diad)	10.5 ± 6.6	24.7 ± 26.8	16.9 ± 19.9
Fucothanxin (Fuco)	59.0 ± 21.0	41.0 ± 27.1	50.9 ± 25.4
Peridinin (Peri)	7.3 ± 12.8	0.8 ± 4.4	4.3 ±10.4
ß-carotene	6.9 ± 8.8	20.8 ± 17.7	13.2 ± 15.2

* [Total accessory pigment] = [Chl *b*] + [Chl c_2] + [ß-carotene] + [Diad] + [Fuco] + [Peri]

Specifically, a mild diatom bloom of *Skeletonema costatum* (2,640 cells mL^{-1}) was confirmed in the Hudson/Raritan Bay (NJDEP 2008b) during the 2008 summer sampling period. In addition to the two samples in the autumn and winter (from a total of 51), peridinin was detected in spring and summer samples, indicating the pervasiveness of dinoflagellates (Figure 7.1 a) (Jeffrey et al., 1997). The contributions of most pigments with the exception of diadinoxanthin showed seasonal changes (Figure 7.1c) suggesting seasonal variability in the algal community.

The proportion of accessory pigments to the Chl *a* concentration was a function of the season (Figure 7.2). Only a few samples contained Chl *b*, indicating the sparing

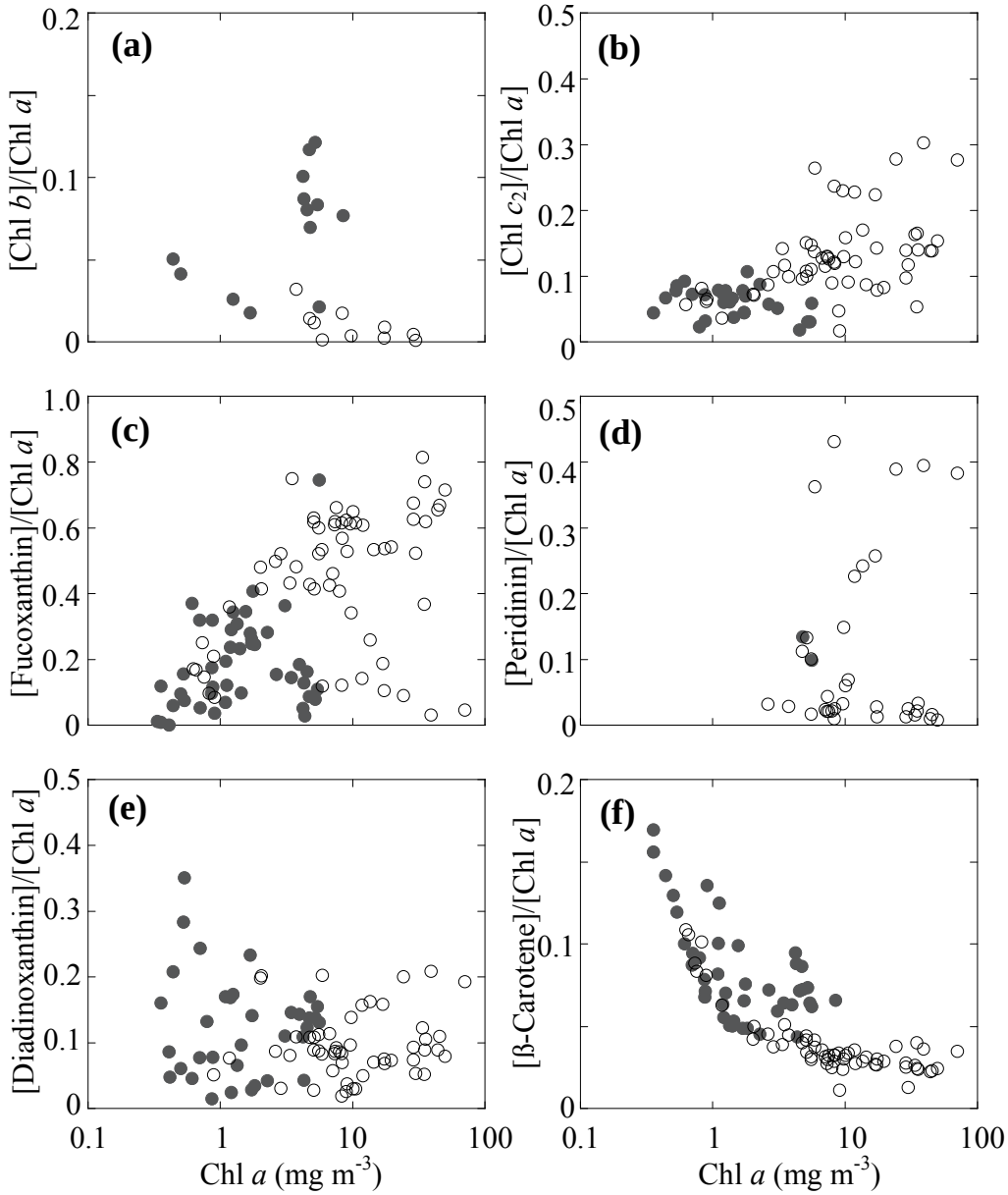

Figure 7.2 Ratios of the accessory pigment concentration to Chl *a* concentration as a function of Chl *a* concentration for autumn and winter (●) and spring and summer (○) samples. (a) Chl *b*; (b) Chl c_2; (c) Fucoxanthin; (d) Peridinin; (e) Diadinoxanthin; and (f) ß-carotene.

presence of picophytoplankton (7.2 a) (Bricaud et al., 2004). The [Chl *b*]/ [Chl *a*] ratio varied greatly between 0.05 and 0.45 in autumn and winter, while only as much as 0.1 for spring and summer (Figure 7.2 a). In contrast to Chl *b,* [Chl c_2]/ [Chl *a*] ratio showed greater variation in spring and summer samples (up to 0.3) than in autumn and winter ones (up to 0.1) (Figure 7.2 b).

The detected photosynthetic carotenoids (PSC) (Stuart et al., 1998) included fucothanxin and peridinin. The greater variation of [PSC]/[Chl *a*] was observed in spring and summer samples (Figure 7.2 c and d) than in autumn and winter ones, suggesting the greater diversity of diatom and dinoflagellate. For example, [Fucothanxin]/[Chl *a*] was up to 0.8 in spring and summer with almost no peridinin detected in autumn and winter. Generally, samples with high Chl *a* have a relatively high proportion of PSC (Stuart et al., 1998).

On the other hand, the detected non-photosynthetic carotenoids (NPC) (or photoprotecting carotenoids (PPC)) (Stuart et al., 1998) were diadinoxanthin and ß-carotene. In contrast with [PSC]/[Chl *a*], greater variation of [NPC]/[Chl *a*] was observed in autumn and winter samples (Figure 7.2 e and f) and is consistent with work of Bricaud et al. (1995) and Stuart et al. (1998).

7.2 Variation of Specific Absorption Coefficient

An important parameter in retrieving water quality information from ocean color is the specific absorption coefficient ($a^*_{ph}(\lambda)$, m^2/mg Chl *a*), the absorption coefficient by per unit Chl *a*. Given the phytoplankton absorption, Chl *a* concentrations are obtained by dividing $a^*_{ph}(\lambda)$ by a_{ph}. However, $a^*_{ph}(\lambda)$ varies greatly from coast to coast. For a

particular region, such as NY/NJ Harbor Estuary, $a^*_{ph}(\lambda)$ is needed to optimize the existing remote sensing models. The specific absorption coefficient at 440 nm, $a^*_{ph}(440)$, decreased with increasing concentration of Chl *a* (Figure 7.3 a). Similar with previous studies (Bricaud et al., 1995, 2004; Babin et al., 2003) this result is attributed to the pigment composition and/or package effect (Bricaud et al., 1995). The trend was apparent at wavelengths as great as 490 nm (Figure 7.3 b) tailing off at 676 nm (7.3 c), which is due to weak absorption by accessory pigments and less to the package effect at the red band (Bricaud et al., 1995, 2004). Because of the more significant impact of the package effect and accessory pigment absorption at 440 nm, this wavelength was selected for further study of the specific absorption coefficient (Bricaud et al., 2004). For the NY/NJ Harbor Estuary, $a^*_{ph}(440)$ ranged from 0.03 to 0.34 m^2 mg^{-1} Chl *a* with a mean of 0.13 ± 0.08 m^2 mg^{-1} Chl *a*. In agreement with other studies (Bricaud et al., 1995), $a^*_{ph}(440)$ is exponentially related to the Chl *a* concentration

$$a^*_{ph}(440) = 0.18(chl\,a)^{-0.424} \quad (r^2 = 0.72) \tag{7.1}$$

for the NY/NJ Harbor Estuary. When the Chl *a* concentration was greater than 10 mg m^{-3}, $a^*_{ph}(440)$ varied within a narrower range compared to that at lower Chl *a* concentrations (< 10 mg m^{-3}) (Figure 7.3a), demonstrating the possible constant package effect.

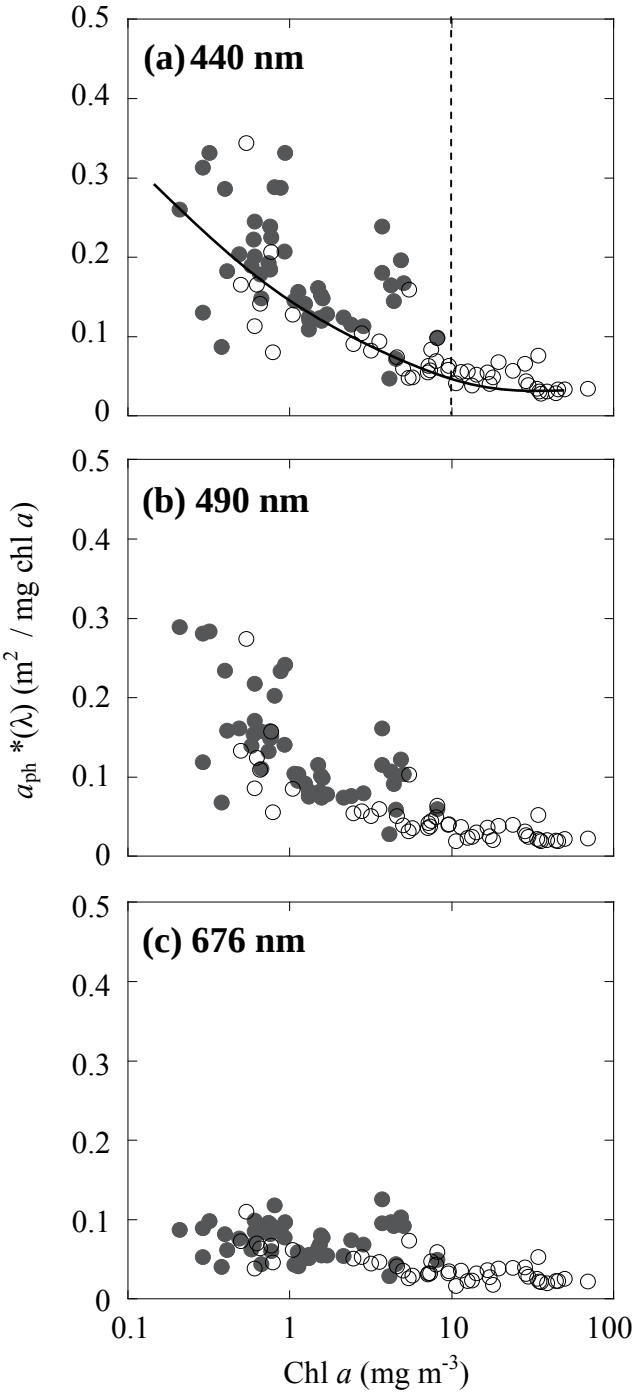

Figure 7.3 Specific absorption coefficient (m^2 / mg Chl *a*) at (a) 440 nm, (b) 490 nm, and (c) 676 nm for autumn and winter (●) and spring and summer (○) samples.

7.3 Effect of Pigment Composition

Theoretically, the phytoplankton absorption coefficient is the sum of the absorption coefficients for the individual pigments, which can be expressed as (Bidigare et al., 1990)

$$a_{sol,i} = C_i \, a^*_{sol,i}(\lambda) \tag{7.2}$$

where, $a_{sol,i}(\lambda)$ is the absorption coefficient of individual pigment dissolved in solvent, m^{-1}, C_i is the concentration of the individual pigment, mg m^{-3}, and, $a^*_{sol,i}(\lambda)$ is the weight-specific absorption coefficient of the individual pigment dissolved in solvent, m^2 mg^{-1} pigment, determined through HPLC analysis (Bidigare et al., 1990; Goericke and Repeta, 1993). Because of the variability in the degree to which a pigment absorbs light, *i.e.*, $a^*_{sol,i}(\lambda)$, the accessory pigments with greater concentrations do not necessarily make a greater contribution to absorption. For example, although fucoxanthin was the dominant accessory pigment (Figure 7.1 a), its absorption resulted in the equivalent contribution as diadinoxanthin and Chl c_2 at 440 nm when Chl *a* was 1 to 10 mg m^{-3} for autumn and winter samples (Figure 7.4 a). This effect is due to the greater weight-specific absorption coefficient of diadinoxanthin and Chl c_2 than that of fucoxanthin. For spring and summer samples, however, fucoxanthin was not only the dominant accessory pigment (Figure 7.1 b), but was also the dominant absorption contribution (Figure 7.4 b) because of its average contribution to total pigment was as much as 24% in spring and summer, while only 11% in autumn and winter (Figure 7.1 c).

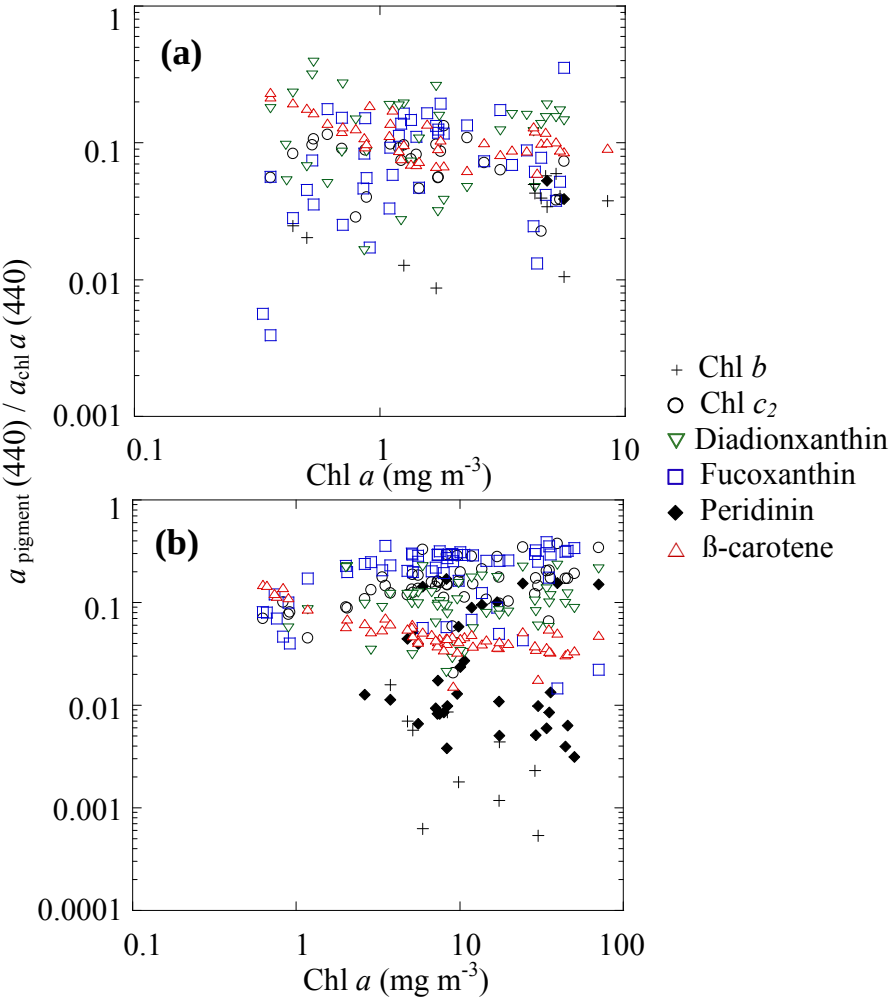

Figure 7.4 Ratio of absorption coefficient contributed from accessory pigments to Chl *a* for (a) autumn and winter samples, and (b) spring and summer samples.

Theoretically, the specific absorption coefficient, $a^*_{pigment}(\lambda)$, for accessory pigments is expressed as (Bricaud et al., 2004)

$$a^*_{pigment}(\lambda) = \frac{\sum C_i \, a^*_{sol,i}(\lambda)}{C_{chl\,a}} \tag{7.3}$$

where, $C_{Chl\,a}$ is the Chl *a* concentration. Based on HPLC pigment results, the calculated $a^*_{pigment}(440)$ of accessory pigments (Figure 7.5) did not show the same change in trend as $a^*_{ph}(440)$ (Figure 7.3 a), suggesting accessory pigment composition was not the major factor in explaining $a^*_{ph}(440)$ variability for the research area. At low Chl *a* concentrations (< 10 mg m^{-3}), accessory pigments may play a more significant role because of their greater variability than at higher Chl *a* concentrations (> 10 mg m^{-3}) (Figure 7.5).

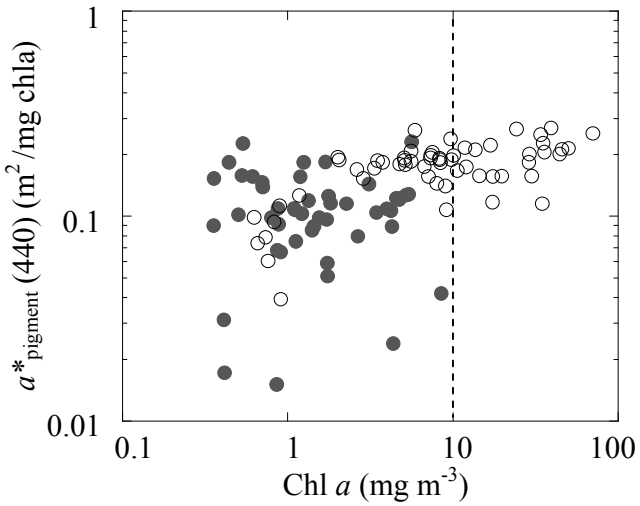

Figure 7.5 Variation of Chl *a*-specific absorption coefficient of accessory pigments at 440 nm, $a^*_{pigment}(440)$, of autumn and winter (●) and spring and summer (○) samples.

7.4 Package Effect

The package effect (the flattening effect) describes the reduced absorption of pigments in phytoplankton cells compared with the absorption potential for the same amount of pigment in solution (Morel and Bricaud, 1981; Kirk, 1994). The pigment packaging increases with the increase of internal pigment concentration or cell size. The package effect, $Q_a^*(\lambda)$, is defined as

$$Q_a^*(\lambda) = a_{ph}(\lambda) / a_{sol}(\lambda) \tag{7.4}$$

where $a_{ph}(\lambda)$ is the actual phytoplankton absorption coefficient, and $a_{sol}(\lambda)$ is the absorption coefficient of the same cellular matter ideally dispersed into solution, (Morel and Bricaud, 1981).

Previous studies (Bricaud et al., 2004) have found that $Q_a^*(\lambda)$ may be greater than 1 and hypothesized a term representing "missing pigments" (carotenoids or phycobiliproteins, not measured by HPLC). The coefficient $a_{sol}(440)$ was therefore corrected as

$$a_{sol}(440) = \sum C_i a^*_{sol,\,i}(440) + 0.0525[\text{chl}\,a]^{0.855} \tag{7.5}$$

Similar to the variation of $a^*_{ph}(440)$ (Figure 6.1a), $Q_a{}^*(440)$ decreases with increasing of Chl *a* concentrations (Figure 7.6), which demonstrates that the package effect is the major factor in explaining the variability of $a^*_{ph}(440)$. The effect of "package" decreases the absorption by as much as 70%, i.e. $Q_a{}^*(440) = 0.3$, at high Chl *a* concentrations (> 40

mg m^{-3}). The package effect is more significant in spring and summer than autumn and winter because the occurrence of the greater diatom population in spring and summer.

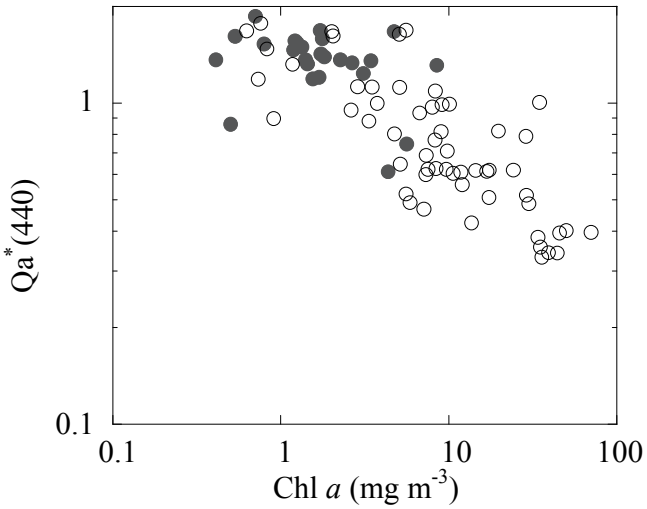

Figure 7.6 Package effect at 440 nm, $Q_a^*(440)$, as a function of Chl *a* concentration for autumn and winter (●) and spring and summer (○) samples.

As mentioned earlier, both cell size and intracellular pigment composition contribute to the package effect. In this research, the pigment composition was not the main cause for variation of $a_{ph}^*(440)$. However, it is important to note that the pigment composition certainly contributes to the variability of $a_{ph}^*(440)$, especially at low Chl *a* concentrations (< 10 mg m^{-3}) (Figure 7.5). The cell size is the main reason for the variation of $a_{ph}^*(440)$ in large algal cells. Specifically, these algae are made up of the diatom and dinoflagellate for the research area during the sampling period (NJDEP, 2008a, 2009), where the cell sizes are up to 60 μm and 120 μm, respectively (Table 7.3). For ocean waters containing picophytoplankton, nanophytoplankton, and

microphytoplankton Bricaud et al. (2004) concluded that both pigment composition and cell size were able to explain the variation of $a^*_{ph}(440)$ at Chl $a > 2$ mg m^{-3}, and cell sizes showed greater effect than pigment composition at Chl $a < 2$ mg m^{-3}.

Table 7.3 Cell Sizes of Diatom and Dinoflagellate During the Sampling Period, August 2008 - June 2009

Division/Class	Genus /Species [a]	Size (μm) [b]
Diatom	*Skeletonema costatum*	Diameter : 2 - 21 Pervalvaraxis 2 - 61
	Thalassiosira minima	Diameter: 5 - 15
	Chaetoceros sp.	4 - 6
Dinoflagellate	*Cerataulina pelagica*	Diameter : 7 - 56 Pervalvaraxis : 55 - 120
	Dynophysis spp	25 - 70

Source: [a] NJDEP (2008b, 2009)
[b] www.smhi.se

Vidussi et al. (2001) developed a size index to investigate the relationship between cell sizes and Chl *a* concentration, where the cell sizes are determined based on HPLC pigment analysis. Bricaud et al. (2004) found an inverse relation based on samples for oceans worldwide. However, the size index could not be developed for the NY/NJ Harbor Estuary primarily because of the absence of marker pigments for

nanophytoplankton and the observation of only one marker pigment for picophytoplankton (where only Chl *b* was detected).

7.5 Summary

The specific absorption coefficient at 440 nm, $a_{ph}^{*}(440)$, showed significant variability in the NY/NJ Harbor Estuary. The pigment composition and package effect analysis revealed that cell size was the main reason for the variability. Furthermore, pigment composition likely plays a role in contributing to the variability of the $a_{ph}^{*}(440)$ at low Chl *a* concentrations, specifically less than 10 mg m^{-3}.

CHAPTER 8

PIGMENTS RETREVAL FROM PHYTOPLANKTON ABSORPTION SPECTRA

An important aspect of real time water quality monitoring is to evaluate the phytoplankton rapidly without the need for HPLC analysis. Based on characteristics of phytoplankton absorption spectra discussed in previous chapters, this chapter is focused on retrieving pigment contributions from decomposing phytoplankton spectra.

8.1 Phytoplankton Spectra Decomposition

Phytoplankton absorption spectra (Figure 8.1) show greater absorption in spring and summer as opposed to autumn and winter as discussed in Chapter 6. Jamaica Bay exhibits greater absorption than Inner Harbor and Hudson/Raritan Bay because of its high phytoplankton contribution. Interestingly, the non-algal spectra did not show a significant difference among the three areas. The phytoplankton absorption spectra were obtained by subtracting NAP spectra from the total spectra. A curve fitting program was initially developed by French et al. (1967) and modified by Hoepffner and Sathyendranath (1991) to decompose phytoplankton absorption spectra. Each absorption spectrum of phytoplankton, a_{ph} (m^{-1}), could be decomposed into 13 Gaussian bands representing absorption by the major phytoplankton pigments, *i.e.*, Chl *a*, *b*, and *c*, and carotenoids (Table 8.1, Figure 8.2). Gaussian bands centered around 384, 413, 435, 623, 676, and 700 nm correspond to absorption by Chl *a*; those at 464 and 655 nm to Chl *b*; those at 461, 583, and 644 nm to Chl *c*; and, those at 490 and 532 nm to total carotenoids (Table 8.1).

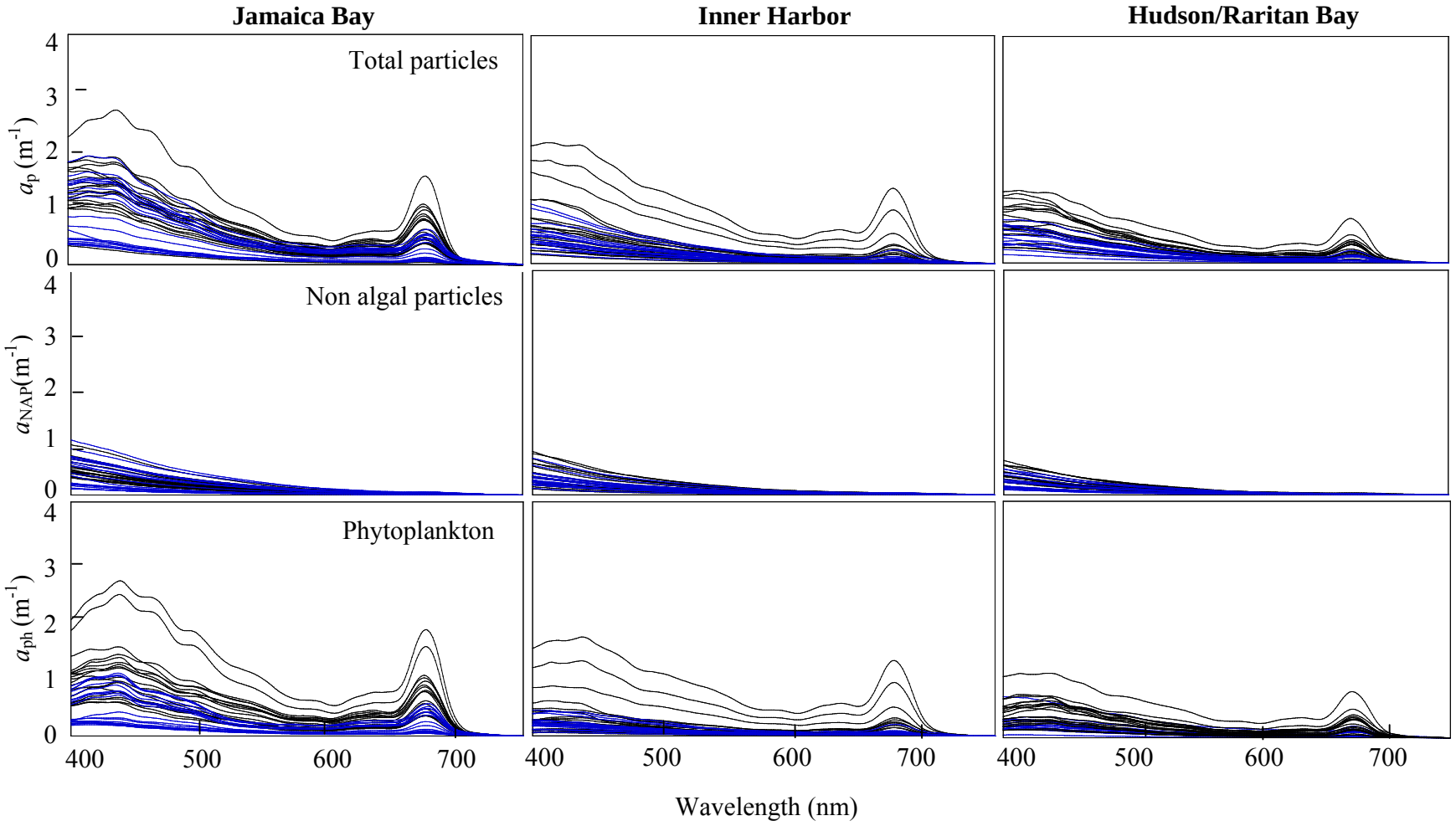

Figure 8.1 Absorption spectra of total particles (a_p), non algal particles (a_{NAP}), and phytoplankton (a_{ph}) in spring and summer (black lines) and autumn and winter (blue lines) in the NY/NJ Harbor Estuary.

Table 8.1 Initial Center-wavelengths and Heights for Spectra Decomposition

Band center (nm)	Half bandwidth (nm)	Pigment represented
384	53.8	Chl *a*
413	21.3	Chl *a*
440 (435)	32.1	Chl *a*
461	27.2	Chl *c*
464	45.0	Chl *b*
490	45.4	Carotenoid
532	45.9	Carotenoid
583	46.3	Chl *c*, *a*
623	35.0	Chl *a*
644	28.9	Chl *c*
655	24.4	Chl *b*
676	21.6	Chl *a*
700	33.5	Chl *a*

Sources: Hoepffner and Sathyendranath (1991), and Stuart et al. (1998).

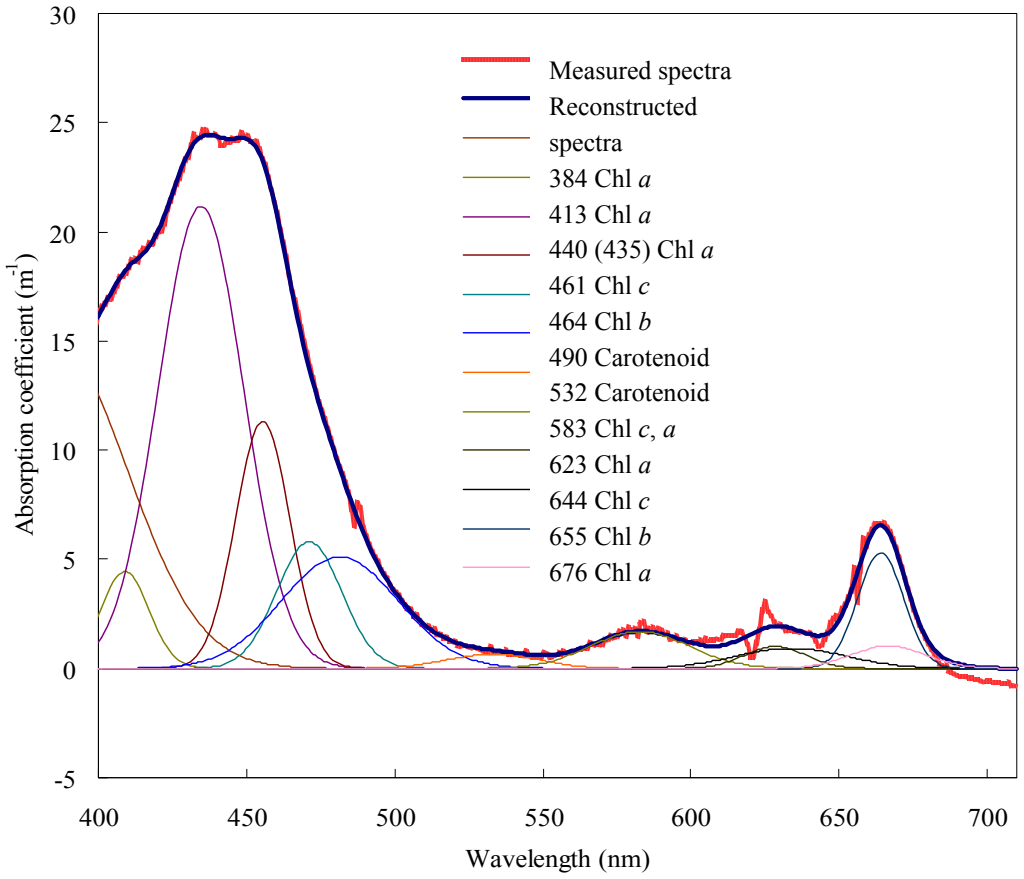

Figure 8.2 Example of discomposing a phytoplankton spectrum into Gaussian curves. Numbers after each line represent the center (nm) of each Gaussian curve.

The absorption coefficient, $a_{ph}(\lambda)$, is therefore expressed as (Hoepffner and Sathyendranath, 1991)

$$a_{ph}(\lambda) = \sum C_i a_i^*(\lambda_{mi}) \exp[\frac{(\lambda - \lambda_{mi})^2}{2\sigma_i^2}] \qquad (8.1)$$

where, λ_{mi} is the position of maximum absorption for the i^{th} Gaussian band, nm; C_i is the concentration of the associated pigment, mg m^{-3}; $a_i^*(\lambda_{mi})$ is the specific absorption coefficient of the i^{th} pigment at wavelength λ_{mi}; and, σ_i is the half width of the peak at the half maximum height. To be consistent with former chapters, the initial wavelength for Chl *a* at 435 nm was adjusted to 440 nm; this approach was also used by Stuart et al. (1998). The input specifications for spectra decomposition include: (1) phytoplankton spectra; and, (2) the band center and half-widths. The program was then setup to run a maximum of 25 iterations per spectrum or terminate earlier if the convergence criterion was met. The output includes (1) retrieved phytoplankton spectra; and, (2) the modified band center and half-widths.

At low pigment concentrations (< 3 mg m^{-3}) a linear relationship between the Gaussian height and pigment concentration was previously observed (Hoepffner and Sathyendranath, 1991). However, a non-linear relationship was confirmed with increasing pigment concentrations (up to 15 mg m^{-3}) (Stuart et al., 1998). Similar to the relationship observed between $a_{ph}(440)$ and Chl *a* concentration (Figure 6.5), the power relationships were observed between Gaussian heights and pigment concentrations (Table 8.2, Figure 8.3 (select wavelengths)) for samples from the NY/NJ Harbor Estuary.

For the six Gaussian bands of Chl *a*, the closest correlation between absorption and Chl *a* concentration was observed at 676 nm (r^2 = 0.95) due to the minimal role of the package effect and accessory pigment contribution (Table 8.2, Figure 8.3 a (selective)) (Babin et al., 2003; Bricaud et al., 2004). The low correlations between absorption and Chl *b* at 464 and 655 nm were due to the low Chl *b* concentrations (< 0.9 mg m^{-3}) (Figure 7.1) in the collected samples (Figure 8.3 b). Gaussian heights at 461 and 644 nm showed

Table 8.2 Values of the Parameters A and B for $G_\lambda = A[Pigment]^B$ Relating the Height (G) of Gaussian Bands Associated with Chl *a*, *b*, and *c*, and Total Carotenoids to the Respective Pigment Concentrations

Pigments	Band center (nm)	A	B	r^2
Chl *a*	384	0.1883	0.3353	0.71
	413	0.0585	0.5335	0.87
	440	0.1386	0.5477	0.93
	623	0.02121	0.6039	0.90
	676	0.0490	0.8056	0.95
	700	0.0118	0.3075	0.50
Chl *b*	464	0.2423	0.6221	0.75
	655	0.1988	0.7064	0.69
Chl *c*	461	0.2180	0.4084	0.89
	583*	0.0939	0.3877	0.85
	644	0.0729	0.4907	0.92
Carotenoids	490	0.1188	0.3665	0.91
	532	0.0843	0.3825	0.89

Data are presented for the cruises in the New York / New Jersey Harbor Estuary from August 2008 to June 2009.

* Absorption was partially contributed by Chl *a*.

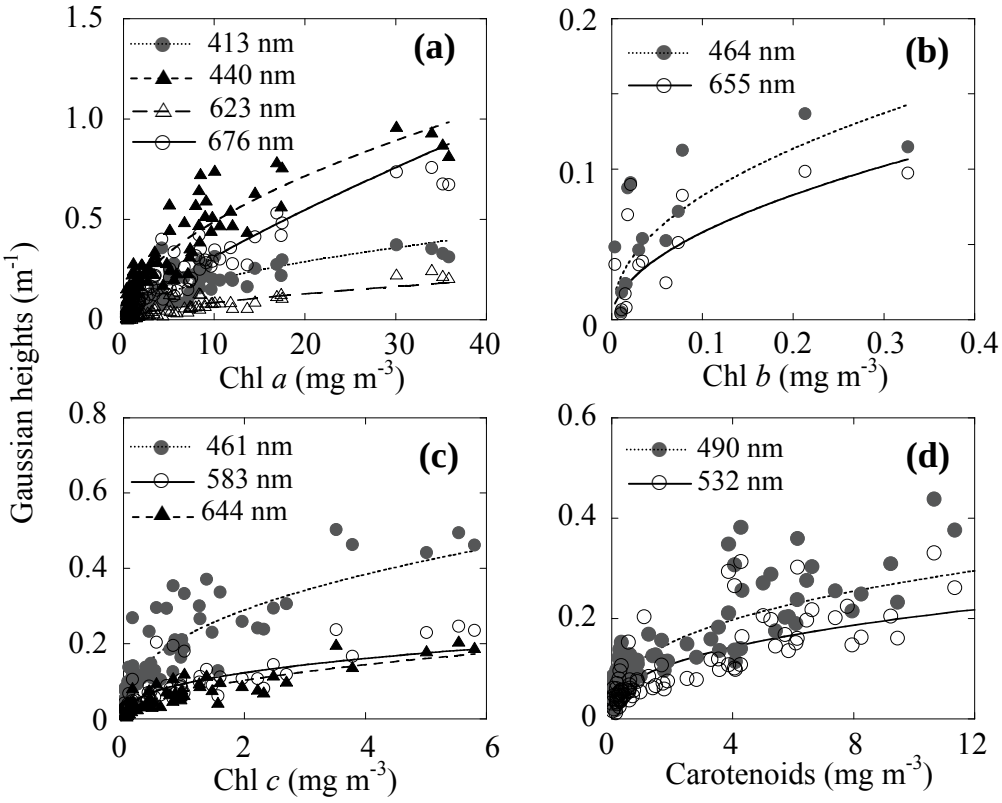

Figure 8.3 Gaussian heights versus pigment concentrations for (a) Chl *a*, (b) Chl *b*, (c) Chl *c*, and (d) Carotenoids.

a strong correlation with Chl *c* concentrations (r^2 = 0.90) (Table 8.2, Figure 8.3 c). Slightly lower correlations were found at 583 nm (r^2 = 0.85) and may be due to the absorption contributions from Chl *a* at this wavelength (Stuart et al., 1998). At 490 and 532 nm, Gaussian heights showed good correlations (r^2 = 0.90) with carotenoids (Table 8.2, Figure 8.3 d), including diadinoxanthin (diad), fucoxanthin (fuco), peridinin (peri), and ß-carotene (ß-caro). To better understand the contribution from each carotenoid, multilinear regression was applied to the 27 samples containing these four carotienoids with Gaussian heights at 490 nm (G_{490}) and 532 nm (G_{532}) expressed as:

$G_{490} = 0.137 + 0.0064[diad] + 0.0096[fuco] + 0.0258[peri] + 0.125[ß\text{-}caro]$, $r^2 = 0.67$ (8.2)

$G_{532} = 0.097 + 0.0081[diad] + 0.0106[fuco] + 0.0200[peri] + 0.064[ß\text{-}caro]$, $r^2 = 0.71$ (8.3)

Pigment compositions therefore explained 67% and 71% of the variance in Gaussian heights at 490 nm and 532 nm, respectively, comparable to that (68% and 70%, respectively) found by Stuart et al. (1998).

8.2 Calculated Pigment Concentrations Versus HPLC Results

Based on the parameters (Table 8.2) developed from decomposition of phytoplankton spectra, the wavelengths used to link calculated pigment concentrations to HPLC measurements are chosen as 676, 464, 644, and 490 nm for Chl *a*, Chl *b*, Chl *c*, and carotenoids, respectively (Figure 8.4). The resulting equations are (8.4) - (8.7):

$$[\text{Chl } a]_{calc} = 0.8187 + 0.8344\ [\text{Chl } a]_{HPLC},\ r^2 = 0.95 \quad (8.4)$$

$$[\text{Chl } b]_{calc} = 0.0685 + 0.7593\ [\text{Chl } b]_{HPLC},\ r^2 = 0.76 \quad (8.5)$$

$$[\text{Chl } c]_{calc} = -0.0540 + 1.2609\ [\text{Chl } c]_{HPLC},\ r^2 = 0.91 \quad (8.6)$$

$$[\text{Carotenoids}]_{calc} = -0.4555 + 1.7415\ [\text{Carotenoids}]_{HPLC},\ r^2 = 0.91 \quad (8.7)$$

Chl *a* concentrations can be accurately estimated from spectra by Eq. (8.4) with strong correlation coefficients (>0.95) (Figure 8.4 a), suggesting a successful spectra decomposition process. The correlation coefficient for estimating Chl *b* is relatively lower (Figure 8.4 b), $r^2 = 0.76$, compared to that for Chl *a*. This result may be due to only 20% of collected samples containing (lower) Chl *b* concentrations (Figure 7.1). Both calculated Chl *c* and carotenoids concentrations showed good correlations with HPLC

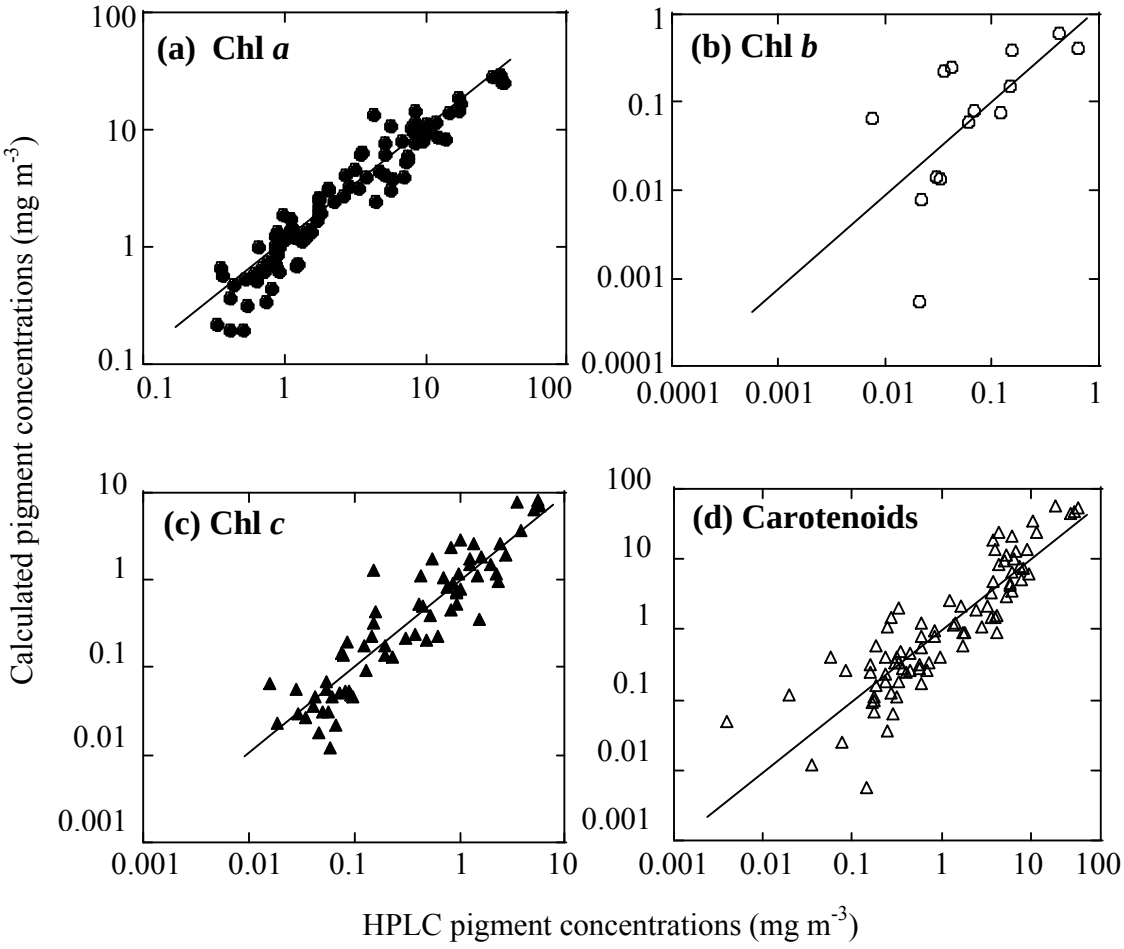

Figure 8.4 Computed concentration of pigments versus HPLC results.

results, r^2 = 0.91 (Figure 8.4 c and d). Hoepffner and Sathyendranath (1991) also obtained good correlations (r^2 = 0.97, 0.77, 0.92, and 0.96 for Chl *a*, *b*, and *c*, and carotenoids, respectively) between the calculated and measured pigment concentrations. However their equations were based on low pigment concentrations, < 3.0, < 0.4, < 0.3, and < 2.0 mg m^{-3} for Chl *a*, *b*, and *c*, and carotenoids, respectively, while concentrations

were greater in this research: < 40, < 0.6, < 4, and < 12 mg m^{-3}, respectively (Table 8.3). This difference indicates the equations developed in this research are more practical for coastal waters, where the pigment concentrations are generally greater than that in open oceans.

8.3 Implication for Remote Sensing Application

To utilize remote sensing for retrieve water quality conditions, atmospheric correction is a required (Gordon and Clark, 1981; Gordon, 1997). The associated procedures have been applied to the CZCS (Coastal Zone Color Scanner), MODIS (Moderate Resolution Imaging Spectroradiometer), SeaWiFS (Sea-viewing Wide Field-of-view Sensor), and MERIS (Medium Resolution Imaging Spectrometer) (Moore et al., 1999). Subsequently, CDOM and NAP contributions can be subtracted, and the phytoplankton spectra may be used to estimate the marker phytoplankton pigments for the NY/NJ Harbor Estuary based on the equations developed, (8.4) - (8.7). The efficiency of the method has been tested with SeaWIFS bands (Hoepffner and Sathyendranath, 1991). However, because of the overlapping maximum wavelength of the carotenoids, further accessory (marker) pigments such as fucoxanthin, diadinoxanthin, and peridinin, cannot be separated from absorption spectra at this time. Nevertheless, the results presented here provide insights for investigating algal species from pigment concentrations for at least Chl *a*, *b*, and *c*. In systems where one algal class dominates, absorption spectra can clarify algal bloom structure and function, for example, dianoflagellate blooms caused by *Gymnodinium breve* (Millie et al., 1997) and *Alexandrium tamarense* (Leong and Taguchi, 2006).

Table 8.3 Comparison of the Pigment Concentration Ranges Tested to Develop Equations for Estimating Pigment Concentrations from Gaussian Bands Obtained by Decomposing Phytoplankton Absorption Spectra

Pigments	Concentration range (μg L^{-1})		r^2	
	Hoepffner and Sathyendranath (1991)	This study	Hoepffner and Sathyendranath (1991)	This study
Chl *a*	< 3.0	< 40	0.97	0.95
Chl *b*	< 0.4	< 0.6	0.77	0.76
Chl *c*	< 0.3	< 4	0.92	0.91
Carotenoids	< 2.0	< 12	0.96	0.91

CHAPTER 9

CONCLUSIONS AND FUTURE WORK

Water quality is a function of the adjacent land use and affects the characteristics of the algal community in the NY/NJ coastal water, including the NY/NJ Bight and the NY/NJ Harbor Estuary. One significant bloom in the NY/NJ Bight is brown tides caused by *Aureococcus anophagefferens*, and the effect of heavy metal on its blooms is one aspect addressed in this research. Red, blue, and green tides caused by diatom and dinoflagellate dominate the NY/NJ Harbor Estuary, and hence application of bio-optical characteristics used in remote sensing for rapid detection of these blooms is another important aspect of this research.

The effects of macronutrients (N and P) on brown tides blooms have been well studied. This study focused on interaction of heavy metals, Cd, Cu, Ni, and Zn, with brown tide alga *A. anophagefferens* which has bloomed in the NY/NJ Bight since 1985. Culture studies conducted in the laboratory showed that *A. anophagefferens* is sensitive to Cd and less sensitive to Cu compared with other species. The presence of dissolved Zn in coastal water resulted in growth inhibition for *A. anophagefferens*. Most strikingly, the environmentally relevant Ni concentrations ($10^{-11.23}$ - $10^{-8.23}$ M Ni^{2+}) stimulated growth of *A. anophagefferens* by as much as 77% of the control (no Ni addition). As a result, shallow coastal water with Ni concentrations typical for the area may promote brown tide blooms. Furthermore, metal (Cd, Ni, and Zn) bioaccumulation by *A. anophagefferens* was quantified in short-term (48 - 72 h) experiments and modeled using the Langmuir isotherm. As an application of short-term results, a hypothetical Category 3 bloom of 10^6

cell/mL in the Narragansett Bay, RI, may remove approximately 10.23 - 12.95% Cd, 0.44 - 0.74% Ni, and 2.61 - 7.43% Zn from the water column. The fate of metals in turn may influence other algal species.

Therefore, future work recommended includes testing the relationship between brown tides and heavy metals with field incubation experiments, and further probing the molecular mechanism(s) influencing growth in the presence of Ni. This focus should include investigating sub-intracellular Ni distribution and related enzymatic reactions.

For the NY/NJ Harbor Estuary, namely Jamaica Bay, Hudson/Raritan Bay, and Inner Harbor, rapidly determining the formation of blooms is a major mission for water quality control in the area. This research focuses on the development of a temporal and spatial database of bio-optical characteristics to improve the accuracy of existing remote sensing modeling.

Seasonal (August 2008 - June 2009) sampling was conducted to investigate variations of the light absorption coefficient, $a(\lambda)$, with contributions from CDOM, phytoplankton, and NAP. The absorption budget showed that the NAP contribution was relatively constant, 18 ± 6% for the entire area, with phytoplankton making up the dominant contribution for Jamaica Bay (44 ± 15%) and CDOM for the Inner Harbor (57 ± 16%) and Hudson/Raritan Bay (50 ± 17%). Because the NAP contribution was relatively constant, it may be subtracted from the total spectra. The exponential slope of the CDOM spectra, S_{CDOM}, 0.0160 ± 0.002 nm^{-1} is comparable to typical coastal water. The wide range of S_{CDOM} (0.0080 - 0.0227 nm^{-1}) and its narrow variation (0.0160 ± 0.0020) suggests in situ CDOM sources dominate along with terrigenous sources. On the other hand, the slope of NAP, S_{NAP}, 0.0138 ± 0.0015 nm^{-1} is greater than that reported for

most other coastal waters, indicating organic particles as the primary source. Based on the HPLC pigment analysis and the packaging effect, cell size was confirmed as the major factor contributing to the variability observed in the specific absorption coefficient with the dominance of large algal cells, diatoms and dinoflagellates. Moreover, pigment composition may be contribute as well to variability of the specific absorption coefficient at low Chl *a* concentrations (<10 mg m^{-3}) as compared to greater ones (>10 mg m^{-3}).

To connect remote sensing data to the results from this study, obtained phytoplankton spectra were decomposed into Gaussian bands, representing major pigments, Chl *a*, *b*, and *c*, and carotenoids. Relationships between heights of Gaussian curves and the HPLC pigment concentrations were established and resulted in high correlation coefficients, 0.95, 0.76, 0.91, and 0.91 for Chl *a*, *b*, and *c*, and carotenoides, respectively. Using these equations, pigment concentrations may be estimated from the remote sensing reflectance spectra after preprocessing for air-correction and retrieval through a bio-optical model.

Based on the temporal and spatial database of bio-optical characteristics, algal bloom distribution may be rapidly characterized from absorption spectra in the future. Furthermore, the dynamic analysis of absorption may provide useful information in the developing predictions of poor water quality conditions. For example, the change in trend of the CDOM spectra, NAP spectra, and pigment concentration will be helpful to forecast pollution from dissolved organic matter, suspended particles, and algal communities. Future work associated with water quality monitoring in the NY/NJ Harbor Estuary can include application of parameters (such as S_{CDOM}, S_{NAP}, and a_{ph}^{*} (440)) developed in this research to update the existing remote sensing models and further examine their utility.

APPENDIX A

COMPOSITION OF AQUIL-SI MEDIUM

This appendix lists the composition of Aquil-Si medium.

Table A.1 Composition of Aquil-Si Medium

Substance	Final Concentration (M)
Synthetic ocean water (SOW) (Appendix B)	
Nutrients	
$NaH_2PO_4 \cdot 6H_2O$	1.00×10^{-5}
$NaNO_3$	3.00×10^{-4}
Trace metals	
Na_2EDTA	5.00×10^{-6}
$FeCl_3 \cdot 6H_2O$	4.51×10^{-7}
$ZnSO_4 \cdot 7H_2O$	4.00×10^{-9}
$MnCl_2 \cdot 4H_2O$	2.30×10^{-8}
$CoCl_2 \cdot 6H_2O$	2.50×10^{-9}
$CuSO_4 \cdot 5H_2O$	9.97×10^{-10}
$Na_2MoO_4 \cdot 2H_2O$	1.0×10^{-7}
Na_2SeO_3	1.0×10^{-8}
Vitamins	
B_{12}	5.50×10^{-7} g/L
Biotin	5.00×10^{-7} g/L
Thiamine HCl	1.00×10^{-4} g/L

Source: Price et al. (1988/1989).

APPENDIX B

COMPOSITION OF SYNTHETIC OCEAN WATER (SOW)

This appendix lists the composition of synthetic ocean water (SOW).

Table B.1 Composition of SOW

Substance	Final Concentration (M)
NaCl	4.2×10^{-1}
Na_2SO_4	2.88×10^{-1}
KCl	9.39×10^{-3}
$NaHCO_3$	2.38×10^{-4}
KBr	8.40×10^{-4}
H_3BO_3	4.85×10^{-5}
NaF	7.14×10^{-5}
$MgCl_2\cdot6H_2O$	5.46×10^{-2}
$CaCl_2\cdot2H_2O$	1.05×10^{-2}
$SrCl_2\cdot6H_2O$	6.38×10^{-5}

Source: Price et al. (1988/1989).

APPENDIX C

SAMPLING CONDITIONS
IN THE NEW YORK / NEW JERSEY HARBOR ESTUARY, 2008 - 2009

This appendix presents condition of sampling locations in the New York/New Jersey Harbor Estuary during 2008 -2009.

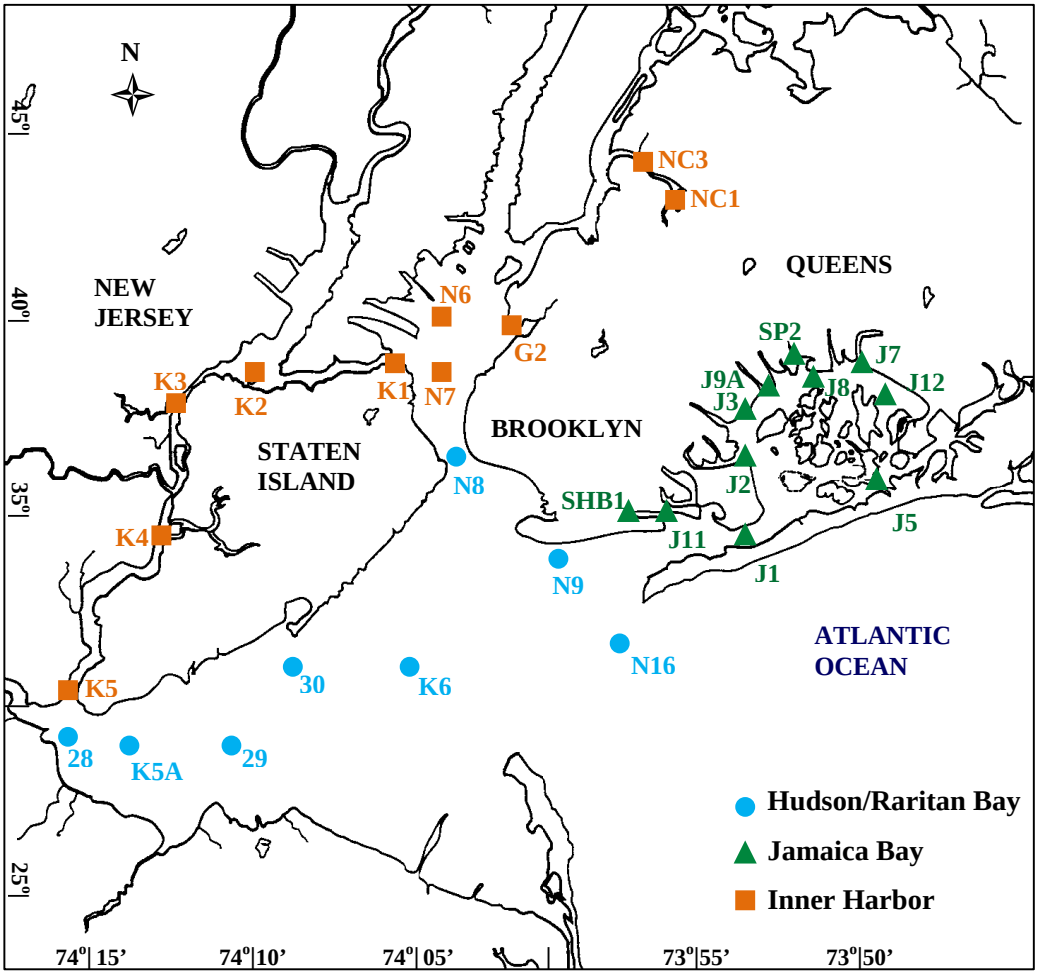

Figure C.1 Sampling locations at New York / New Jersey Harbor Estuary including Hudson/Raritan Bay (blue), Jamaica Bay (green), and Inner Harbor (brown). Sampling at sites of 28, 29, and 30 were conducted in collaboration with Passaic Valley Sewerage Commissioners (PVSC), and all others (J1, J2, J3, J4, J5, J7, J8, J9A, J11, J12, SP2, SHB1, K1, K2, K3, K4, K5, K5A, K6, N6, N7, N8, N9, N16, NC1, and NC3) were conducted in collaboration with New York City Department of Environmental Protection (NYCDEP).

Table C.1 Sampling Conditions in the New York / New Jersey Harbor Estuary, August 2008 - June 2009

Date	Site[1]	Latitude ^{o}	Longitude ^{o}	Depth ft	Salinity psu	Temperature ^{o}C	O_2 mg/L	Conductivity S/M	Sigma-T Kg/m^3	pH	Fecal Coliform #/100 mL
8/12/2008	N9	40.569170	-73.985000	3	27.90	21.38	6.78	4.03	19.00	7.62	QD[2]
8/12/2008	N16	40.529330	-73.943670	3	29.22	21.53	6.90	4.21	19.95	7.73	QD
8/12/2008	J11	40.581670	-73.931330	3	28.35	22.39	7.45	4.17	19.07	7.77	QD
8/12/2008	SHB1	40.582500	-73.946830	4	28.51	23.35	7.40	4.27	18.92	7.48	QD
8/12/2008	J1	40.573830	-73.883500	3	28.09	23.76	6.86	4.25	18.49	7.91	QD
8/12/2008	J2	40.608670	-73.885170	4	27.68	23.73	6.71	4.20	18.19	7.89	QD
8/12/2008	J3	40.626830	-73.884000	3	27.79	24.00	5.56	4.23	18.20	7.71	QD
8/12/2008	J9A	40.633500	-73.873330	3	27.41	23.88	5.89	4.17	17.94	7.74	QD
8/12/2008	SP2	40.643170	-73.854170	4	27.25	23.89	3.51	4.15	17.82	7.62	QD
8/12/2008	J8	40.642330	-73.849830	4	27.03	24.04	3.36	4.13	17.61	7.63	300
8/12/2008	J7	40.644330	-73.820170	3	26.19	24.97	2.92	4.09	16.70	7.45	240
8/12/2008	J12	40.633000	-73.805667	4	26.25	24.56	7.08	4.07	16.87	7.80	2
8/12/2008	J5	40.597830	-73.807170	4	27.21	24.02	4.72	4.16	17.75	7.75	34
8/13/2008	G2	40.666000	-74.003670	3	19.25	22.78	8.92	2.96	12.09	7.80	24
8/13/2008	N7	40.643670	-74.052830	5	14.98	23.77	8.93	2.41	8.62	7.73	88
8/13/2008	N8	40.606830	-74.044330	4	17.17	23.60	8.62	2.72	10.31	7.85	64
8/13/2008	K6	40.511170	-74.099830	4	23.68	23.20	7.80	3.61	15.32	7.77	4
8/13/2008	K5A	40.483830	-74.244670	4	23.61	23.86	5.08	3.65	15.09	7.35	2
8/13/2008	K5	40.509830	-74.258670	4	22.29	24.07	5.28	3.47	14.03	7.49	12
8/13/2008	K4	40.565500	-74.213500	4	21.15	24.64	6.21	3.35	13.01	7.62	50

[1] The sites were named by NYC DEP and PVSC (Figure C.1). Only latitude and longitude of the sites were taken into account in this research, and the site names were not mentioned in the text.

[2] QD = Questionable Data.

Table C.1 Sampling Conditions in the New York / New Jersey Harbor Estuary, August 2008 - June 2009 (Continued)

Date	Site	Current		Wind		NO_3/NO_2_N mg/L	NH_3_N mg/L	Ortho_P mg/L	TKN_N mg/L	SiO_2 mg/L	Total P mg/L	TSS mg/L	Chl *a* µg/L	DOC mg/L
		knots	Dir.[3]	mph	Dir.									
8/12/2008	N9	0.8	S	13	N	0.056	0.122	0.045	1.370	0.434	0.099	16.8	1.692	7.30
8/12/2008	N16	1	SE	7	N	0.039	0.116	0.053	1.440	0.382	0.117	12.2	1.664	2.80
8/12/2008	J11	0.1	E	7	N	0.076	0.097	0.056	1.440	0.442	0.142	9.6	9.202	3.40
8/12/2008	SHB1	0.5	S	9	NW	0.090	0.176	0.072	1.790	1.140	0.162	9.6	19.224	4.20
8/12/2008	J1	1.1	SE	10	N	0.065	0.150	0.125	1.910	0.360	0.265	17.6	34.027	4.80
8/12/2008	J2	0.7	S	9	NW	0.135	0.290	0.163	3.810	0.475	0.308	15.2	33.446	3.90
8/12/2008	J3	0.7	SE	10	N	0.122	0.351	0.170	1.770	0.714	0.282	8.0	22.342	5.30
8/12/2008	J9A	0.7	SE	11	N	0.146	0.420	0.190	2.180	0.760	0.314	23.2	25.129	4.30
8/12/2008	SP2	0.6	S	8	N	0.190	0.641	0.236	3.120	0.941	0.399	18.4	32.160	5.10
8/12/2008	J8	0.9	SE	13	N	0.188	0.621	0.235	3.880	0.869	0.381	24.0	24.886	4.40
8/12/2008	J7	0.9	S	12	N	0.136	0.735	0.285	4.030	1.170	0.452	15.2	29.275	3.40
8/12/2008	J12	1.5	SE	10	N	0.217	0.673	0.251	7.420	0.873	0.444	15.2	50.544	4.60
8/12/2008	J5	0.1	SE	6	NW	0.106	0.296	0.197	4.190	0.956	0.346	27.6	32.357	5.20
8/13/2008	G2	0.4	W	2	NW	0.204	0.127	0.064	0.482	0.462	0.126	9.6	13.864	4.20
8/13/2008	N7	1.1	S	9	SW	0.213	0.162	0.069	0.546	0.603	0.118	5.6	16.040	5.30
8/13/2008	N8	1.7	S	12	SE	0.193	0.161	0.066	0.564	0.558	0.114	8.0	10.580	3.50
8/13/2008	K6	0.3	N	8	SE	0.234	0.070	0.077	0.584	0.812	0.160	8.8	7.766	5.30
8/13/2008	K5A	1.3	W	11	E	0.358	0.378	0.152	0.733	1.390	0.223	6.0	6.977	3.50
8/13/2008	K5	0.7	W	9	E	0.416	0.450	0.163	0.786	1.440	0.234	9.6	5.569	6.20
8/13/2008	K4	0.6	NW	11	E	0.444	0.468	0.167	0.797	1.510	0.238	7.2	6.525	4.00

[3] Dir. = Direction

Table C.1 Sampling Conditions in the New York / New Jersey Harbor Estuary, August 2008 - June 2009 (Continued)

Date	Site	Latitude ^{o}	Longitude ^{o}	Depth ft	Salinity psu	Temperature ^{o}C	O_2 mg/L	Conductivity S/M	Sigma-T Kg/m^3	pH	Fecal Coliform #/100 mL
8/13/2008	K3	40.637330	-74.195670	4	37	23.51	6.66	78.58	13.23	7.60	217
8/13/2008	K2	40.641170	-74.153170	5	26	23.16	7.30	81.64	13.06	7.70	28
8/13/2008	K1	40.649670	-74.084000	4	46	23.09	7.92	76.15	12.03	7.77	40
8/13/2008	N6	40.664000	-74.053000	4	50	24.07	10.15	75.95	8.29	8.11	88
8/13/2008	NC1	40.723833	-73.926167	5	17	24.02	11.44	9.84	12.74	7.16	180
8/13/2008	NC3	40.737170	-73.946170	4	22	23.76	2.22	29.20	13.24	7.06	132
9/16/2008	N9	40.568830	-73.983170	4	17	19.57	6.41	82.62	21.40	7.66	2
9/16/2008	N16	40.529500	-73.942670	4	25	19.73	6.49	79.46	21.39	7.74	1
9/16/2008	J11	40.581670	-73.931330	4	20	21.20	5.69	70.45	19.48	7.64	288
9/16/2008	SHB1	40.582670	-73.947170	4	39	21.59	3.48	18.32	18.89	7.49	840
9/16/2008	J1	40.573830	-73.883170	4	30	22.14	5.85	78.00	18.43	7.62	14
9/16/2008	J2	40.609170	-73.885500	4	39	22.61	5.45	66.63	17.84	7.55	37
9/16/2008	J3	40.627000	-73.883000	5	33	22.74	4.99	60.13	17.31	7.49	38
9/16/2008	J9A	40.633830	-73.873330	5	18	22.94	4.86	58.22	16.93	7.48	26
9/16/2008	SP2	40.643000	-73.853830	4	20	23.10	3.75	50.12	16.56	7.39	48
9/16/2008	J8	40.642670	-73.849830	4	22	23.17	3.78	44.48	16.42	7.40	65
9/16/2008	J7	40.645000	-73.820830	4	23	23.27	4.14	38.58	15.84	7.38	48
9/16/2008	28										
9/16/2008	29										
9/16/2008	30										
9/16/2008	J12	40.633170	-73.806000	4	24.77	23.38	5.68	3.77	16.09	7.49	16
9/16/2008	J5	40.598000	-73.807670	4	25.37	23.20	5.11	3.84	16.59	7.48	16
9/17/2008	G2	40.666500	-74.003670	5	23.76	22.16	3.37	3.54	15.66	7.21	184
9/17/2008	N7	40.643500	-74.053830	4	24.49	21.77	4.97	3.61	16.31	7.37	40
9/17/2008	N8	40.606330	-74.043830	4	23.80	21.82	5.27	3.52	15.78	7.37	8

Table C.1 Sampling Conditions in the New York / New Jersey Harbor Estuary, August 2008 - June 2009 (Continued)

Date	Site	Current		Wind		NO_3/NO_2_N mg/L	NH_3_N mg/L	Ortho_P mg/L	TKN_N mg/L	SiO_2 mg/L	Total P mg/L	TSS mg/L	Chl *a* µg/L	DOC mg/L
		knots	Dir.	mph	Dir.									
8/13/2008	K3	0.1	NE	9	SE	0.376	0.484	0.157	0.806	1.400	0.224	9.6	7.000	4.30
8/13/2008	K2	0.9	NE	10	SE	0.300	0.266	0.118	0.579	0.957	0.178	9.2	9.859	4.10
8/13/2008	K1	0.9	NW	8	SE	0.198	0.190	0.074	0.524	0.529	0.134	10.4	12.220	3.30
8/13/2008	N6	1.1	NE	13	S	0.199	0.084	0.052	0.562	0.454	0.106	9.6	19.982	4.00
8/13/2008	NC1	0.2	NW	6	W	0.052	0.616	0.261	1.780	1.020	0.462	9.6	29.200	3.90
8/13/2008	NC3	0.1	W	3	NW	0.175	0.784	0.229	1.550	1.650	0.362	13.6	10.506	3.70
9/16/2008	N9	0.1	W	7	S	0.055	0.118	0.046	0.869	0.444	0.074	6.8	1.232	2.70
9/16/2008	N16	1.4	SE	2	S	0.041	0.080	0.036	1.050	0.368	0.069	4.8	4.794	2.60
9/16/2008	J11	0.1	NW	4	S	0.152	0.262	0.089	1.140	1.000	0.142	5.6	14.770	2.90
9/16/2008	SHB1	0.2	NW	5	S	0.192	0.411	0.120	1.730	1.360	0.190	5.6	9.466	3.60
9/16/2008	J1	1	W	2	S	0.160	0.446	0.166	1.400	1.120	0.215	11.6	16.400	3.60
9/16/2008	J2	0.9	SE	1	S	0.196	0.573	0.171	2.230	1.350	0.251	13.6	17.210	3.70
9/16/2008	J3	1	NW	0	--	0.233	0.903	0.220	2.060	1.660	0.317	8.4	21.080	4.00
9/16/2008	J9A	1	NW	1	S	0.234	0.976	0.232	2.300	1.770	0.343	15.2	22.139	3.70
9/16/2008	SP2	0.9	NW	4	S	0.199	1.120	0.279	2.760	1.930	0.387	10.0	20.518	4.20
9/16/2008	J8	0.3	W	4	S	0.208	1.110	0.287	2.760	1.880	0.400	7.2	18.523	4.20
9/16/2008	J7	0.1	W	1	S	0.249	1.290	0.316	2.730	1.920	0.430	7.2	16.160	4.10
9/16/2008	28												< 2.400	15.00
9/16/2008	29												< 2.400	23.00
9/16/2008	30												2.500	13.00
9/16/2008	J12	0.8	W	0	S	0.194	1.110	0.294	2.380	1.750	0.405	4.0	21.533	4.00
9/16/2008	J5	0.6	SW	2	S	0.208	0.568	0.220	1.930	1.550	0.316	9.6	21.084	4.00
9/17/2008	G2	0.1	W	2	NE	0.381	0.433	0.146	3.550	1.380	0.199	10.4	2.396	3.70
9/17/2008	N7	0.2	S	6	NE	0.335	0.392	0.130	1.270	1.490	0.170	26.4	2.646	3.80
9/17/2008	N8	1.7	S	4	N	0.326	0.398	0.120	1.950	1.500	0.170	8.6	4.260	3.30

Table C.1 Sampling Conditions in the New York / New Jersey Harbor Estuary, August 2008 - June 2009 (Continued)

Date	Site	Latitude ^{o}	Longitude ^{o}	Depth ft	Salinity psu	Temperature ^{o}C	O_2 mg/L	Conductivity S/M	Sigma-T Kg/m^3	pH	Fecal Coliform #/100 mL
9/17/2008	K6	40.510500	-74.100670	5	25.42	22.20	5.93	3.77	16.90	7.41	1
9/17/2008	K5A	40.484170	-74.244670	4	23.09	22.63	4.27	3.48	15.03	7.27	16
9/17/2008	K5	40.510500	-74.258330	4	22.89	22.64	4.03	3.46	14.88	7.25	30
9/17/2008	K4	40.565500	-74.212830	4	20.65	23.18	4.65	3.18	13.04	7.23	84
9/17/2008	K3	40.637670	-74.194830	4	19.41	23.00	5.11	3.00	12.16	7.25	112
9/17/2008	K2	40.640830	-74.153330	4	21.19	22.12	4.98	3.19	13.73	7.28	50
9/17/2008	K1	40.649670	-74.083500	4	23.67	21.63	4.89	3.49	15.73	7.30	4
9/17/2008	N6	40.664830	-74.052330	4	25.05	21.20	5.35	3.64	16.89	7.32	4
9/17/2008	NC1	40.723830	-73.926500	5	22.31	22.63	2.12	3.38	14.44	6.92	40
9/17/2008	NC3	40.737330	-73.946500	4	23.33	22.49	3.18	3.51	15.25	7.09	32
11/18/2008	N9	40.569170	-73.985000				9.51			7.55	17
11/18/2008	N16	40.529500	-73.942670				9.25			7.86	4
11/18/2008	J11	40.581670	-73.931330				9.23			7.67	71
11/18/2008	SHB1	40.582670	-73.947170				8.47			7.75	680
11/18/2008	J1	40.574040	-73.884740				9.37			7.83	12
11/18/2008	J2	40.608580	-73.885600				9.56			7.67	55
11/18/2008	J3	40.626830	-73.884000				9.56			7.80	54
11/18/2008	J9A	40.633500	-73.873330				9.37			7.72	64
11/18/2008	SP2	40.643170	-73.854170				9.42			7.78	372
11/18/2008	J8	40.642330	-73.849830				9.40			7.79	66
11/18/2008	J7	40.644330	-73.820170				9.15			7.72	196
11/18/2008	J12	40.633000	-73.805667				9.71			7.75	180
11/18/2008	J5	40.597830	-73.807170				9.95			7.79	36
11/2020/08	G2	40.666000	-74.003670				9.17			7.83	16

Table C.1 Sampling Conditions in the New York / New Jersey Harbor Estuary, August 2008 - June 2009 (Continued)

Date	Site	Current		Wind		NO_3/NO_2_N mg/L	NH_3_N mg/L	Ortho_P mg/L	TKN_N mg/L	SiO_2 mg/L	Total P mg/L	TSS mg/L	Chl *a* µg/L	DOC mg/L
		knots	Dir.	mph	Dir.									
9/17/2008	K6	1	SE	3	N	0.317	0.258	0.128	1.720	1.590	0.194	4.8	8.310	3.80
9/17/2008	K5A	0.9	SE	2	N	0.442	0.444	0.172	2.080	2.140	0.220	8.8	5.434	4.00
9/17/2008	K5	0.9	S	6	N	0.456	0.477	0.170	2.090	2.120	0.236	19.2	4.460	3.60
9/17/2008	K4	0.8	SW	2	N	0.590	0.662	0.196	1.990	1.920	0.261	15.2	2.812	3.70
9/17/2008	K3	0.3	SW	5	N	0.538	1.430	0.207	3.090	2.240	0.264	7.2	1.860	4.60
9/17/2008	K2	0.3	S	3	N	0.442	0.504	0.159	1.620	1.630	0.212	7.2	1.895	4.00
9/17/2008	K1	0.1	E	7	N	0.366	0.404	0.139	2.330	1.620	0.182	19.2	1.972	3.90
9/17/2008	N6	0.1	E	9	N	0.288	0.528	0.132	1.680	1.470	0.172	13.2	2.740	3.70
9/17/2008	NC1	0.2	S	3	NE	0.153	0.730	0.220	3.420	2.200	0.333	8.8	18.040	3.80
9/17/2008	NC3	0.2	S	1	NE	0.404	0.545	0.191	3.000	2.090	0.242	9.6	5.676	3.80
11/18/2008	N9	0.2	E	10	NE	0.212	0.222	0.062	1.140	0.792	0.092	17.6	1.500	2.20
11/18/2008	N16	0.4	N	19	N	0.088	0.068	0.040	0.884	0.551	0.066	15.2	1.300	2.40
11/18/2008	J11	WEAK	ND	9	N	0.291	0.290	0.072	1.750	1.120	0.102	8.8	4.400	2.20
11/18/2008	SHB1	WEAK	E	8	N	0.472	0.310	0.074	1.080	1.660	0.106	16.4	4.400	2.70
11/18/2008	J1	WEAK	E	15	N	0.232	0.206	0.058	1.020	0.758	0.095	20.8	2.600	2.40
11/18/2008	J1	WEAK	E	15	N	0.232	0.206	0.058	1.020	0.758	0.095	20.8	2.600	2.40
11/18/2008	J2	0.5	S	18	N	0.434	0.542	0.098	1.870	1.200	0.136	16.0	3.400	2.60
11/18/2008	J3	WEAK	W	17	NE	0.432	0.517	0.094	1.530	1.160	0.134	18.4	4.900	2.60
11/18/2008	J9A	0.2	W	17	NE	0.582	0.870	0.141	2.050	1.420	0.213	6.4	4.400	3.30
11/18/2008	SP2	WEAK	W	14	N	0.518	0.650	0.111	1.350	1.380	0.153	21.2	4.500	2.60
11/18/2008	J8	0.5	W	13	N	0.530	0.660	0.120	1.810	1.320	0.153	13.6	4.600	2.80
11/18/2008	J7	0.7	S	14	N	0.725	1.120	0.161	2.720	1.650	0.217	11.2	5.300	3.70
11/18/2008	J12	0.5	W	24	N	0.710	1.330	0.189	2.070	1.730	0.261	14.4	6.600	3.10
11/18/2008	J5	1.2	W	19	N	0.624	0.760	0.124	2.130	1.520	0.171	8.8	4.800	3.20
11/20/2008	G2	0.3	E	10	WNW	0.468	0.388	0.113	1.500	1.330	0.167	6.4	0.900	3.10

Table C.1 Sampling Conditions in the New York / New Jersey Harbor Estuary, August 2008 - June 2009 (Continued)

Date	Site	Latitude ^{o}	Longitude ^{o}	Depth ft	Salinity psu	Temperature ^{o}C	O_2 mg/L	Conductivity S/M	Sigma-T Kg/m^3	pH	Fecal Coliform #/100 mL
11/2020/08	N7	40.643500	-74.053830				9.59			7.66	56
11/2020/08	N8	40.606330	-74.043830				9.65			7.86	38
11/2020/08	K6	40.510940	-74.100020				10.08			7.87	23
11/2020/08	K5A	40.484220	-74.245360				10.13			7.77	40
11/2020/08	K5	40.510890	-74.258660				9.68			7.83	16
11/2020/08	K4	40.565840	-74.213440				9.53			7.72	36
11/2020/08	K3	40.637430	-74.195960				9.47			7.75	48
11/2020/08	K2	40.641160	-74.152940				9.71			7.79	36
11/2020/08	K1	40.649540	-74.082680				9.59			7.87	28
11/2020/08	N6	40.663950	-74.052380				9.77			7.90	28
11/2020/08	NC1	40.723833	-73.926167				5.41			7.09	330
11/2020/08	NC3	40.737170	-73.946170				6.06			7.26	251
12/03/2008	28										
12/03/2008	29										
12/03/2008	30										
3/10/2009	N9	40.568830	-73.983000	3	29.70	4.78	6.94	2.86	23.51	8.03	11
3/10/2009	J11	40.581830	-73.931330	3	29.72	4.66	6.14	2.85	23.53	8.04	49
3/10/2009	SHB1	40.582670	-73.947330	3	27.85	5.00	6.23	2.73	22.00	8.14	192
3/10/2009	J1	40.573500	-73.884170	3	28.84	4.66	6.16	2.78	22.83	8.48	6
3/10/2009	J2	40.608330	-73.885670	3	28.22	4.81	5.48	2.73	22.33	8.48	2
3/10/2009	J3	40.627170	-73.883000	3	27.66	4.77	5.34	2.69	21.88	8.53	2
3/10/2009	J9A	40.633670	-73.873000	3	27.28	4.60	4.91	2.64	21.60	8.58	3
3/10/2009	SP2	40.643000	-73.854000	3	27.00	4.63	4.81	2.61	21.38	8.66	2
3/10/2009	J8	40.642670	-73.850000	3	26.97	4.57	4.51	2.59	21.34	8.61	4
3/10/2009	J7	40.645000	-73.820500	3	25.59	5.61	4.90	2.56	19.74	8.77	2

Table C.1 Sampling Conditions in the New York / New Jersey Harbor Estuary, August 2008 - June 2009 (Continued)

Date	Site	Current		Wind		NO_3/NO_2_N mg/L	NH_3_N mg/L	Ortho_P mg/L	TKN_N mg/L	SiO_2 mg/L	Total P mg/L	TSS mg/L	Chl *a* µg/L	DOC mg/L
		knots	Dir.	mph	Dir.									
11/20/2008	N7	0.5	S	7	W	0.444	0.422	0.103	0.964	1.340	0.131	7.2	1.500	3.00
11/20/2008	N8	0.4	N	12	NW	0.355	0.355	0.093	0.818	1.100	0.113	6.0	1.400	3.10
11/20/2008	K6	0.5	W	13	W	0.355	0.310	0.089	1.080	1.090	0.108	5.6	1.800	3.30
11/20/2008	K5A	WEAK	ND	19	WNW	0.566	0.384	0.120	0.766	2.040	0.144	5.2	1.700	3.40
11/20/2008	K5	WEAK	N	13	NW	0.538	0.333	0.120	0.495	1.670	0.138	12.4	2.100	3.50
11/20/2008	K4	0.6	N	10	NW	0.714	0.603	0.158	1.370	2.160	0.192	6.0	1.400	3.50
11/20/2008	K3	0.6	E	9	W	0.700	0.768	0.148	1.460	2.320	0.182	7.2	1.000	3.40
11/20/2008	K2	0.9	E	13	W	0.615	0.428	0.119	1.250	2.040	0.160	14.8	1.000	4.10
11/20/2008	K1	2	E	9	WNW	0.397	0.352	0.108	1.990	1.270	0.133	16.8	1.200	3.10
11/20/2008	N6	0.7	N	13	WNW	0.404	0.365	0.103	1.310	1.230	0.118	6.8	1.000	3.00
11/20/2008	NC1	SLACK	ND	5.0	NW	0.456	1.010	0.138	1.520	3.150	0.217	6.0	2.700	3.40
11/20/2008	NC3	0.3	E	5	NNW	0.505	0.784	0.135	1.180	2.670	0.187	10.4	1.300	3.10
12/03/2008	28												5.000	18
12/03/2008	29												< 2.400	14
12/03/2008	30												< 2.400	28
3/10/2009	N9	1.1	E	7	E	0.040	0.048	0.011	1.040	< 0.045	0.050	10.8	18.400	2.70
3/10/2009	J11	0.5	E	9	S	0.026	0.030	< 0.010	1.280	< 0.045	0.062	9.6	19.282	2.70
3/10/2009	SHB1	WEAK	E	8	S	0.223	0.058	0.011	0.805	0.081	0.078	10.4	14.893	4.40
3/10/2009	J1	1.1	W	10	S	0.088	0.016	< 0.010	1.340	< 0.045	0.065	8.8	74.547	3.00
3/10/2009	J2	0.6	S	9	S	0.158	0.100	< 0.010	1.210	< 0.045	0.072	8.8	37.330	3.60
3/10/2009	J3	0.8	W	10	S	0.210	0.191	0.012	1.280	< 0.045	0.092	9.6	72.400	4.00
3/10/2009	J9A	0.4	W	10	S	0.248	0.197	0.012	2.140	< 0.045	0.134	10.4	70.240	4.00
3/10/2009	SP2	0.2	W	11	S	0.286	0.227	0.013	1.810	< 0.045	0.166	16.8	68.560	4.10
3/10/2009	J8	0.3	W	11	S	0.287	0.204	< 0.010	2.920	< 0.045	0.215	8.8	71.831	4.20
3/10/2009	J7	0.3	N	9	S	0.437	0.486	0.039	2.630	0.045	0.204	10.4	71.520	4.40

Table C.1 Sampling Conditions in the New York / New Jersey Harbor Estuary, August 2008 - June 2009 (Continued)

Date	Site	Latitude ^{o}	Longitude ^{o}	Depth ft	Salinity psu	Temperature ^{o}C	O_2 mg/L	Conductivity S/M	Sigma-T Kg/m^3	pH	Fecal Coliform #/100 mL
3/10/2009	J12	40.633000	-73.805330	5	27.05	4.28	4.65	2.60	21.47	8.63	3
3/10/2009	J5	40.598000	-73.807330	3	27.38	4.07	4.65	2.61	21.71	8.78	1
3/11/2009	NC0	40.714500	-73.931170	3	21.26	4.03	5.98	2.07	17.71	7.65	68
3/11/2009	NC1	40.723830	-73.926330	3	22.30	4.36	6.49	2.18	17.62	7.90	100
3/11/2009	NC2	40.729000	-73.935170	3	22.24	4.03	5.30	2.16	17.70	8.06	48
3/11/2009	NC3	40.737330	-73.946330	3	19.00	3.73	4.90	1.85	14.31	7.87	48
3/11/2009	N7	40.643500	-74.053830	3	15.70	4.19	5.12	1.57	12.02	7.92	64
3/11/2009	N8	40.606170	-74.043830	3	20.99	3.99	4.65	2.04	14.63	7.98	28
3/11/2009	K6	40.510330	-74.099670	3	24.40	4.51	5.09	1.21	19.33	8.04	2
3/11/2009	K5A	40.484170	-74.245000	3	21.79	4.88	6.31	1.17	17.23	8.32	16
3/11/2009	K5	40.510500	-74.257830	3	23.33	4.57	5.58	2.29	18.11	8.21	10
3/11/2009	K4	40.565830	-74.212330	3	20.65	4.98	4.89	1.07	16.32	7.89	8
3/11/2009	K3	40.637670	-74.195330	3	18.92	4.59	4.26	1.89	14.72	7.76	4
3/11/2009	K2	40.641000	-74.152830	3	19.75	4.57	4.23	1.96	15.57	7.76	12
3/11/2009	K1	40.649500	-74.083330	3	16.04	5.01	4.53	1.64	12.17	7.81	16
3/11/2009	N6	40.664000	-74.052000	3	14.30	3.77	4.79	1.43	8.86	7.74	64
3/11/2009	G2	40.666330	-74.003330	3	18.59	4.04	4.79	1.83	14.60	7.78	16
4/21/2009	N9	40.569170	-73.985000				11.60			7.59	504
4/21/2009	J11	40.582000	-73.931420				11.30			7.82	1340
4/21/2009	SHB1	40.582670	-73.947170				12.83			7.69	4000
4/21/2009	J1	40.573830	-73.883170				11.78			7.91	990
4/21/2009	J2	40.609170	-73.885500				11.31			7.95	2000
4/21/2009	J3	40.627000	-73.883000				11.93			8.01	450
4/21/2009	J9A	40.633830	-73.873330				15.01			8.17	490
4/21/2009	SP2	40.643000	-73.854000				13.11			8.07	530

Table C.1 Sampling Conditions in the New York / New Jersey Harbor Estuary, August 2008 - June 2009 (Continued)

Date	Site	Current		Wind		NO_3/NO_2_N mg/L	NH_3_N mg/L	Ortho_P mg/L	TKN_N mg/L	SiO_2 mg/L	Total P mg/L	TSS mg/L	Chl *a* µg/L	DOC mg/L
		knots	Dir.	mph	Dir.									
3/10/2009	J12	WEAK	N	9	S	0.264	0.084	< 0.010	1.340	< 0.045	0.121	5.6	70.287	4.00
3/10/2009	J5	WEAK	W	8	S	0.081	<0.010	< 0.010	1.270	< 0.045	0.086	9.6	73.040	4.40
3/11/2009	NC1	0.2	N	2	W	0.298	0.142	< 0.010	1.080	0.421	0.087	19.2	65.645	3.80
3/11/2009	NC3	SLACK	--	2	NE	0.320	0.432	0.048	1.200	1.290	0.124	18.0	26.707	3.40
3/11/2009	N7	1.0	S	CALM	--	0.408	0.374	0.050	1.240	2.530	0.083	21.6	11.300	3.30
3/11/2009	N8	2.5	S	CALM	--	0.301	0.352	0.044	0.906	1.440	0.079	20.0	12.544	3.20
3/11/2009	K6	1.1	E	5	W	0.182	0.164	0.015	0.670	0.216	0.057	16.8	41.360	2.70
3/11/2009	K5A	0.6	E	12	W	0.264	0.034	< 0.010	1.200	< 0.045	0.070	13.6	64.602	3.10
3/11/2009	K5	0.4	E	5	W	0.311	0.158	< 0.010	1.170	0.052	0.147	22.4	62.862	3.30
3/11/2009	K4	0.7	S	5	W	0.542	0.636	0.075	1.970	1.060	0.132	14.4	42.160	3.80
3/11/2009	K3	0.6	S	11	SW	0.401	0.412	0.048	1.100	1.730	0.081	13.6	17.054	3.00
3/11/2009	K2	0.6	E	12	W	0.488	0.398	0.052	1.170	2.300	0.084	12.0	16.968	3.60
3/11/2009	K1	0.5	W	7	W	0.395	0.365	0.051	1.420	2.920	0.083	32.8	11.060	6.30
3/11/2009	N6	2.3	S	9	W	0.434	0.366	0.052	1.050	1.520	0.108	13.6	10.120	7.20
3/11/2009	G2	0.3	E	--	--	0.329	0.408	0.050	1.660	1.570	0.102	20.8	23.402	4.70
4/21/2009	N9	0.9	E	CALM	--	0.182	0.140	0.028	1.120	0.984	0.102	7.6	21.900	2.90
4/21/2009	J11	SLACK	--	6	E	0.251	0.045	0.016	1.370	0.674	0.126	12.0	72.200	2.88
4/21/2009	SHB1	SLACK	W	3	E	1.600	0.089	0.031	1.320	5.020	0.113	13.6	30.600	3.20
4/21/2009	J1	0.4	E	CALM	--	0.358	0.370	0.076	1.700	0.580	0.172	21.0	87.800	3.88
4/21/2009	J2	0.7	N	CALM	--	0.484	0.601	0.107	2.000	0.697	0.202	13.4	49.700	3.79
4/21/2009	J3	0.6	E	3	E	0.512	0.652	0.108	3.960	0.770	0.257	12.0	46.000	3.68
4/21/2009	J9A	0.3	E	3	E	0.556	0.814	0.136	3.580	0.971	0.394	17.4	108.800	3.70
4/21/2009	SP2	0.2	E	4	E	0.529	0.782	0.132	3.850	0.936	0.334	9	92.800	3.71

Table C.1 Sampling Conditions in the New York / New Jersey Harbor Estuary, August 2008 - June 2009 (Continued)

Date	Site	Latitude ^{o}	Longitude ^{o}	Depth ft	Salinity psu	Temperature ^{o}C	O_2 mg/L	Conductivity S/M	Sigma-T Kg/m^3	pH	Fecal Coliform #/100 mL
4/21/2009	J8	40.642330	-73.849830				11.15			7.89	590
4/21/2009	J7	40.644330	-73.820170				13.59			8.09	480
4/21/2009	J12	40.633000	-73.805667				18.92			8.38	590
4/21/2009	J5	40.597830	-73.807170				11.34			7.96	217
4/30/2008	28										
4/30/2008	29										
4/30/2008	30										
5/21/2009	N9	40.569060	-73.982820	3	25.51	13.28	7.90	3.10	19.02	7.54	18
5/21/2009	N16	40.526300	-73.942000	3	25.19	14.19	8.82	3.13	18.57	7.69	1
5/21/2009	J11	40.582000	-73.931420	3	27.01	16.45	8.90	3.51	19.51	7.72	24
5/21/2009	J1	40.574040	-73.884740	3	26.60	15.99	10.13	3.43	19.30	7.82	2
5/21/2009	J2	40.608580	-73.885600	3	25.86	17.22	9.03	3.44	18.46	7.88	8
5/21/2009	PB2	40.628280	-73.909940	3	25.68	17.92	11.70	3.46	18.13	8.17	70
5/21/2009	PB3	40.623640	-73.899560	3	25.72	18.05	12.72	3.49	18.18	8.12	2
5/21/2009	J3	40.627480	-73.883220	3	25.62	17.47	11.37	3.43	18.23	7.92	33
5/21/2009	J9A	40.633900	-73.873440	3	25.67	17.29	9.81	3.42	18.32	7.89	32
5/21/2009	SP2	40.643220	-73.853440	3	25.32	17.41	10.75	3.39	18.01	8.05	2
5/21/2009	J8	40.642840	-73.849960	3	25.34	17.45	10.63	3.39	18.02	7.90	8
5/21/2009	J7	40.645220	-73.820640	3	23.91	18.31	16.37	3.28	16.70	8.15	3
5/21/2009	J12	40.633660	-73.805920	3	25.05	17.19	12.58	3.34	17.85	8.01	3
5/21/2009	J5	40.598020	-73.807880	3	26.18	16.18	9.87	3.40	18.94	7.97	5
5/28/2009	NC1	40.723940	-73.926670	3	21.92	16.06	7.07	2.88	15.70	7.35	390
5/28/2009	NC3	40.737400	-73.946720	3	22.46	15.67	7.01	2.92	16.19	7.39	220
5/28/2009	N7	40.644870	-74.054230	3	24.14	15.51	7.25	3.11	17.52	7.58	132
5/28/2009	N8	40.606840	-74.045860	3	25.30	15.28	7.45	3.23	18.45	7.74	128

Table C.1 Sampling Conditions in the New York / New Jersey Harbor Estuary, August 2008 - June 2009 (Continued)

Date	Site	Current		Wind		NO_3/NO_2_N mg/L	NH_3_N mg/L	Ortho_P mg/L	TKN_N mg/L	SiO_2 mg/L	Total P mg/L	TSS mg/L	Chl *a* µg/L	DOC mg/L
		knots	Dir.	mph	Dir.									
4/21/2009	J8	0.3	W	CALM	--	0.517	0.768	0.130	2.920	0.842	0.263	1.8	33.900	3.36
4/21/2009	J7	SLACK	--	6	E	0.564	1.010	0.165	4.940	1.220	0.592	18.2	169.700	4.32
4/21/2009	J12	0.3	N	6	SE	0.558	0.801	0.145	3.960	1.120	0.554	22.3	169.700	4.73
4/21/2009	J5	0.5	E	10	SSE	0.382	0.322	0.081	2.080	0.689	0.166	6.8	33.500	3.50
4/30/2008	28												4.600	23
4/30/2008	29												3.500	24
4/30/2008	30												3.800	29
5/21/2009	N9	0.8	E	7	S		19	0.170	0.148	0.038	0.503	0.761	0.079	1.0
5/21/2009	N16	0.8	S	10	S		19	0.194	0.136	0.039	0.624	0.646	0.070	4.6
5/21/2009	J11	0.2	N	6	S		19	0.304	0.149	0.041	0.668	0.908	0.098	4.8
5/21/2009	J1	1.0	E	14	S		19	0.402	0.265	0.076	1.190	0.344	0.178	4.6
5/21/2009	J2	0.6	N	8	S		19	0.536	0.556	0.112	1.700	0.260	0.244	6.2
5/21/2009	J3	0.7	E	13	S		19	0.581	0.610	0.120	1.770	0.162	0.255	8.6
5/21/2009	J9A	0.5	E	15	S		19	0.604	0.698	0.133	1.940	0.176	0.273	12.6
5/21/2009	SP2	1.3	E	18	S		19	0.542	0.723	0.127	2.180	0.086	0.293	
5/21/2009	J8	0.8	E	19	S		25	0.574	0.663	0.126	1.960	0.107	0.274	10.6
5/21/2009	J7	0.5	N	18	S		25	0.721	0.732	0.134	2.060	0.094	0.318	12.6
5/21/2009	J12	0.4	W	19	S		25	0.512	0.632	0.114	1.870	0.070	0.260	10.0
5/21/2009	J5	1.2	E	20	S		25	0.440	0.222	0.074	1.310	0.279	0.206	17.4
5/28/2009	NC1	0.2	S	7	N		19	0.354	0.230	0.066	1.010	0.975	0.178	6.8
5/28/2009	NC3	0.2	E	3	N		19	0.354	0.331	0.086	0.838	0.920	0.165	7.2
5/28/2009	N7	1.7	N	7	S		19	0.224	0.284	0.062	0.715	0.773	0.089	10.0
5/28/2009	N8	1.2	N	11	S		19	0.186	0.230	0.056	0.672	0.658	0.086	6.6

Table C.1 Sampling Conditions in the New York / New Jersey Harbor Estuary, August 2008 - June 2009 (Continued)

Date	Site	Latitude ^{o}	Longitude ^{o}	Depth ft	Salinity psu	Temperature ^{o}C	O_2 mg/L	Conductivity S/M	Sigma-T Kg/m^3	pH	Fecal Coliform #/100 mL
5/28/2009	K6	40.510940	-74.100020	3	25.21	15.32	8.30	3.22	18.37	7.85	1
5/28/2009	K5A	40.484220	-74.245360	3	21.46	17.24	6.67	2.90	15.10	7.62	2
5/28/2009	K5	40.510890	-74.258660	3	21.87	17.31	6.96	2.96	15.40	7.71	12
5/28/2009	K4	40.565840	-74.213440	3	20.25	18.03	6.18	2.80	14.01	7.44	20
5/28/2009	K3	40.637430	-74.195960	3	19.68	17.84	6.14	2.72	13.62	7.40	12
5/28/2009	K2	40.641160	-74.152940	3	19.98	16.82	6.89	2.70	14.06	7.53	8
5/28/2009	K1	40.649540	-74.082680	3	21.09	16.29	7.00	2.80	15.02	7.57	8
5/28/2009	N6	40.663950	-74.052380	3	22.98	15.74	7.46	2.99	16.58	7.70	4
5/28/2009	G2	40.666420	-74.003480	3	23.17	15.68	6.78	3.01	16.73	7.58	40
6/04/2009	28										
6/04/2009	29										
6/04/2009	30										

Table C.1 Sampling Conditions in the New York / New Jersey Harbor Estuary, August 2008 - June 2009 (Continued)

Date	Site	Current		Wind		NO_3/NO_2_N mg/L	NH_3_N mg/L	Ortho_P mg/L	TKN_N mg/L	SiO_2 mg/L	Total P mg/L	TSS mg/L	Chl *a* µg/L	DOC mg/L
		knots	Dir.	mph	Dir.									
5/28/2009	K6	1.5	E	20	E		19	0.202	0.136	0.043	0.707	0.558	0.085	21.2
5/28/2009	K5A	0.8	E	21	E		12	0.418	0.574	0.064	1.300	0.726	0.118	9.8
5/28/2009	K5	0.9	S	17	E		12	0.412	0.294	0.053	0.791	0.566	0.112	9.4
5/28/2009	K4	0.6	S	7	E		12	0.630	0.507	0.115	0.943	1.590	0.162	15.0
5/28/2009	K3	SLK		6	E		12	0.622	1.140	0.151	1.700	2.170	0.203	10.0
5/28/2009	K2	0.3	E	7	S		12	0.479	0.441	0.098	0.901	1.930	0.138	13.8
5/28/2009	K1	1.4	E	6	S		12	0.394	0.448	0.109	0.857	1.540	0.134	12.4
5/28/2009	N6	1.8	S	6	S		12	0.280	0.328	0.070	0.927	1.040	0.104	11.0
5/28/2009	G2	WEAK	E	6	S		12	0.314	0.346	0.168	0.778	1.060	0.132	10.0
6/04/2009	28												1.000	14
6/04/2009	29												1.100	18
6/04/2009	30												1.500	30

REFERENCES

Ahner, B. A.; Morel, F. M. M. Phytochelatin production in marine algae. 2. Induction by various metals. *Limnology and Oceanography.* **1995**, *40(4)*, 658-665.

Andersen, R. A.; Saunders, G. W.; Paskind, M. P.; Sexton, J. P. Ultrastructure and 18S rRNA gene sequence for Pelagomonas calceolata gen. et sp. nov. and the description of a new algal class, the Pelagophyceae classis nov. *Journal of Phycology.* **1993**, *29(5)*, 701-715.

Astoreca, R.; Rousseau, V.; Lancelot, C. Coloured dissolved organic matter (CDOM) in Southern North Sea waters: Optical characterization and possible origin. *Estuarine, Coastal and Shelf Science.* **2009**, *85(4)*, 633-640.

Babin, M.; Stramski, D.; Ferrari, G. M.; Claustre, H.; Bricaud, A.; Obolensky, G.; Hoepffner, N. Variations in the light absorption coefficients of phytoplankton, nonalgal particles, and dissolved organic matter in coastal waters around Europe. *Journal of Geophysical Research.* **2003**, *108(C7)*, 3211.

Bagheri, S.; Peters, S.; Yu, T. Retrieval of marine water constituents from AVIRIS data in the Hudson/Raritan Estuary. *International Journal of Remote Sensing.* **2005**, *26(18)*, 4013-4027.

Bagheri, S.; Rijkeboer, M.; Gons, H. J. Inherent and apparent optical measurements in the Hudson/Raritan Estuary. *Aquatic Ecology.* **2002**, *36(4)*, 559-562.

Bailey, J. C.; Andersen, R. A. Analysis of clonal cultures of the brown tide algae Aureococcus and Aureoumbra (Pelagophyceae) using 18S rRNA, rbcL, and rubisco spacer sequences. *Journal of Phycology.* **1999**, *35(3)*, 570-574.

Baker, K. M.; Gobler, C. J.; Collier, J. L. Urease gene sequences from algae and heterotrophic bacteria in axenic and nonaxenic phytoplankton cultures. *Journal of Phycology.* **2009**, *45(3)*, 625-634.

Beatley, T.; Brower, D. J.; Schwab, A. K. *An introduction to coastal zone management*; Island Press: Washington, DC, 2002.

Bidigare, R. R., et al. Photosynthetic pigment composition of the brown tide alga: Unique chlorophyll and carotenoid derivatives. In *Novel phytoplankton blooms: causes and impacts of recurrent brown tides and other unusual blooms*; Cosper, E.; Carpenter, E. J.; Bricelj, M. Eds.; Springer: Berlin 1989; pp. 57–75.

Bidigare, R. R.; Ondrusek, M. E.; Morrow, J. H.; Kiefer, D. A. 1990. In vivo absorption properties of algal pigments. *Proc. SPIE*, *1302*, pp. 290-302.

Binding, C. E.; Jerome, J. H.; Bukata, R. P.; Booty, W. G. Spectral absorption properties of dissolved and particulate matter in Lake Erie. *Remote Sensing of Environment.* **2008**, *112(4)*, 1702-1711.

Boesch, DF. *Harmful algal blooms in coastal waters: Options for prevention, control and mitigation*; US Dept. of Commerce, National Oceanic and Atmospheric Administration, Coastal Ocean Office, 1997.

Bowers, D. G.; Harker, G. E. L.; Stephan, B. Absorption spectra of inorganic particles in the Irish Sea and their relevance to remote sensing of chlorophyll. *International Journal of Remote Sensing.* **1996**, *17(12)*, 2449-2460.

Brand, L. E.; Sunda, W. G.; Guillard, R. R. L. Reduction of marine phytoplankton reproduction rates by copper and cadmium. *Journal of Experimental Marine Biology and Ecology.* **1986**, *96(3)*, 225-250.

Breuer, E.; Sañudo-Wilhelmy, S. A.; Aller, R. C. Trace metals and dissolved organic carbon in an estuary with restricted river flow and a brown tide bloom. *Estuaries.* **1999**, *22(3A)*, 603-615.

Bricaud, A.; Babin, M.; Morel, A.; Claustre, H. Variability in the chlorophyll-specific absorption coefficients of natural phytoplankton: analysis and parameterization. *Journal of Geophysical Research.* **1995**, *100(C7)*, 13321-13332.

Bricaud, A.; Claustre, H.; Ras, J.; Oubelkheir, K. Natural variability of phytoplanktonic absorption in oceanic waters: Influence of the size structure of algal populations. *Journal of Geophysical Research C: Oceans.* **2004**, *109(11)*, C11010.

Bricaud, A.; Sathyendranath, S. 1981. Spectral signatures of substances reponsible for the change in ocean colour. *Spectral Signatures of Objects in Remote Sensing*, Avignon, France, pp. 41-55.

Bricelj, V. M.; Lonsdale, D. J. *Aureococcus anophagefferens*: Causes and ecological consequences of brown tides in U.S. mid-Atlantic coastal waters. *Limnology and Oceanography.* **1997**, *42(5, part 2)*, 1023-1038.

Buskey, E. J.; Stockwell, D. A., et al. Effects of a persistent brown tides on zooplankton populations in the Laguna Madre of South Texas. In *Toxic Phytoplankton Blooms in the Sea*; Smayda T. J.; Shimizu, Y. Eds.; Elsevier: Amsterdam 1993; pp. 659-666.

Carder, K. L.; Chen, F. R.; Lee, Z. P.; Hawes, S. K.; Kamykowski, D. Semianalytic Moderate-Resolution Imaging Spectrometer algorithms for chlorophyll α and absorption with bio-optical domains based on nitrate-depletion temperatures. *Journal of Geophysical Research C: Oceans.* **1999**, *104(C3)*, 5403-5421.

Carder, K. L.; Gregg, W. W.; Costello, D. K.; Haddad, K.; Prospero, J. M. Determination of Saharan dust radiance and chlorophyll from CZCS imagery. *Journal of Geophysical Research.* **1991**, *96(D3)*, 5369-5378.

Carder, K. L.; Steward, R. G.; Harvey, G. R.; Ortner, P. B. Marine humic and fulvic acids: their effects on remote sensing of ocean chlorophyll. *Limnology and Oceanography.* **1989**, *34(1)*, 68-81.

Caron, D. A.; Lim, E. L.; Kunze, H.; Cosper, E. M.; Andersen, D. M., et al. Trophic interactions between nano- and microzooplankton and the"brown tide". In *Novel phytopankton blooms: causes and impacts of recurrent brown tides and other unusual blooms*; Cosper, E. M.; Bricelj, M., Carpenter, E. J. Eds.; Springer-Verlag: Berlin 1989; pp. 265-294.

Castro, P.; Huber, M. E. *Marine Biology, 6th Edition*; McGraw Hill: New York, 2007.

Chang, G. C.; Gould, R. W. Jr. Comparisons of optical properties of the coastal ocean derived from satellite ocean color and in situ measurements. *Optics Express.* **2006**, *14(22)*, 10149-10163.

Clark, L. B.; Gobler, C. J.; Sanudo-Wilhelmy, S. A. Spatial and temporal dynamics of dissolved trace metals, organic carbon, mineral nutrients, and phytoplankton in a coastal lagoon: Great South Bay, New York. *Estuaries and Coasts.* **2006**, *29(5)*, 841-854.

Cloern, J. E. Phytoplankton bloom dynamics in coastal ecosystems: A review with some general lessons from sustained investigation of San Francisco Bay, California. *Reviews of Geophysics.* **1996**, *34(2)*, 127-168.

Cosper, EM; Dennison, WC; Carpenter, EJ; Bricelj, VM; Mitchell, JG; Kuenstner, SH; Colflesh, D; Dewey, M. Recurrent and persistent brown tide blooms perturb coastal marine ecosystem. *Estuaries and Coasts.* **1987**, *10(4)*, 284-290.

D'Sa, E. J.; Miller, R. L.; Del Castillo, C. Bio-optical properties and ocean color algorithms for coastal waters influenced by the Mississippi River during a cold front. *Applied Optics.* **2006**, *45(28)*, 7410-7428.

Debelius, B.; Forja, J.M.; DelValls, Á.; Lubián, L.M. Toxicity and bioaccumulation of copper and lead in five marine microalgae. *Ecotoxicology and Environmental Safety.* **2009**, *72(5)*, 1503-1513.

Dennison, W. C.; Marshall, G. J.; Wigand, C., et al. Effect of “brown tide” shading on eelgrass (Zostera marina L.) distributions. In *Novel phytoplankton blooms: causes and impacts of recurrent brown tides and other unusual blooms*; Cosper, E. M.; Bricelj, M., Carpenter, E. J. Eds.; Springer-Verlag: Berlin 1989; pp. 675-692.

DeYoe, HR; Stockwell, DA; Bidigare, RR; Latasa, M; Johnson, PW; Hargraves, PE; Suttle, CA. Description and characterization of the algal species Aureoumbra lagunensis gen. et sp. nov. and referral of Aureoumbra and Aureococcus to the Pelagophyceae. *Journal of Phycology.* **1997**, *33(6)*, 1042-1048.

Dooley, P. *Brown tide research initiative(Report# 9)*. New York Sea Grant, 2006.

Dupont, C. L.; Barbeau, K.; Palenik, B. Ni uptake and limitation in marine Synechococcus strains. *Applied and environmental microbiology.* **2008**, *74(1)*, 23-31.

Dupont, C. L.; Buck, K. N.; Palenik, B.; Barbeau, K. Nickel utilization in phytoplankton assemblages from contrasting oceanic regimes. *Deep-Sea Research Part I: Oceanographic Research Papers.* **2010**, *57(4)*, 553-566.

Dzurica, S.; Lee, C.; Cosper, E. M.; Carpenter, E. J. Role of environmental variables, specifically organic compounds and micronutrients, in growth of the" brown tide" organism. *Lecture Notes on Coastal and Estuarine Studies.* **1989**, *35*, 229-252.

Eaton, A. D.; Cleasceri, L. S.; Rice, E. W.; Greenberg, A. E., Eds. *Standard Methods for the Examination of Water & Wastewater (21st Edition)*; Amer Public Health Association: Washington, DC, 2005.

Errécalde, O.; Campbell, P. G. C. Cadmium and zinc bioavailability to *Selenastrum capricornutum* (Chlorophyceae): Accidental metal uptake and toxicity in the presence of citrate. *Journal of Phycology.* **2000**, *36(3)*, 473-483.

Ferrari, G. M.; Dowell, M. D. CDOM absorption characteristics with relation to fluorescence and salinity in coastal areas of the southern Baltic Sea. *Estuarine, Coastal and Shelf Science.* **1998**, *47(1)*, 91-105.

Ferrari, G. M.; Tassan, S. A method using chemical oxidation to remove light absorption by phytoplankton pigments. *Journal of Phycology.* **1999**, *35(5)*, 1090-1098.

Ferreira, A.; Garcia, V. M. T.; Garcia, C. A. E. Light absorption by phytoplankton, non-algal particles and dissolved organic matter at the Patagonia shelf-break in spring and summer. *Deep-Sea Research Part I: Oceanographic Research Papers.* **2009**, *56(12)*, 2162-2174.

Fisher, N. S.; Bohe, M.; Teyssie, J. L. Accumulation and toxicity of Cd, Zn, Ag, and Hg in four marine phytoplankters. *Marine Ecology Progress Series.* **1984**, *19(3)*, 201-213.

Förstner, U.; Wittmann, G. T. W; Prosi, F.; Van Lierde, J. H.; Goldberg, E. D. *Metal pollution in the aquatic environment*; Springer-Verlag: New York, 1979.

French, C. S.; Brown, J. S.; Prager, L.; Lawrence, M. C. Analysis of spectra of natural chlorophyll complexes. *Carnegie Inst. Washington, Year Book.* **1967**, *67*, 536-546.

Gainey, L. F. Jr; Shumway, S. E. The physiological effect of *Aureococcus anophagefferens* ("brown tide") on the lateral cilia of bivalve mollusks. *The Biological Bulletin.* **1991**, *181(2)*, 298-306.

Gao, Y.; Nelson, E. D.; Field, M. P.; Ding, Q.; Li, H.; Sherrell, R. M.; Gigliotti, C. L.; Van Ry, D. A.; Glenn, T. R.; Eisenreich, S. J. Characterization of atmospheric trace elements on PM2.5 particulate matter over the New York-New Jersey harbor estuary. *Atmospheric Environment.* **2002**, *36(6)*, 1077-1086.

Gastrich, M. D.; Lathrop, R.; Haag, S.; Weinstein, M. P.; Danko, M.; Caron, D. A.; Schaffner, R. Assessment of brown tide blooms, caused by *Aureococcus anophagefferens*, and contributing factors in New Jersey coastal bays: 2000-2002. *Harmful Algae.* **2004**, *3(4)*, 305-320.

Gastrich, M. D.; Wazniak, C. E. A brown tide bloom index based on the potential harmful effects of the brown tide alga, Aureococcus anophagefferens. *Aquatic Ecosystem Health & Management.* **2002**, *5(4)*, 435-441.

Giner, J. L.; Boyer, G. L. Sterols of the brown tide alga Aureococcus anophagefferens. *Phytochemistry.* **1998**, *48(3)*, 475-477.

Gobler, C. J.; Berry, D. L.; Dyhrman, S. T.; Wilhelm, S. W.; Salamov, A.; Lobanov, A. V.; Zhang, Y.; Collier, J. L.; Wurch, L. L.; Kustka, A. B.; Dill, B. D.; Shah, M.; VerBerkmoes, N. C.; Kuo, A.; Terry, A.; Pangilinan, J.; Lindquist, E. A.; Lucas, S.; Paulsen, I. T.; Hattenrath-Lehmann, T. K.; Talmage, S. C.; Walker, E. A.; Koch, F.; Burson, A. M.; Marcoval, M. A.; Tang, Y. Z.; LeCleir, G. R.; Coyne, K. J.; Berg, G. M.; Bertrand, E. M.; Saito, M. A.; Gladyshev, V. N.; Grigoriev, I. V. Niche of harmful alga Aureococcus anophagefferens revealed through ecogenomics. *Proceedings of the National Academy of Sciences of the United States of America.* **2011**, *108(11)*, 4352-4357.

Gobler, C. J.; Hutchins, D. A.; Fisher, N. S.; Cosper, E. M.; Sañudo-Wilhelmy, S. A. Release and bioavailability of C, N, P, Se, and Fe following viral lysis of a marine chrysophyte. *Limnology and Oceanography.* **1997**, *42(7)*, 1492-1504.

Gobler, C. J.; Lonsdale, D. J.; Boyer, G. L. A review of the causes, effects, and potential management of harmful brown tide blooms caused by Aureococcus anophagefferens (Hargraves et Sieburth). *Estuaries.* **2005**, *28(5)*, 726-749.

Gobler, C. J.; Renaghan, M. J.; Buck, N. J. Impacts of nutrients and grazing mortality on the abundance of Aureococcus anophagefferens during a New York brown tide bloom. *Limnology and Oceanography.* **2002**, *47(1)*, 129-141.

Gobler, C. J.; Sañudo-Wilhelmy, S. A. Temporal variability of groundwater seepage and brown tide blooms in a Long Island embayment. *Marine Ecology Progress Series.* **2001**, *217*, 299-309.

Goericke, R.; Repeta, D. J. Chlorophylls a and b and divinyl chlorophylls a and b in the open subtropical North Atlantic Ocean. *Marine Ecology Progress Series.* **1993**, *101(3)*, 307-313.

Gordon, H. R. Atmospheric correction of ocean color imagery in the Earth observing system era. *Journal of Geophysical Research D: Atmospheres.* **1997**, *102(14)*, 17081-17106.

Gordon, Howard R.; Clark, Dennis K. Clear water radiances for atmospheric correction of coastal zone color scanner imagery *Applied Optics.* **1981**, *20(24)*, 4175-4180.

Gould, R. W. Jr; Arnone, R. A. Remote sensing estimates of inherent optical properties in a coastal environment. *Remote Sensing of Environment.* **1997**, *61(2)*, 290-301.

Graneli, E.; Risinger, L. Effects of cobalt and vitamin-B-12 on the growth of *Chrysochromulina polylepis* (Prymnesiophyceae). *Marine Ecology Progress Series.* **1994**, *113(1-2)*, 177-184.

Greenfield, D. I. (2002). The Influence of Variability in Plankton Community Composition on the Growth of Juvenile Hard Clams Merecenaria Mercenaria (L.), Master Thesis, State University of New York at Stony Brook.

Greenfield, D. I.; Lonsdale, D. J.; Cerrato, R. M.; Lopez, G. R. Effects of background concentrations of Aureococcus anophagefferens (brown tide) on growth and feeding in the bivalve Mercenaria mercenaria. *Marine Ecology Progress Series.* **2004**, *274*, 171-181.

Groom, S.; Martinez-Vicente, V.; Fishwick, J.; Tilstone, G.; Moore, G.; Smyth, T.; Harbour, D. The Western English Channel observatory: Optical characteristics of station L4. *Journal of Marine Systems.* **2009**, *77(3)*, 278-295.

Hallegraeff, G. M. A review of harmful algal blooms and their apparent global increase. *Phycologia.* **1993**, *32(2)*, 79-99.

Havskum, H.; Schlüter, L.; Scharek, R.; Berdalet, E.; Jacquet, S. Routine quantification of phytoplankton groups-microscopy or pigment analyses? *Marine Ecology Progress Series.* **2004**, *273*, 31-42.

Hellweger, F. L.; Schlosser, P.; Lall, U.; Weissel, J. K. Use of satellite imagery for water quality studies in New York Harbor. *Estuarine, Coastal and Shelf Science.* **2004**, *61(3)*, 437-448.

Henriksen, P.; Riemann, B.; Kaas, H.; Sorensen, H.M.; Sorensen, H. L. Effects of nutrient-limitation and irradiance on marine phytoplankton pigments. *Journal of Plankton Research.* **2002**, *24(9)*, 835.

Ho, T. Y.; Quigg, A.; Finkel, Z. V.; Milligan, A. J.; Wyman, K.; Falkowski, P. G.; Morel, F. M. M. The elemental composition of some marine phytoplankton. *Journal of Phycology.* **2003**, *39(6)*, 1145-1159.

Hoepffner, N.; Sathyendranath, S. Effect of pigment composition on absorption properties of phytoplankton. *Marine Ecology Progress Series.* **1991**, *73(1)*, l-23.

Hoepffner, N.; Sathyendranath, S. Bio-optical characteristics of coastal waters: absorption spectra of phytoplankton and pigment distribution in the western North Atlantic. *Limnology & Oceanography.* **1992**, *37(8)*, 1660-1679.

Hu, C.; Chen, Z.; Clayton, T. D.; Swarzenski, P.; Brock, J. C.; Muller-Karger, F. E. Assessment of estuarine water-quality indicators using MODIS medium-resolution bands: Initial results from Tampa Bay, FL. *Remote Sensing of Environment.* **2004**, *93(3)*, 423-441.

Hudson, R. J. M. Which aqueous species control the rates of trace metal uptake by aquatic biota? Observations and predictions of non-equilibrium effects. *Science of the Total Environment.* **1998**, *219(2-3)*, 95-115.

Ingle, R. M.; Martin, D. F. Prediction of the florida red tide by means of the iron index. *Environmental Letters.* **1971**, *1(1)*, 69-74.

IOCCG. *Remote Sensing of Ocean Colour in Coastal, and Other Optically-Complex, Waters*. Sathyendranath, S. (ed.). Reports of the International Ocean-Colour Coordinating Group, No.3. IOCCG, Dartmouth, Canada, 2000.

IOCCG. *Remote sensing of inherent optical properties: fundamentals, tests of algorithms, and applications*. Lee, Z.-P. (ed.). Reports of the International Ocean-Colour Coording Group, No. 5. IOCCG, Dartmouth, Canada, 2006.

Jeffrey, S. W.; Mantoura, R. F. C.; Wright, S. W., Eds. *Phytoplankton pigments in oceanography: guidelines to modern methods*; UNESCO: Paris, 1997.

Jerlov, NG. *Optical oceanography*; Elsevier, 1968.

Kirk, J. T. O. A theoretical analysis of the contribution of algal cells to the attenuation of light within natural waters I. General treatment of suspensions of pigmented cells. *New phytologist.* **1975**, *75(1)*, 11-20.

Kirk, J. T. O. *Light and photosynthesis in aquatic ecosystems*; Cambridge University Press, 1994.

Koike, Y.; Nakaguchi, Y.; Hiraki, K.; Takeuchi, T.; Kokubo, T.; Ishimaru, T. Species and concentrations of selenium and nutrients in Tanabe Bay during red tide due to *Gymnodinium nagasakiense*. *Journal of Oceanography.* **1993**, *49(6)*, 641-656.

Komada, T.; Schofield, O. M. E.; Reimers, C. E. Fluorescence characteristics of organic matter released from coastal sediments during resuspension. *Marine Chemistry.* **2002**, *79(2)*, 81-97.

Kozelka, P. B.; Bruland, K. W. Chemical speciation of dissolved Cu, Zn, Cd, Pb in Narragansett Bay, Rhode Island. *Marine Chemistry.* **1998**, *60(3-4)*, 267-282.

Landsberg, J. H. The effects of harmful algal blooms on aquatic organisms. *Reviews in Fisheries Science.* **2002**, *10(2)*, 113-390.

LaRoche, J.; Nuzzi, R.; Waters, R.; Wyman, K.; Falkowski, P. G.; Wallance, D. Brown tide blooms in Long Island's coastal waters linked to interannual variability in groundwater flow. *Global Change Biology.* **1997**, *3(5)*, 397-410.

Lee, J. G.; Ahner, B. A.; Morel, F. M. M. Export of cadmium and phytochelatin by the marine diatom *Thalassiosira weissflogii*. *Environmental Science and Technology.* **1996**, *30(6)*, 1814-1821.

Lee, Z. P.; Carder, K. L.; Arnone, R. A. Deriving inherent optical properties from water color: a multiband quasi-analytical algorithm for optically deep waters. *Applied Optics.* **2002**, *41(27)*, 5755-5772.

Leong, S. C. Y.; Taguchi, S. Detecting the bloom-forming dinoflagellate Alexandrium tamarense using the absorption signature. *Hydrobiologia.* **2006**, *568(1)*, 299-308.

Llewellyn, C. A.; Fishwick, J. R.; Blackford, J. C. Phytoplankton community assemblage in the English Channel: a comparison using chlorophyll a derived from HPLC-CHEMTAX and carbon derived from microscopy cell counts. *Journal of Plankton Research.* **2005**, *27(1)*, 103.

Lomas, M. W.; Gobler, C. J. Aureococcus anophagefferens research: 20 years and counting. *Harmful Algae.* **2004**, *3(4)*, 273-277.

Lomas, M. W.; Kana, T. M.; MacIntyre, H. L.; Cornwell, J. C.; Nuzzi, R.; Waters, R. Interannual variability of Aureococcus anophagefferens in Quantuck Bay, Long Island: natural test of the DON hypothesis. *Harmful Algae.* **2004**, *3(4)*, 389-402.

Lonsdale, D. J.; Cosper, E. M.; Kim, W. S.; Doall, M.; Divadeenam, A.; Jonasdottir, S. H. Food web interactions in the plankton of Long Island bays, with preliminary observations on brown tide effects. *Marine Ecology Progress Series.* **1996**, *134(1)*, 247-263.

Luoma, S. N.; Van Geen, A.; Lee, B. G.; Cloern, J. E. Metal uptake by phytoplankton during a bloom in South San Francisco Bay: Implications for metal cycling in estuaries. *Limnology and Oceanography.* **1998**, *43(5)*, 1007-1016.

MacIntyre, H. L.; Lomas, M. W.; Cornwell, J.; Suggett, D. J.; Gobler, C. J.; Koch, E. W.; Kana, T. M. Mediation of benthic-pelagic coupling by microphytobenthos: an energy-and material-based model for initiation of blooms of Aureococcus anophagefferens. *Harmful Algae.* **2004**, *3(4)*, 403-437.

Mackey, M. D.; Mackey, D. J.; Higgins, H. W.; Wright, S. W. CHEMTAX-A program for estimating class abundances from chemical markers: Application to HPLC measurements of phytoplankton. *Marine Ecology Progress Series.* **1996**, *144(1-3)*, 265-283.

Mahoney, J. B.; McLaughlin, J. J. A. The association of phytoflagellate blooms in Lower New York Bay with hypertrophication. *Journal of Experimental Marine Biology and Ecology.* **1977**, *28(1)*, 53-65.

Marshall, H. G.; Cohn, M. S. Phytoplankton composition of the New York Bight and adjacent waters. *Journal of Plankton Research.* **1987**, *9(2)*, 267-276.

Mehran, R. (1996). Effects of Aureococcus anophagefferens on microzooplankton grazing and growth rates in the Peconic Bays system, Long Island, New York, Master Thesis, State University of New York at Stony Brook.

Miao, A. J.; Wang, W. X. Cadmium toxicity to two marine phytoplankton under different nutrient conditions. *Aquatic Toxicology.* **2006**, *78(2)*, 114-126.

Miao, A. J.; Wang, W. X.; Juneau, P. Comparison of Cd, Cu, and Zn toxic effects on four marine phytoplankton by pulse-amplitude-modulated fluorometry. *Environmental toxicology and chemistry.* **2005**, *24(10)*, 2603-2611.

Millie, D. F.; Schofield, O. M.; Kirkpatrick, G. J.; Johnsen, G.; Tester, P. A.; Vinyard, B. T. Detection of harmful algal blooms using photopigments and absorption signatures: a case study of the Florida red tide dinoflagellate, Gymnodinium breve. *Limnology and Oceanography.* **1997**, *42(5)*, 1240-1251.

Milligan, A. J.; Cosper, E. M. Growth and photosynthesis of the'brown tide'microalga Aureococcus anophagefferens in subsaturating constant and fluctuating irradiance. *Marine Ecology Progress Series.* **1997**, *153(1-3)*, 67-75.

Mitchell, B. G.; Bricaud, A.; Carder, K.; Cleveland, J.; Ferrari, G.; Gould, R.; Kahru, M.; Kishino, M.; Maske, H.; Moisan, T.; Moore, L.; Nelson, N.; Phinney, D.; Reynolds, R.; Sosik, H.; Stramski, D.; Tassan, S.; Trees, C.; Weidemann, A.; Wieland, J.; Vodacek, A. *Determination of spectral absorption coefficients of particles, dissolved material and phytoplankton for discrete water samples*. NASA Technical Memorandum (209966). 2000.

Mitchell, B. G.; Kieper, D. A. Variability in pigment particulate fluorescence and absorption spectra in the northeastern Pacific Ocean. *Deep Sea Research Part A, Oceanographic Research Papers.* **1988**, *35(5)*, 665-689.

Montagnes, D. J. S.; Franklin, D. J. Effect of temperature on diatom volume, growth rate, and carbon and nitrogen content: reconsidering some paradigms. *Limnology and Oceanography.* **2001**, *46(8)*, 2008-2018.

Moore, G. F.; Aiken, J.; Lavender, S. J. The atmospheric correction of water colour and the quantitative retrieval of suspended particulate matter in Case II waters: Application to MERIS. *International Journal of Remote Sensing.* **1999**, *20(9)*, 1713-1733.

Morel, A.; Bricaud, A. Theoretical results concerning light absorption in a discrete medium, and application to specific absorption of phytoplankton. *Deep Sea Research Part A, Oceanographic Research Papers.* **1981**, *28(11)*, 1375-1393.

Morel, F. M. M.; Price, N. M. The biogeochemical cycles of trace metals in the oceans. *Science.* **2003**, *300(5621)*, 944-947.

Mulholland, M. R.; Gobler, C. J.; Lee, C. Peptide hydrolysis, amino acid oxidation, and nitrogen uptake in communities seasonally dominated by Aureococcus anophagefferens. *Limnology and Oceanography.* **2002**, *47(4)*, 1094-1108.

Nelson, N. B.; Siegel, D. A.; Michaels, A. F. Seasonal dynamics of colored dissolved material in the Sargasso Sea. *Deep-Sea Research Part I: Oceanographic Research Papers.* **1998**, *45(6)*, 931-957.

Newman, M. C.; Roberts, M. H. Jr.; Hale, R. C., Eds. *Coastal and Estuarine Risk Assessment*; Lewis: Boca Raton, Florida, 2002.

Nichols, D. B.; Satchwell, M. F.; Alexander, J. E.; Martin, N. M.; Baesl, M. T.; Boyer, G. L. (2001). Iron nutrition in the brown tide alga, *Aureococcus anophagefferens*: Characterization of a ferric chelate reductase activity. Harmful Algal Blooms 2000. Hallegraeff, G. M., Blackburn, S. I., Bolch, C. J., Lewis, R. J. . Hobart, Tasmania, Intergovermental Oceanographic Commission of UNESCO**:** 340-343.

NJDEP. *Annual Summary of Phytoplankton Blooms and Related Condidtions in the New Jersey Coastal Waters Summer of 1999*. New Jersey Department of Environmental Protection: Trenton, New Jersey, 1999: http://www.state.nj.us/dep/bmw/Reports/phytorpt99.pdf.

NJDEP. *Harmful Algal Blooms in coastal waters of New Jersey*. New Jersey Department of Environmental Protection: Trenton, NJ, 2000: www.state.nj.us/dep/dsr/coastal/hab2.pdf.

NJDEP. *Annual summary of phytoplankon blooms and related conditions in the New Jersey coastal waters summer of 2005*. New Jersey Department of Environmental Protection: Trenton, NJ, 2008a: www.state.nj.us/dep/bmw/Reports/Phyto2005Final.pdf.

NJDEP. *Report of Algal Conditions in New Jersey Coastal Waters Week of August 18, 2008*. New Jersey Department of Environmental Protection: Trenton, NJ, 2008b: www.state.nj.us/dep/bmw/Phytoplankton/082008report.pdf.

Nuzzi, R.; Olsen, P.; Mahoney, J. B.; Zodl, G. *The first Aureococcus anophagefferens brown tide in New Jersey*. Harmful Algae News, IOC Newsletter. 1996, No. 15.

NYCDEP. *New York Harbor water quality report*. New York City Department of Environmental Protection: New York, NY, 2009: http://www.nyc.gov/html/dep/pdf/hwqs2009.pdf.

Odriozola, A. L.; Varela, R.; Hu, C.; Astor, Y.; Lorenzoni, L.; Müller-Karger, F. E. On the absorption of light in the Orinoco River plume. *Continental Shelf Research.* **2007**, *27(10-11)*, 1447-1464.

Oubelkheir, K.; Claustre, H.; Bricaud, A.; Babin, M. Partitioning total spectral absorption in phytoplankton and colored detrital material contributions. *Limnology and Oceanography: Methods.* **2007**, *5(NOV)*, 384-395.

Payne, C. D.; Price, N. M. Effects of cadmium toxicity on growth and elemental composition of marine phytoplankton. *Journal of Phycology.* **1999**, *35(2)*, 293-302.

Perkins, M.; Effler, S. W.; Strait, C.; Zhang, L. Light absorbing components in the Finger Lakes of New York. *Fundamental and Applied Limnology.* **2009**, *173(4)*, 305-320.

Phillips, D. M.; Kirk, J. T. O. Study of the spectral variation of absorption and scattering in some Australian coastal waters (Jervis Bay). *Australian Journal of Marine & Freshwater Research.* **1984**, *35(6)*, 635-644.

Pope, R. M.; Fry, E. S. Absorption spectrum (380–700 nm) of pure water. II. Integrating cavity measurements. *Applied Optics.* **1997**, *36(33)*, 8710-8723.

Price, N. M.; Harrison, G. I.; Hering, J. G.; Hudson, R. J. M.; Nirel, P. M. V.; Palenik, B.; Morel, F. M. M. Preparation and chemistry of the artificial algal culture medium Aquil. *Biological oceanography.* **1988/1989**, *6(5-6)*, 443-461.

Price, N. M.; Morel, F. M. M. Cadmium and cobalt substitution for zinc in a marine diatom. *Nature.* **1990**, *344(12)*, 658-660.

Prieur, L.; Sathyendranath, S. An optical classification of coastal and oceanic waters based on the specific spectral absorption curves of phytoplankton pigments, dissolved organic matter, and other particulate materials. *Limnology and Oceanography.* **1981**, *26(4)*, 671-689.

Pustizzi, F.; MacIntyre, H.; Warner, M. E.; Hutchins, D. A. Interaction of nitrogen source and light intensity on the growth and photosynthesis of the brown tide alga Aureococcus anophagefferens. *Harmful Algae.* **2004**, *3(4)*, 343-360.

Raven, J. A.; Evans, M. C. W.; Korb, R. E. The role of trace metals in photosynthetic electron transport in O_2-evolving organisms. *Photosynthesis Research.* **1999**, *60(2-3)*, 111-150.

Rodriguez, F.; Varela, M.; Zapata, M. Phytoplankton assemblages in the Gerlache and Bransfield Straits (Antarctic Peninsula) determined by light microscopy and CHEMTAX analysis of HPLC pigment data. *Deep Sea Research Part II: Topical Studies in Oceanography.* **2002**, *49(4-5)*, 723-747.

Roesler, C. S.; Perry, M. J.; Carder, K. L. Modeling in situ phytoplankton absorption from total absorption spectra in productive inland marine waters. *Limnology & Oceanography.* **1989**, *34(8)*, 1510-1523.

Sanders, J. G.; Riedel, G. F. Trace element transformation during the development of an estuarine algal bloom. *Estuaries.* **1993**, *16(3)*, 521-532.

Sasaki, H.; Miyamura, T.; Saitoh, S. I.; Ishizaka, J. Seasonal variation of absorption by particles and colored dissolved organic matter (CDOM) in Funka Bay, southwestern Hokkaido, Japan. *Estuarine, Coastal and Shelf Science.* **2005**, *64(2-3)*, 447-458.

Saunders, G. W.; Potter, D.; Andersen, R. A. Phylogentic Affinities of the Sarcinochrysidales and Chrsomeridales (Heterokonta) Based on Analyses of Molecular and Combinaed Data 1 *Journal of Phycology.* **1997**, *33(2)*, 310-318.

Schecher, W. (2001). Thermochemical data used in MINEQL+ version 4.5 with comparisons to versions 4.07 and earlier. Environmental Research Software. Hallowell, ME.

Schlüter, L.; Møhlenberg, F.; Havskum, H.; Larsen, S. The use of phytoplankton pigments for identifying and quantifying phytoplankton groups in coastal areas: testing the influence of light and nutrients on pigment/chlorophyll a ratios. *Marine Ecology Progress Series.* **2000**, *192*, 49-63.

Seidl, M.; Huang, V.; Mouchel, J. M. Toxicity of combined sewer overflows on river phytoplankton: The role of heavy metals. *Environmental Pollution.* **1998**, *101(1)*, 107-116.

Sellner, K. G.; Doucette, G. J.; Kirkpatrick, G. J. Harmful algal blooms: causes, impacts and detection. *Journal of Industrial Microbiology and Biotechnology.* **2003**, *30(7)*, 383-406.

Sieburth, J. M. N. ; Johnson, P. W.; Hargraves, P. E. Ultrastructure and ecology of Aureococcus anophagefferens gen. et sp. nov.(Chrysophyceae): the dominant picoplankter during a bloom in Narragansett Bay, Rhode Island, summer 1985. *Journal of Phycology.* **1988**, *24(3)*, 416-425.

Sindermann, C. J. *Coastal Pollution: Effects on Living Resources and Humans*; CRC/Taylor & Francis: Boca Raton, Florida, 2006.

Slaveykova, V. I.; Karadjova, I. B.; Karadjov, M.; Tsalev, D. L. Trace metal speciation and bioavailability in surface waters of the black sea coastal area evaluated by HF-PLM and DGT. *Environmental Science and Technology.* **2009**, *43(6)*, 1798-1803.

Small, C.; Cohen, J. E. Continental physiography, climate, and the global distribution of human population. *Current Anthropology.* **2004**, *45(2)*, 269-277.

Smith, R. C.; Baker, K. S. Optical properties of the clearest natural waters (200-800 nm). *Applied Optics.* **1981**, *20(2)*, 177-184.

Stedmon, C. A.; Markager, S. The optics of chromophoric dissolved organic matter (CDOM) in the Greenland Sea: An algorithm for differentiation between marine and terrestrially derived organic matter. *Limnology & Oceanography.* **2001**, *46(8)*, 2087-2093.

Strathmann, R. R. Estimating the organic carbon content of phytoplankton from cell volume or plasma volume. *Limnology & Oceanography.* **1967**, *12(3)*, 411-418.

Stuart, V.; Sathyendranath, S.; Platt, T.; Maass, H.; Irwin, B. D. Pigments and species composition of natural phytoplankton populations: Effect on the absorption spectra. *Journal of Plankton Research.* **1998**, *20(2)*, 187-217.

Sunda, W. G., et al. Trace metals and harmful algal blooms. In *Ecology of Harmful Algae*; Granéli, E.; Turner, J. T. Eds.; Springer: Berlin 2006; pp. 203-214.

Tassan, S.; Ferrari, G. M. A sensitivity analysis of the'Transmittance-Reflectance'method for measuring light absorption by aquatic particles. *Journal of Plankton Research.* **2002**, *24(8)*, 757.

Tester, P. A.; Geesey, M. E.; Guo, C.; Paerl, H. W.; Millie, D. F. Evaluating phytoplankton dynamics in the Newport River estuary (North Carolina, USA) by HPLC-derived pigment profiles. *Marine Ecology Progress Series.* **1995**, *124(1)*, 237-245.

Twardowski, M. S.; Lewis, M. R.; Barnard, A. H.; Zaneveld, J. R. V., et al. In-water instrumentation and platforms for ocean color remote sensing applications. In *Remote Sensing of Coastal Aquatic Environments*; Miller, R. L.; Castillo, C. E. D.; McKee, B. A. Eds.; Springer: Dordrecht 2005; pp. 69-100.

Veldhuis, M. J. W.; Kraay, G. W. Phytoplankton in the subtropical Atlantic Ocean: towards a better assessment of biomass and composition. *Deep Sea Research Part I: Oceanographic Research Papers.* **2004**, *51(4)*, 507-530.

Vidussi, F.; Claustre, H.; Manca, B.B.; Luchetta, A.; Marty, J. C. Phytoplankton pigment distribution in relation to upper thermocline circulation in the eastern Mediterranean Sea during winter. *Journal of Geophysical Research.* **2001**, *106(C9)*, 19939.

Wang, M.; Wang, W. X. Cadmium toxicity in a marine diatom as predicted by the cellular metal sensitive fraction. *Environmental Science and Technology.* **2008**, *42(3)*, 940-946.

Warnock, R. E.; Gieskes, W. W. C.; Van Laar, S. Regional and seasonal differences in light absorption by yellow substance in the Southern Bight of the North Sea. *Journal of Sea Research.* **1999**, *42(3)*, 169-178.

Wei, L.; Donat, J. R.; Fones, G.; Ahner, B. A. Interactions between Cd, Cu, and Zn influence particulate phytochelatin concentrations in marine phytoplankton: Laboratory results and preliminary field data. *Environmental Science and Technology.* **2003**, *37(16)*, 3609-3618.

Wells, M. L.; Smith, G. J.; Bruland, K. W. The distribution of colloidal and particulate bioactive metals in Narragansett Bay, RI. *Marine Chemistry.* **2000**, *71(1-2)*, 143-163.

Westall, J. C.; Zachary, J. L.; Morel, F. M. M. *MINEQL: A computer program for the calculation of chemical equilibrium composition of aqueous systems*. Tech. Note No. 18 R. M. Parons Lab for Water Resources and Environmental Engineering. MIT, Cambridge, Dept. of Civil Engineering, 1976.

Wolfe, G. V.; Steinke, M.; Kirst, G. O. Grazing-activated chemical defence in a unicellular marine alga. *Nature.* **1997**, *387(6636)*, 894-897.

Wright, S. W.; Jeffrey, S. W.; Mantoura, R. F. C.; Llewellyn, C. A.; Bjørnland, T.; Repeta, D.; Welschmeyer, N. Improved HPLC method for the analysis of chlorophylls and carotenoids from marine phytoplankton. *Marine Ecology Progress Series.* **1991**, *77(2-3)*, 183-196.

Zimmer, B. J.; Groppenbacher, S. *New Jersey Ambient Monitoring Program Report on Marine and Coastal Water Quality, 1993-1997* New Jersey Department of Environmental Protection: New Jersey, 1999: http://www.state.nj.us/dep/bmw/Reports/estmon-99.pdf.